MICROPLASTICS IN AGRICULTURAL SOIL AMENDED WITH ALKALINE-TREATED BIOSOLIDS

by

Charles A. Little

Submitted in partial fulfillment of the requirements
for the degree of Master of Science

at

Dalhousie University
Halifax, Nova Scotia
April 2025

Dalhousie University is located in Mi’kma’ki,
the ancestral and unceded territory of the Mi’kmaq.
We are all Treaty people.

TABLE OF CONTENTS

LIST OF TABLES

LIST OF FIGURES

ABSTRACT

Microplastics (MPs) are emerging ubiquitous environmental contaminants that risk agricultural sustainability and food security through the land application of biosolids. This research quantified MPs in alkaline-treated biosolids (ATBs) and evaluated their accumulation, persistence, and vertical movement in agricultural soils over 15 years. ATBs contained an average of 138 600 MP particles kg^{-1} (dry weight), predominantly fragments. Repeated ATB applications led to significant MP accumulation in surface soils (0–15 cm), with an 8.7-fold increase observed under 14 tonnes ha^{-1} applications. MPs persisted long-term, even in single-application plots, and smaller MPs preferentially migrated deeper into the soil profile. To enhance MP characterisation, thermogravimetric analysis (TGA) paired with differential scanning calorimetry (DSC) and Fourier-transformed infrared (FTIR) spectroscopy was used to successfully identify polypropylene (PP), polyethene (PE), and polystyrene (PS). These findings underscore the need for improved regulatory oversight and monitoring strategies to mitigate MP contamination and protect agricultural sustainability and food security.

LIST OF ABBREVIATIONS USED

ATB	Alkaline-Treated Biosolids
CEC	Cation Exchange Capacity
cm	Centimeter
^{o}C	Degrees Celcius
DOM	Dissolved Organic Matter
DSC	Differential Scanning Calorimetry
FTIR	Fourier Transform Infrared Spectroscopy
g	Gram
g/cm^3	Grams per Cubic Centimeter (Density)
H_2O_2	Hydrogen Peroxide
ha	Hectare
kg	Kilogram
kg^{-1}	Per Kilogram
L	Liter
mg	Milligram
mL	Milliliter
MPs	Microplastics
µg	Microgram
µL	Microliter
µm	Micrometer (Micron)
µm^2	Square Micrometer
µV	Microvolt
UV	Ultraviolet
NIAS	Non-intentionally Added Substances
NR	Nile Red
PBT	Persistent, Bioaccumulative and Toxic
PE	Polyethylene
PET	Polyethylene Terephthalate
PLA	Polylactide
PMMA	Poly (methyl methacrylate)
PoTSs	Potentially Toxic Substances
PP	Polypropylene
ppm	Parts per Million
PS	Polystyrene
PVC	Polyvinyl Chloride
SEM	Scanning Electron Microscopy
SOC	Soil Organic Carbon
SOM	Soil Organic Matter
TGA	Thermogravimetric Analysis
w/w	Weight per Weight

ACKNOWLEDGEMENTS

I would like to express my sincere gratitude to my supervisor, Dr. Gordon Price, for his guidance and support; thank you for providing me with this opportunity and challenging me to grow as an independent researcher. I extend my thanks to my committee members; thank you, Dr. Adam Gillespie, for your generosity with access to your lab and equipment that supported this research; and thank you, Dr. Chijioke, for your insights on analytical instruments.

I would like to extend my appreciation to Sherri Matheson; thank you for your kindness and automatic willingness to help. The many hours spent counting microplastics would not have been possible without you.

I also appreciate and thank my Integrated Waste Management (IWM) lab mates, who consistently pulls together and offer support and guidance when needed. I was fortunate to form valued friendships that brought encouragement, motivation, and moments of levity, making this journey even more rewarding.

Finally, I am sincerely grateful to my close friends and family for their unwavering support, encouragement and belief in me. To my parents, thank you for always being my greatest source of strength and encouragement; none of this would be possible without you.

CHAPTER 1: INTRODUCTION

The invention of the first synthetic polymer, Bakelite, by Leo Baekeland in 1907 marks the beginning of the plastics industry, setting the stage for an unprecedented rise in global plastic production (Baekeland, 1909). Since plastics became widely adopted in the mid-20th century, their production has surged more than 230-fold, increasing from 2 million tonnes in 1950 to over 460 million tonnes annually (Geyer et al., 2017; OECD, 2022). Its mass production has resulted in massive amounts of plastic waste that persistently amass in ecosystems worldwide, ultimately fragmenting into microplastics (MPs), pieces smaller than 5 mm (UNEP, 2019; US EPA, 2022).

Due to plastics versatility, they have been adopted into a wide range of industries, from textiles and packaging to construction materials, pharmaceuticals, agricultural products, electronics, and more (Government of Canada, 2023; Halliwell, 2002; Lupton, 2010; Scarascia-Mugnozza et al., 2011; Soni & Joseph, 2021). However, mishandling and improper disposal practices have resulted in over half of the cumulatively produced 9 billion tonnes of plastic being directly landfilled, with less than nine per cent recycled (Geyer et al., 2017; OECD, 2022). Consequently, there are now significant accumulations of fragmented polymers contaminating all environmental compartments (Abbasi et al., 2023; Martin et al., 2020), even infiltrating biota, drinking water, food products, and different parts of the human body (Çelen et al., 2023; Cui et al., 2022; Jenner et al., 2022; Kirstein et al., 2021; Kumar et al., 2022; Leslie et al., 2022; Ragusa et al., 2022).

Despite the widespread prevalence of MPs across all environmental compartments, contemporary research has yet to address their occurrence, distribution, and potential impacts fully. To date, the focus of MP research has been on aquatic environments, with the preceding sense that most MPs migrate to these environments regardless of their original disposal (Almeida et al., 2023; Crossman et al., 2020; Zhang et al., 2021). However, more recent research suggests that terrestrial environments, particularly agricultural soils, could be a significant MP sink with the land application of agricultural amendments such as compost (Iswahyudi et al., 2024), manure (Sheriff et al., 2023; Wang et al., 2024a), plastic mulch (Hao et al., 2024), irrigation water (Pérez-Reverón et al., 2022), and sewage sludge (Crossman et al., 2020; Schell et al., 2022; Zhang et al., 2020).

Still, agricultural soils have received comparatively little attention and remain critically understudied. Fundamental and necessary information such as MP sources, persistence, migration, different polymer types, and the size and shape of MP particles in agricultural soils are unidentified. As a result, the dispersion and weathering mechanisms, the potential effects on soil physical and chemical properties, interactions with soil organisms, and transfer to humans through the tropic food web are underdeveloped topics. The constraining factor in gleaning such knowledge is reliable and standardised extraction and analytical methodologies. Since agricultural soil underpins global food security and provides critical ecosystem services, understanding MP dynamics in these systems is urgently needed. Such research gaps, especially when pertaining to such a fundamental pillar of food security, need to be filled.

Given these significant knowledge gaps regarding MP presence in agricultural soils, this research investigates alkaline-treated biosolids (ATBs) as a source of MP contamination. Utilising a long-term agricultural research site with over a decade of ATB applications to evaluate agricultural soil as a potentially significant MP sink. In the following chapters, MP accumulation, persistence and vertical movement will be assessed in response to ATB applications while examining MP morphology (shape and size), and a more novel approach to MP chemical characterisation using TGA-DSC-FTIR is employed.

CHAPTER 2: LITERATURE REVIEW

2.1 NOVELTY OF RESEARCH

Using SCOPUS, one of the largest databases of peer-reviewed literature, various terms were searched within article titles, abstracts and keywords between 2004 and 2024 to assess the extent of MP research. The term 'microplastics' returned 22,343 documents, with nearly half (49%) published in 2023 and 2024 (Fig 1). Of these documents, 40% of publications are within environmental science subject areas and approximately 76% (17,030) are primary research articles. The search was then narrowed to include 'soil AND agriculture AND microplastics', returning only 510 documents (Fig 1). Of these, approximately 74% (378) were primary research articles, and none were published before 2016. The past shortage of research articles paired with a recent surge of documents emphasises the novelty of MP research. These findings highlight a significant research gap, underscoring the limited focus on agricultural soil and the need for further investigation into MPs in these systems.

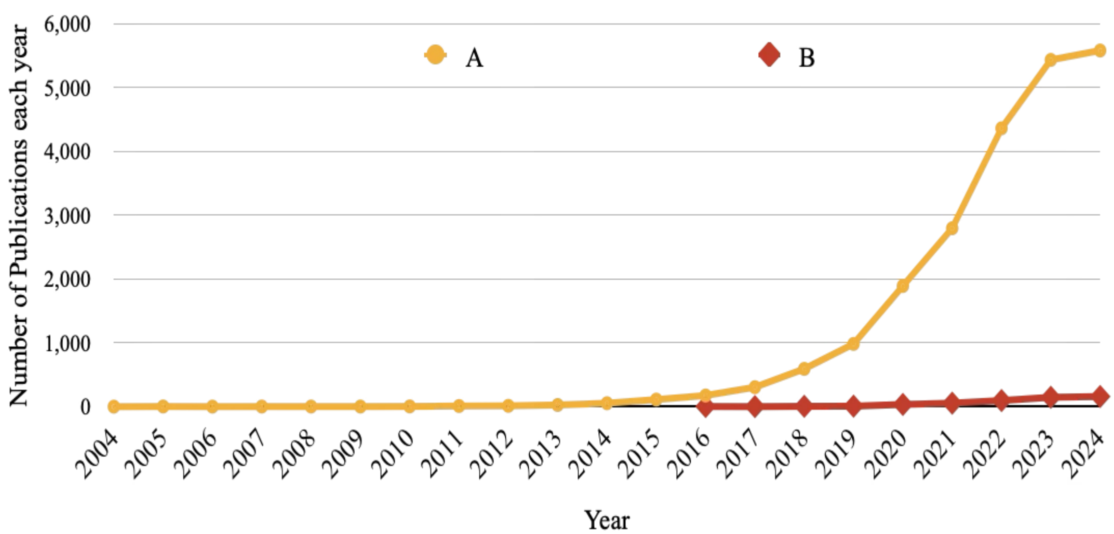

Figure 1. SCOPUS document search for (A) 'microplastics' and (B) 'soil AND agriculture AND microplastics' between 2004 and 2024.

2.2 IMPORTANCE OF SOIL HEALTH

Agricultural soil is a complex and multifaceted ecological system necessary for global food and nutritional security. Soil provides more than 95% of the world's food supply while silently offering nearly all ecosystem services necessary for life to exist on Earth (Vargas, 2022). While traditionally, the focus of agricultural soil has been on nutrient status and crop productivity, broader ecosystem services that the soil provides are of equal importance. Such ecosystem services include but are not limited to, carbon sequestration, water purification, pollutant bioremediation, recycling of organic wastes, and climate regulation (Blume et al., 2016; Hou, 2023; Paul & Frey, 2023). A healthy soil cycles nutrients, supports root growth, absorbs and purifies water, promotes biodiversity, and sequesters carbon more efficiently (Telo da Gama, 2023). All these factors enhance agricultural productivity; soils need fewer inputs, e.g. synthetic fertilisers, pesticides, and herbicides, have increased predictability of crop yield, provide economic stability for agriculturalists, and provide food security. Introducing MPs in these systems could result in soil health degradation, compromising crop productivity and posing risks to food safety through the transfer of toxic substances associated with MPs. If left unchecked, MP contamination could progressively degrade soil quality. This may result in reduced agricultural output, lower food quality, and economic instability within the agricultural sector.

2.3 DEFINING MICROPLASTICS

The term MP is used loosely in literature to include pieces of plastic smaller than 5 mm but with undefined or differing lower size limits between 1mm to 0.1 μm (Hartmann et al., 2019; Wu et al., 2022; Yuan et al., 2022; Kadac-Czapska et al., 2023; Liu et al., 2024). These MPs either directly enter the environment in their small size, termed primary MPs, or indirectly via fragmentation of larger plastics, termed secondary MPs. In addition, they occur in different shapes; common forms include microbeads, microfibers, and fragments. Microbeads or spheres are primary MPs produced for cosmetics and cleaning products and are predominantly found in wastewater streams (Environment and Climate Change Canada, 2015; Boucher & Friot, 2017). Microfibers, also primary MPs, originate from synthetic textiles and are again prevalent in wastewater streams (Boucher & Friot, 2017; Kim et al., 2023; Radford et al., 2023). In contrast, fragments are secondary MPs, resulting from the fragmentation of any plastic item, from PVC pipes and agrochemical containers to plastic single-use cups, plastic water bottles, plastic toys, and more (Andrady, 2017; Boucher & Friot, 2017; Pfohl et al., 2022). Other forms of MPs include foams and films but have been found in much less abundance (Crossman et al., 2020; Letwin et al., 2024).

Further, MPs are synthetic polymers composed primarily of organic compounds synthesized from hydrocarbons derived from fossil fuels such as coal, natural gas, and crude oil. They are high-molecular-weight compounds synthesized through polymerization processes, including polycondensation or polyaddition reactions, and broadly classified according to their thermal response; either thermoplastics consist of linear chains of monomers formed through polyaddition reactions, enabling them to be repeatedly softened and reshaped with heat; or thermosets, formed through polycondensation reactions, and are rigid and cannot be remoulded once cured (Aquino et al., 2022; McKeen, 2014). Thermoplastics can be recycled; they are further characterised based on their recyclability, illustrated through standardised recycling codes in Table 1.

Table 1. The most abundant plastic types, their recyclability codes, and chemical formulas.

Recycling Codes	**Name**	**Acronym**	**Chemical Formula**
1	Polyethene terephthalate	PET	$(C_{10}H_8O_4)_n$
2	High-density polyethene	HDPE	Linear $(C_2H_4)_n$
3	Polyvinyl chloride	PVC	$(C_2H_3Cl)_n$
4	Low-density polyethene	LDPE	Branched $(C_2H_4)_n$
5	Polypropylene	PP	$(C_3H_6)_n$
6	Polystyrene	PS	$(C_8H_8)_n$
7*	Acrylonitrile butadiene styrene	ABS	$(C_8H_8 \cdot C_4H_6 \cdot C_3H_3N)_n$
7*	Polylactic Acid	PLA	$(C_3H_4O_2)_n$
7*	Polycarbonate	PC	$(C_{16}H_{14}O_3)_n$
7*	Polyamide (Nylon)	PA	Nylon 1,6: $(C_6H_{11}NO)_n$ Nylon 6,6: $(C_{12}H_{22}N_2O_2)_n$
7*	Polyurethane (PU)	PU	$(C_{27}H_{36}N_2O_{10})_n$
7*	Polymethyl methacrylate (Acrylic)	PMMA	$(C_5O_2H_8)_n$

*Recycling code 7 includes various other plastic types and mixed resins; listed here are typical examples and not an extensive list.

2.4 BIOSOLIDS AS A SOURCE OF MICROPLASTICS

Biosolids are the processed nutrient-rich organic material recovered from sewage sludge in wastewater treatment plants (WWTPs). The sewage sludge can be processed or treated through anaerobic digestion, aerobic digestion, alkaline stabilisation, or composting to stabilise the organic material, reduce contaminants, and make it safe for handling (Canadian Council of Ministers of the Environment, 2012; Fitzmorris et al., 2009; Sivarajah et al., 2023). Biosolids are employed to maintain soil health and productivity by providing nutrients and organic matter while facilitating the recycling of organic wastes (Collivignarelli et al., 2019). Biosolids have been implemented in agricultural practices for over thirty years in Europe, the US, and Canada, enhancing soil fertility and recycling organic wastes towards a circular economy (Lebeau, 2023). Despite the agronomic benefits of biosolids, their role in introducing MPs to agricultural soils raises significant concerns regarding their long-term environmental impact and soil health implications.

WWTPs become contaminated with MPs from stormwater or domestic and industrial sources, and it has been estimated that in Vancouver, Canada, approximately 1.76 ± 0.31 trillion MPs enter one of their primary WWTPs annually (Gies et al., 2018). WWTPs then demonstrate high efficacy in MP removal, having between 97 and 99% removal rates retained in sewage sludge (Carr et al., 2016; Gies et al., 2018; Horton et al., 2021). A case study assessing the MP content of sewage sludge from 22 WWTPs across nine provinces in Canada found between 228 000 – 1 353 000 MP particles kg^{-1} with a median of 636 000 particles kg^{-1} (Sivarajah et al., 2023). Another study in Canada estimated that at a single WWTP, up to 1.28 ± 0.54 trillion MPs settle into primary sludge and 0.36 ± 0.22 trillion into secondary sludge annually (Gies et al., 2018). Similarly, in Spain, 183 000 ± 84 000 plastic particles kg^{-1} wet sludge and 165 000 ± 37 000 plastic particles kg^{-1} dried sludge were found (Edo et al., 2020). Also, in the UK, between 301 000 and 10 380 000 MPs kg^{-1} (dry weight) were found (Horton et al., 2021).

When sludges are then treated to become biosolids, MP concentrations have been shown to persist. In the UK, samples taken at multiple stages of the sewage treatment process, from wastewater to sewage sludge to processed biosolids, contained MPs at all stages, ranging from 37 700 – 286 500 MP particles kg^{-1} of sludge dry weight and 37 700 – 97 200 MP particles kg^{-1} biosolids dry weight (Harley-Nyang et al., 2022). A case study by Letwin et al. (2024) assessed the MP load of biosolid samples processed using liquid, dewatered, pelletised, and alkali-stabilised biosolids, from 11 sources across southern Ontario and found all samples to contain MP concentrations ranging from 188 200 (± 24 161) to 512 000 (± 28 571) MPs kg^{-1} dry weight and from 4122 (± 231) to 453 746 (± 38 194) MPs kg^{-1} wet weight. Similarly, Crossman et al. (2020) found between 8700 and 14 000 MPs kg^{-1} biosolids and estimated that between 410 trillion and 1 trillion 300 billion MPs kg^{-1} are added to agricultural soils annually with current guidelines in Ontario, Canada. These findings highlight the presence of MPs throughout wastewater treatment processes, raising concerns over their introduction into agricultural soils when biosolids are land-applied as organic amendments. However, no regulatory guidelines currently exist to monitor or limit MP presence in biosolids intended for land application.

2.5 CHEMICAL ADDITIVES IN MICROPLASTICS

Plastics are engineered products, and during manufacturing, they are often blended with other synthetic polymers and additives to enhance their properties (Marturano et al., 2017). Additives are essential in plastics production, enhancing durability, flexibility, heat resistance, and processing efficiency. However, their composition is highly variable, as manufacturers put proprietary blends of substances into plastic resins, making comprehensive identification of all plastic-associated chemicals difficult (McKeen, 2023). In addition, combining multiple compounds can often lead to non-intentionally added substances (NIAS), including impurities, breakdown products, and reaction by-products, further complicating plastic composition and potential environmental impacts (Groh et al., 2019).

Additives can be broadly classified into fillers, plasticisers, flame retardants, colourants, stabilisers, lubricants, foaming agents, and antistatic agents, listed in decreasing order of tonnage used (Groh et al., 2019). The grouping of stabilisers further encompasses several other categories with more specific functions, such as antistatic additives, antimicrobials, UV stabilisers, thermal stabilisers, and antioxidants (Groh et al., 2019; McKeen et al., 2019). There are also many other additives used in lesser amounts, such as catalysts, optical brighteners, pigment extenders, dyes, combustion modifiers, nucleating agents, oxygen scavengers, odour absorbers, and desiccants (Groh et al., 2019; McKeen, 2014). Plasticisers are the most abundant additives, predominantly comprised of phthalic acid esters (PAEs), a group of synthetically produced compounds, and short, medium, and long chains of chlorinated paraffins (SCCP/MCCP/LCCP), used to increase the durability and flexibility of plastics (Groh et al., 2019; Hahladakis et al., 2018). Fillers, the second most abundant additive group, reduce manufacturing costs and improve mechanical properties by incorporating materials such as clay, talc, mica, calcium carbonate, kaolin, and barium sulphate (McKeen, 2014). While, flame retardants, including brominated and chlorinated flame retardants (BFRs/CFRs), are widely used in plastics to reduce flammability (Hahladakis et al., 2018).

A significant concern with plastic additives is that, in nearly all instances, they are not covalently bound to the plastic polymer matrix, making them susceptible to leaching into surrounding environments throughout the plastics lifecycle (Hahladakis et al., 2018). Zimmermann et al. (2021) examined the aqueous migration of chemical additives from 24 common plastic items representing eight polymer types (HDPE, LDPE, PET, PS, PP, PVC, PUR, PLA) after 10 days of incubation at 40°C. The study detected between 17 and 8,681 chemical migrates, of which only 8% were identifiable, highlighting the extensive list of unknown chemicals accompanying plastics that are readily leached.

Examples of leached chemicals include but are not limited to BPA, shown to continually leach from PC plastics while being readily adsorbed and desorbed by LDPE in aquatic matrices (Sajiki & Yonekubo, 2004; Sun et al., 2021); different phthalates such as di-n-octyl phthalate (DOP), diethyl hexyl phthalate (DEHP), dimethyl phthalate (DMP), benzyl butyl phthalate (BBP), and di-n-butyl phthalate (DnBP), shown to readily leach from PVC into aquatic matrices and can make up to 28.76% of the plastic by weight (Andjelković et al., 2021); polybrominated diphenol esters (PBDEs), numerous PAE's, and antimony, all shown to leach from PE plastics in aquatic matrices (Shotyk & Krachler, 2007; Andra et al., 2012); BFRs are amply detected in leachates from landfills as well in laboratory testing (Kim et al., 2006); heavy metals like cadmium (Cd), tin (Sn), and lead (Pb) are released from PVC pipes when exposed to UV-radiation and or acidic environments >50 times the maximum permissible levels set by the US environmental protection agency (USEPA) (2022) (Al-Malack, 2001); and formaldehyde and acetaldehyde, known to readily leach from PET plastics in an aquatic matrix and persist

(Mutsuga et al., 2006); as well, benzene has been shown to continuously leache from PS (Ahmad & Bajahlan, 2007).

Many of these additives associated with plastics are currently classified as potentially toxic substances (PoTSs), an abbreviation introduced by Hahladakis et al. (2018) to address the uncertainties surrounding plastic additives, as they need to be released or leached before any toxicity is expressed. The United Nations Environmental Programme (UNEP) (2023) highlighted these concerns in its technical report on the chemicals in plastics, identifying over 13,000 chemicals associated with plastics, of which 7000 have been studied extensively, and more than 3,200 have been identified as substances of potential concern. Given the widespread presence of these additives in plastics, understanding toxicological impacts on soil systems is essential to maintaining soil health and food safety.

2.6 TOXICOLOGICAL EFFECTS OF MICROPLASTICS

MPs themselves are not inherently toxic but are a contamination pathway for hazardous chemical additives, facilitating their transport and release and raising concerns about bioavailability and toxicity. MPs have been found to move from soil with concentrations of 870 ± 1900 particles kg^{-1} to earthworm cast with 14 800 ± 28 800 particles kg^{-1} to chicken gizzards with 10 200 ± 13 800 particles kg^{-1} (Huerta Lwanga et al., 2016). Demonstrating the potential for significant trophic transfer of MPs and, consequently, PoTSs.

Earthworms are widely used for soil health assessments as bioindicators to provide insights into pollutant uptake and toxicity. When earthworms have been exposed to MPs, adverse effects have been seen on the growth, behaviour, oxidative stress response, gene expression, and gut microbiota (Cui et al., 2022). A study was performed by Gaylor et al. (2013) to assess the accumulation of plastic additive polybrominated diphenyl ether (PBDE), a brominated flame retardant, in earthworms. Earthworms were exposed to artificial soil containing sand, kaolinite, peat moss, and dolomite, which was spiked with either PBDE or PU foam MPs, anaerobically digested biosolids (ADB), or composted biosolids (CB) in increasing concentrations. Earthworms exposed to PU foam MPs for 28 days showed PBDE burdens up to 3740mg/kg lipid levels. Similar responses were seen in both CB and ADB treatments, and after 28 days, lipid PBDE burdens were 5-fold higher.

This study demonstrates the significant bioavailability of a PoTS associated with plastics using a brominated flame retardant and the possibility of bioaccumulation.

From an agricultural perspective, the toxicological threat of MP contamination is food contamination and adverse effects on human health. For example, phthalic acid esters (PAEs), a common plasticiser, are now the most abundant chemicals humans are in contact with and are prevalent in all environmental compartments (Net et al., 2015). In humans, phthalates are documented carcinogens and endocrine disruptors which are linked to obesity (Lind et al., 2012), allergies and asthma (Bertelsen et al., 2013), decreased sperm counts and quality (Duty et al., 2003), low gestation age of a fetus and endometriosis (Latini et al., 2003). The in-vitro toxicity using a Microtox® assay, oxidative stress response using an AREc32 assay, and endocrine activity using a yeast-based reporter gene was performed on eight different polymer types (HDPE, LDPE, PET, PS, PP, PVC, PUR, and PLA) was performed by Zimmermann et al. (2021). In all cases, the leachates induced baseline toxicity in vitro, and the oxidative stress response was activated in response to all plastics except for HDPE and PLA. PVC was the only plastic found to leach estrogen receptor agonists. Meanwhile, PUR, HDPE, LDPE, and PVC exhibited androgen agonistic capabilities. Such effects raise significant concerns for food and nutritional safety.

2.7 MICROPLASTIC FRAGMENTATION AND PERSISTENCE

Plastics are highly resistant to degradation. Even under optimum laboratory conditions, the degradation of plastics is limited, and plastics can persist for centuries once in marine and terrestrial environments (Chamas et al., 2020). Rather than degrade, plastics change physically and chemically when exposed to environmental factors called weathering; the terms weathering, fragmentation, degradation, and ageing are often used interchangeably in the literature. Environmental factors include UV exposure, mechanical abrasion, and microbial degradation, leading to surface oxidation (Stapleton et al., 2023; Zhang et al., 2021). As a result, plastics undergo structural weakening, becoming brittle and fragmenting when exposed to these environmental conditions, leading to secondary MP particles and beyond into nanoparticle sizes (Pfohl et al., 2022). A depiction of the weathering process of MPs is seen in Figure 2, showing the progressive structural degradation and fragmentation (Andrady et al., 2017). There is currently no theoretical limit to how small synthetic plastics can fragment aside from reaching the molecular level.

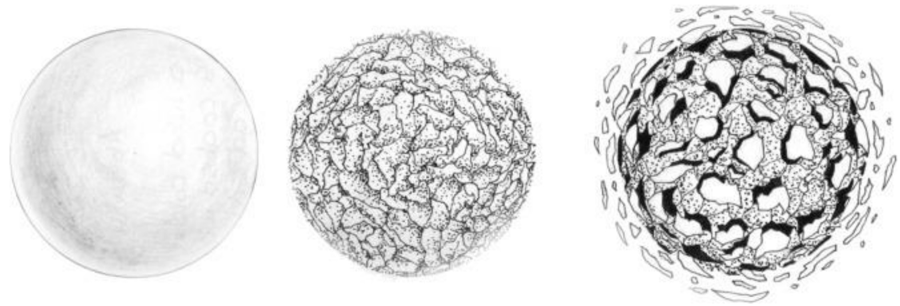

Figure 2. Depiction of MP fragmentation process taken from Andrady et al. (2017); left: particle as produced, middle: weathered particle displaying surface cracking, and right: fragmented surface layer of the particle.

These structural changes increase the relative surface-to-volume ratios of the particles and increase porosity (Andrady et al., 2017; Guo et al., 2020). As a result, weathering of polymers enhances the leaching of plastic additives (Luo et al., 2022a). It also makes them highly susceptible to sorption and desorption processes, allowing them to act as vectors for persistent organic pollutants (POPs), heavy metals, and other environmental pollutants, potentially transporting them and increasing their persistence (Fajardo et al., 2022; Hahladakis et al., 2018). Additionally, as MPs fragment, their bioavailability increases, perpetuating their toxicological risks (Luo et al., 2022b). The combination of their high surface area, increased porosity, and ability to sorb and transport environmental contaminants raises concerns about their long-term implications for soil structure, food security and nutritional safety, and overall soil function.

2.8 MICROPLASTICS IN SOIL

Once MPs enter agricultural soils, they interact with soil components, biota, and crops, raising concerns about their long-term consequences. Unlike other pollutants, MPs are persistent contaminants due to their resistance to degradation and ability to fragment into smaller particles over time. These fragments can accumulate in soil, where their movement, persistence, and effects remain poorly understood. Their vertical and horizontal migration may be affected by several factors such as plastic-type, size, shape, bioturbation, soil texture, and agricultural practices such as tillage, seeding, irrigation, and crop rotation (Guo et al., 2020). These activities may facilitate the transport of MPs deeper into soils, promote fragmentation, potentially alter soil physicochemical properties, disrupt nutrient cycling, and impact soil biota.

2.8.1 Soil Properties

MP particles in the soil can alter key agronomic properties, including cation exchange capacity (CEC), pH, bulk density, porosity, water retention, nitrification, and aggregate stability (Boots et al., 2019; de Souza et al., 2018; Guo et al., 2020; Meng et al., 2022). The extent of these effects may be significantly influenced by MP type, size, shape, and abundance. Alterations to these properties have direct effects on soil fertility and crop production.

A study by Zhang & Liu (2018) investigating the abundance and distribution of plastic particles among soil aggregates found that 72% of MP particles are associated with soil aggregates, influencing soil structure and stability. For instance, when HDPE was introduced at a concentration of 0.1% w/w, soil aggregate stability declined, and pH decreased (Boots et al., 2019). In contrast, PP at a much higher concentration of 28% w/w increased dissolved organic matter (DOM) content, including dissolved organic carbon, nitrogen, phosphorus, nitrate, phosphate, and humic substances (Liu et al., 2017). MPs have also been shown to impact water infiltration and retention in clay and sandy soils by reducing soil pore size and altering soil aeration and hydraulic conductivity, with more pronounced effects in soils with higher organic content and larger MP particle sizes (Guo et al., 2022). When a sandy loam till was exposed to concentrations of MPs, either PMMA fibres, PA beads, PET fibres, or PE fragments up to 2% for 5 weeks, in all cases, there was a functional change between microbial activity and water-stable aggregates, with PET fibres increasing water holding capacity, while PE fragments, PMMA fibres, and PA beads all lowered bulk density (de Souza Machado et al., 2018). These findings suggest that MP particles' impacts are highly context-dependent, driven by MP size, shape, abundance, and local soil conditions. Such changes could directly affect plant available water, increasing the susceptibility of soils to drought stress and reducing crop yield.

2.8.2 Soil Biota

Soil biota is essential in maintaining soil structure, decomposing organic matter, and driving nutrient cycling, all of which are critical for the proper function of soil ecosystems. However, the presence of MPs introduces new ecological stressors, particularly for larger soil fauna that can ingest MPs, which can cause internal abrasions, energy depletion, inhibited development, and even mortality (Costa et al., 2018; Cui et al., 2022). Additionally, soil fauna can contribute to MPs distribution and further fragmentation through ingestion and excretion, creating secondary MPs of varying shapes and sizes and amplifying their impact on soil physicochemical properties (Waldman & Rillig, 2020). The ingestion of particles also exposes organisms to toxic chemicals, as discussed previously.

MPs may also influence soil microbial communities, providing new surfaces for microbial colonization by forming a terrestrial plastisphere that alters microbial community composition (MacLean et al., 2021). This may alter soil microbial communities by increasing microbial biomass but decreasing overall microbial diversity (Li et al., 2023; MacLean et al., 2021). Soil matrix characteristics like texture and porosity may influence the interactions between MPs and soil biota. For instance, changes in soil porosity may alter oxygen flows and influence the distribution of aerobic and anaerobic populations (Guo et al., 2020). Below-ground microbial communities regulate aboveground plant-soil interactions through tropic connections that regulate plant health, nutrient cycling, and broader ecosystem stability (Bardgett & van der Putten, 2014). These changes may have unforeseen consequences for microbial-driven nutrient cycles, directly impacting soil fertility and plant growth.

2.8.3 Agricultural Crops

The addition of MPs to soil may negatively affect plant growth and development. A study on perennial ryegrass (*Lolium perenne)* by Boots et al. (2019) found that after 30 days of exposure to PLA at 0.1% w/w and 10mg kg^{-1} MP fibres, a 6 and 7% reduction in germination rates were observed, respectively, and lower shoot heights were seen with PLA exposure. Similarly, Dong et al. (2022) found measurable reductions in seed germination of rapeseed (*Brassia campestris L.*) when exposed to PMMA. Further, studies indicate MPs accumulate in roots and reduce root elongation and dry biomass production (Jia et al., 2023). PE and PP MPs both inhibited the shoot extensions of amaranth (*Amaranthus mangostanus L.*), while PP reduced root length to a greater extent (Wang et al., 2023). In addition to potentially hindering growth, fruits and vegetables such as carrots, lettuce, and apples have been shown to contain MPs (<10 μm) ranging from 52,050 to 233,000 particles g^{-1} (Conti et al., 2020). Providing a direct mode of transportation for chemical additives and other soil contaminants to enter the food chain. Studies like these reveal the potential of MPs to hinder crop growth and productivity and contaminate produce, reducing agricultural outputs and directly contaminating food, threatening food and nutritional security.

2.9 ANALYTICAL METHODS AND METHODOLOGICAL CHALLENGES

Accurately analysing MPs in complex matrices such as soils remains methodologically challenging due to the heterogeneous nature of soils and MPs varied physical and chemical properties (Crossman et al., 2020; Groh et al., 2019). Currently, there is no standardised protocol for MP extraction and identification from soil, leading to variability between studies and an inability to compare results or methods directly. Most methodologies follow a multi-stage process, which generally includes organic matter removal, plastic extraction, and plastic identification. Each step presents unique challenges, particularly when working with complex matrices like biosolids and soils.

2.9.1 Organic Matter Removal

Any non-plastic material, particularly SOM, can interfere with sample analysis and should be removed. SOM and plastics share similar densities (0.9 -1.6g cm^{-3}), making density-based separation difficult (Thomas et al., 2020). In addition, plastic particles can be embedded within soil aggregates, reducing extraction efficiency if organic matter is not removed first (Zhang & Liu, 2018). Plastic recovery efficiencies have consistently been lower in studies using organic-rich soils (Radford et al., 2021). Reagents that can be used to reduce organic matter include hydrogen peroxide (H_2O_2), Fenton's reagent, an alkaline digestant of sodium hydroxide (NaOH) or potassium hydroxide (KOH), or an acid digestant like hydrochloric acid (HCl), nitric acid (HNO_3), or sulfuric acid (H_2SO_4) (Li et al., 2020). However, strong alkaline reagents have been shown to degrade nylon, polyethene (PE) fragments, polystyrene (PS), polycarbonate (PC), and polyethene terephthalate (PET) (Cole et al., 2014; Hurley et al., 2018; Tan et al., 2022). Fenton's reagent is widely used but is highly exothermic and has been recorded at temperatures exceeding 80ºC, potentially degrading plastic particles (Hurley et al., 2018; Radford et al., 2021). The choice of reagent, therefore, requires a trade-off between maximising organic matter removal and preserving the plastic portion of the sample. A comparison of organic removal efficiencies and polymer degradations using similar methodologies in soil samples can be found in Appendix A, Table A9.

2.9.2 Density Separation

Density separation is the most widely used MP extraction technique, exploiting the low density of plastics relative to soil minerals (Thomas et al., 2020; Kadac-Czapska et al., 2023). The success of this method depends on selecting a suitable brine solution with an appropriate density range to float MPs while retaining heavier soil particles. The densities of common synthetic polymers are shown in Table 2 (Grigorescu et al., 2019; Tan et al., 2022), and the densities of the most utilised solutions are shown in Table 3 (Quinn et al., 2017; Thomas et al., 2020; Withana et al., 2024).

Table 2. Densities of common synthetic polymer types.

Plastic Type	Abbreviation	Density g/cm^{-3}
Polypropylene	PP	0.90-0.91
Low-density polyethene	LDPE	0.91-0.93
High-density polyethene	HDPE	0.94-0.97
Acrylonitrile butadiene	ABS	0.99-1.10
Polystyrene	PS	1.04-1.07
Acrylonitrile styrene	AS	1.070
Polyurethane	PU	1.080
Polyamide	PA	1.140
Polycarbonate	PC	1.200
Poly methyl methacrylate	PMMA	1.200
Polylactide	PLA	1.21-1.43
Polyethene terephthalate	PET	1.38-1.39
Polyvinyl chloride	PVC	1.35-1.45

Table 3. Densities of commonly used saturated solutions.

Density Solution	Abbreviation	Density g/cm^{-3}
Water	H_2O	1.0
Sodium chloride	NaCl	1.2
Calcium chloride	$CaCl_2$	1.3-1.5
Sodium bromide	NaBr	1.4-1.6
Zinc chloride	$ZnCl_2$	1.5-1.8
Sodium Iodide	NaI	1.8
Zinc bromide	$ZnBr_2$	1.7- 4.2

Density solutions such as H_2O, NaCl, and $CaCl_2$, have been widely used but have a limited density, reducing their ability to separate denser MP polymers like PET and PVC (Grause et al., 2022; Quinn et al., 2017; Radford et al., 2021). While higher-density solutions like zinc chloride $ZnCl_2$ have been shown to improve extraction efficiency more than 15 times when compared to lower-density solutions like NaCl (Mattsson et al., 2022). However, $ZnCl_2$ is costly and requires stringent handling protocols due to environmental and health hazards (Han et al., 2023).

When selecting an optimal solution, key considerations like environmental toxicity and reusability should be considered in addition to density. Unfortunately, not many studies focus on these additional factors. To consider toxicity, the LD_{50} (oral-rat) of solutions can be ranked: $ZnCl_2$ (350 mg/kg) > $CaCl_2$ (1000 mg/kg) $ZnBr_2$ (1447 mg/kg) > NaCl (3000 mg/kg) > NaBr (3500 mg/kg) > NaI (4340 mg/kg). In terms of reusability, Li et al. (2021) tested NaBr and found that reusing it up to five times had no adverse effect on plastic recovery rates. Unfortunately, the reusability of other solutions is unknown. Selecting the best solution will differ depending on the specific research needs, balancing MP recovery rates, environmental safety, reusability, and cost. A comparison of the efficiencies of each solution using similar methodological techniques for MP extraction in soil can be found in Appendix A, Table A10.

2.9.3 Microplastic Identification

Following organic matter removal and density separation, multiple analytical techniques have been applied to characterise MPs in soil both physically and chemically. However, no single method provides a comprehensive analysis due to variations in polymer types, degradation states, and matrix interferences. As a result, MP analysis typically requires a combination of non-destructive techniques, which assess the size, shape, color, and particle count, and destructive techniques, which provide polymer identification.

Microscopy

Stereomicroscopy remains one of the most widely used approaches for MP analysis due to its accessibility and utility in providing three-dimensional images using reflected light (Mariano et al., 2021). This method has successfully been used to identify MP abundance, size, shape, and colour (Crossman et al., 2020; Letwin et al., 2023; Mercy et al., 2023). However, it lacks the resolution to confidently detect particles below 100 µm, increasing the risk of misidentification (Schell et al., 2022; Zhang et al., 2023). With small particles consistently being reported as challenging to capture and analyse (Blair et al., 2019; Harley-Nyang et al., 2022; Wang et al., 2024b). To improve accuracy, fluorescence microscopy is often employed by staining MPs with Nile Red (NR), a hydrophobic dye that enhances MP visibility (Çelen Erdem et al., 2023; Grause et al., 2022; Meyers et al., 2022; Nalbone et al., 2021). NR is typically chosen over other dyes as it has a high affinity for hydrophobic plastics, a wide excitation wavelength range, and does not interfere with subsequent chemical analysis (Maes et al., 2017). NR-based methods have been reported to increase MP identification to between 80–87% accuracy (Gerigny et al., 2024). However, microscopy-based methods cannot confirm polymer chemical composition and are often paired with spectroscopic or thermal analysis for chemical information. An overview of the advantages and limitations of different microscopy techniques for MP analysis can be found in Appendix A, Table A11.

Spectroscopy

Spectroscopic methods such as Raman and Fourier-transform infrared (FTIR) spectroscopy provide chemical fingerprinting of MPs, allowing differentiation based on polymer composition by identifying polymer-specific vibrational signatures (Mariano et al., 2021). Raman spectroscopy irradiates samples with laser radiation, causing inelastic scattering that generates spectra corresponding to specific atomic bonds (Ribeiro-Claro et al., 2017). Conventional Raman detects MPs down to 10 μm, but micro-Raman (μ-Raman) extends detection to 1 μm (Mariano et al., 2021). However, organic matter interference can limit its effectiveness. FTIR spectroscopy measures infrared absorbance and identifies molecular vibrations (Huang et al., 2023). Attenuated total reflectance (ATR-FTIR) works well for MPs >500 μm, whereas micro-FTIR (μ-FTIR) is required for MPs down to 10 μm (Mariano et al., 2021). FTIR struggles with small particle sizes and is also hindered by the presence of organic matter. Both FTIR and Raman are powerful identification tools but require extensive sample pre-treatment to isolate MPs. They also require spectral reference libraries to identify materials based on their unique spectral ‘fingerprint’, presenting challenges with the identification of novel materials such as weathered MPs. Spectroscopic techniques are not used as stand-alone techniques as they cannot determine particle abundance, size, or shape. Instead, they are used to supplement other analyses by chemically identifying polymer types.

Thermal Analysis

Thermal analysis methods, such as thermogravimetric analysis (TGA) and differential scanning calorimetry (DSC), offer key advantages for polymer identification in complex matrices. TGA measures mass loss as a function of temperature, providing polymer decomposition profiles that help distinguish synthetic materials from natural organic matter (Mariano et al., 2021). DSC, on the other hand, detects enthalpy changes by measuring heat flux during phase transitions, aiding in the identification of material-specific thermal events (Majewsky et al., 2016). While TGA and DSC alone lack specificity in distinguishing individual MP types in complex matrices, their strength lies in their ability to be paired with evolved gas analysis (TGA-FTIR or TGA-DSC-FTIR). This integration allows for the real-time transfer of evolved gases via a heated line to an FTIR detector, where the chemical signature of polymer degradation products can be identified. For instance, TGA-FTIR successfully identified PS and PVC MPs in seawater (Yu et al., 2019), while TGA-DSC has been applied to detect PP and PE in wastewater effluent (Majewsky et al., 2016). Further, TGA-DSC was used to identify a broad range of polymers, including PP, PS, PET, nylon, PE, and PVC, in water samples (Abbasi et al., 2023). Despite its successful application in aquatic environments, TGA-based methods have not yet been widely adopted in soil analyses. However, their ability to decompose organic matter and differentiate MPs based on degradation temperature makes them highly promising for soil matrices, where organic interference is a significant challenge. Additionally, detecting gas-phase degradation products can help identify MPs that are too small to be visually isolated and analyzed by traditional techniques.

CHAPTER 3: OBJECTIVES AND HYPOTHESIS

The study of MPs in terrestrial environments is gaining much-needed attention, although significant gaps in knowledge remain. Laboratory studies have made notable progress in exploring the properties of MPs, yet long-term field studies are still lacking. Key knowledge gaps include defining MP long-term presence, accumulation, persistence, and movement within soil systems. Further, few studies have connectedly measured MP shape in combination with size in a soil environment and provided actionable data. This study aims to investigate the long-term presence, persistence, and vertical movement of MPs in agricultural soils amended with ATBs. The specific objectives of this research are:

1. Quantify and characterise (size, shape) MP content within ATBs used in agricultural applications to determine their role as a source of MPs in soil.
2. Quantify and characterise (size, shape) MP content within agricultural soils that have received ATB applications.
3. Assess the long-term accumulation and persistence of MPs in soil following ATB applications to identify soil as a potential MP sink.
4. Evaluate the vertical movement of MPs in soil profiles after ATB applications to assess soils as a MP sink.
5. Chemically identify MP polymers in ATBs and soil that has received ATB applications using TGA-DSC-FTIR.

The hypotheses of this study are that the long-term repeated application of ATBs will result in the accumulation and vertical movement of MPs in agricultural soils; if ATBs are land applied at higher treatment rates, then the amount of MP accumulation and vertical movement will increase; if vertical movement of MP is observed, then MP size and shape will be a significant factor; and if ATBs are land-applied only once, MP presence will not accumulate but persist for long periods.

Establishing long-term MP abundance, accumulation, and distribution in soils, mainly owing to an established and commonly used agricultural amendment, will yield actionable data, deepening our understanding of MP presence and behaviour in soil matrices. Such research is imperative to filling these knowledge gaps and assessing the implications for soil health, ecosystem function, and global food security.

CHAPTER 4: MICROPLASTIC ACCUMULATION, PERSISTENCE AND VERTICAL MOVEMENT IN AGRICULTURAL SOIL AMENDED WITH ALKALINE-TREATED BIOSOLIDS

ABSTRACT

Microplastics (MPs) are emerging contaminants in agricultural soils, with biosolid amendments serving as a major source. This study quantified MPs in alkaline-treated biosolids (ATBs), finding an average of 138 600 (117 444, 159 757) MP particles kg^{-1} of ATB (dry weight), predominantly fragments (84%), followed by fibres (13%), and then spheres (3%). Using archived soil samples over 15 years, MP accumulation and persistence were evaluated under different application rates (0, 14, 42 tonnes ATB (wet weight) ha^{-1}) and management practices (single vs. annual). Vertical movement (0-100 cm) was also evaluated using archived soil samples after 13 years of different application rates (0, 14, 42 tonnes ATB (wet weight) ha^{-1}) and management practices (single vs. annual). Results revealed significant MP accumulation in surface soils, with vertical migration decreasing as soil depth increased. Annual ATB applications led to a cumulative effect, while even a single application showed long-term MP persistence. Smaller MPs permeated to deeper soil layers, indicating preferential migration. These findings underscore the need for improved biosolid treatment processes and regulatory frameworks to mitigate MP contamination in agricultural soils and protect ecosystem health.

KEYWORDS

Agriculture; Alkaline-Treated Biosolids (ATBs); Microplastics; Soil contaminant

HIGHLIGHTS

- MPs in ATBs averaged 138 600 (117 444, 159 757) MP particles kg^{-1} of ATB (dry weight).
- Repeated ATB application led to MP accumulation in the surface soil (0-15 cm), with an 8.7x increase in MP abundance at 14 tonnes ha^{-1} over 15 years.
- MPs persisted in soil beyond the initial ATB application, with measurable increases in single-application and control plots.
- Vertical movement of MPs was observed, with smaller particles preferentially migrating deeper into the soil profile.
- Agricultural soil is a sink of MP contamination and a source to surrounding environments.

4.1 INTRODUCTION

Conventional agriculture can gradually lose soil nutrients and soil organic matter (SOM), a dynamic and highly heterogeneous mixture of plant- and animal-derived litter at different stages of decomposition (Canadian Council of Ministers of the Environment, 2012; Thomas et al., 2020). Maintaining SOM is a significant challenge in the agricultural sector but is necessary to maintain crop productivity; too little can result in soil compaction, erosion, and desertification due to changes in soil structure (Fließbach et al., 2007; Osman, 2014). To combat this gradual loss of SOM, organic amendments are often used, many of which are recycled organic wastes, such as manure, compost, and treated sewage sludges (i.e. biosolids), all shown to increase SOM, improve soil structure, water infiltration and retention, and reduce the need for synthetic and inorganic fertilisers (Tian et al., 2013; Lin et al., 2019; Wright et al., 2022).

Biosolids are the treated solid by-product, or sewage sludge, from wastewater treatment plants (WWTPs). The treatment aims to stabilise the organic material, reduce contaminants, and make it safe for handling and use so that the nutrients and organic matter that are beneficial for soil health and productivity can be utilised (Canadian Council of Ministers of the Environment, 2012). Sewage sludge treatment can be done by implementing various methods, including anaerobic digestion, aerobic digestion, alkaline stabilisation, and composting (Fitzmorris et al., 2009; Sivarajah et al., 2023). Depending on the remaining pathogen and heavy metal content, biosolids are classified as either Class A, which contain pathogens below detectable limits and are safe for unrestricted use in agriculture or Class B, which contain reduced levels of pathogens and have restricted use as soil amendments, typically requiring buffer zones and limited public access (Canadian Council of Ministers of the Environment, 2012).

However, the land application of biosolids has been scrutinised for ongoing concerns over emerging contaminants, such as pharmaceuticals, musks, industrial chemicals, and more recently, microplastics (MPs); MPs are defined as pieces of synthetic polymers (plastic) smaller than 5 mm (Hartmann et al., 2019). This research aims to quantify and characterise MP contamination within ATBs and then characterise MPs by size and shape, both over time and vertically, within agricultural soil after ATB application. MP accumulation will be determined from a research site receiving annual applications of

ATBs at different application rates over a 15-year timeframe. MP persistence will be determined from the same research site where only a single application of ATBs occurred, at different application rates, and with no additional biosolid applications over a 15-year timeframe. The vertical movement of MPs in the soil will be assessed using a 1 m soil core taken 13 years after either the annual or single application of ATBs at different treatment rates. The objectives of this study are to determine if soils act as a long-term sink with the accumulation and vertical movement of MPs.

4.2 MATERIALS AND METHODS

4.2.1 Site Description

In 2008, a long-term field study was initiated at the Bio-Environmental Engineering Complex (BEEC), an environmental management research site associated with the Faculty of Agriculture, Dalhousie University, located in Bible Hill, Nova Scotia, Canada (45°23’19.8 “N 63°14’02.9” W). The soil at the site is classified as an Ortho-Humic Podzol and is described as a highly acidic, reddish-brown sandy loam till (Price et al., 2015).

The biosolids field study consists of an 82 m x 60 m section of agricultural field designated for research purposes. The allocated land was subdivided into four blocks containing 12 treatment plots. Each plot measures 5 m x 12 m, with a 2 m buffer between plots and a 4 m buffer between blocks. The treatments applied at the site include an alkaline-treated biosolid (ATB) obtained from the Halifax Biosolids Facility, operated by Walker Industries Ltd., located in Halifax, Nova Scotia, Canada. ATB from this facility is generated from municipal sources and treated by the N-Viro™ process, a patented stabilisation process using a second residual stream (cement kiln dust) for alkalinity that produces Class A municipal biosolids. A schematic of the patented N-viro process can be found in Appendix C, Figure 1C. A pelletised dolomitic lime treatment was also applied, sourced from Shaw Resources Inc. in Shubenacadie, Nova Scotia, Canada.

A split-plot randomised complete block design was used, with two management practices: ‘single’ and ‘annual.’ The ‘single’ application plots received ATB treatments at the beginning of the study, split over the fall of 2008 and spring 2009, with no further applications thereafter, while the ‘annual’ plots similarly received ATB treatment applications each year, from 2008 onwards to the present day. The rates of ATBs were initially based on an agronomic recommendation for nitrogen in Nova Scotia for growing corn, which suggested a rate of 14 tonnes of ATB ha^{-1} (Price et al., 2015). In total, six treatments were applied for each management practice: a lime treatment of 2 tonnes ha^{-1} and ATBs at a half rate of 7 tonnes ha^{-1}, a full rate of 14 tonnes ha^{-1}, a double rate of 28 tonnes ha^{-1}, and a triple rate of 42 tonnes ha^{-1}. Treatments were weighed, uniformly spread over the plot by raking, and tilled to a depth of ~10 cm each year using a tractor-mounted rototiller.

The site was initially cropped to soybean (*Glycine max*) in 2008, prior to ATB treatment applications. After the fall of 2008 harvest, half of the assigned biosolid rates were applied to each plot. The second half of the biosolid rates were applied in the following spring of 2009, after which the plots were cropped to corn (*Zea mays*). All subsequent applications were full-rate, applied each spring, except for 2020, when treatments were not applied due to the COVID-19 pandemic. The cropping sequence continued as follows: corn from 2009 to 2012, barley (*Hordeum vulgare*) from 2013 to 2015, soybean in 2016, corn from 2017 to 2021, soybean in 2022, and corn in 2023.

4.2.2 Sample Collection and Storage

Sampling was conducted over the growing seasons, once in the spring pre-plant, before annual treatment applications, and then repeated monthly until post-harvest. The samples used in this study were collected from the final post-harvest sampling event each year. Soil samples were collected using a soil corer with a 1.9 cm radius to a depth of 0 to 15 cm. A systematic sampling approach was employed to gather 10 soil cores strategically from all areas within each plot and combine them to form a 10-core composite sample for each plot. Once collected, samples were air-dried in a greenhouse for more than 72 hours. Once dry, the samples were sieved using a Cole-Palmer brass sieve with a 2mm mesh and stored in a soil archive for future analysis. At the end of the 2021 sampling season, a deeper soil core was taken from the centre of each plot, reaching an approximate depth of 100 cm, depending on soil compaction. This core was then separated into the following depths: 0-15, 15-30, 30-60, and > 60 up to 100 cm. The deeper soil core samples were handled identically to the annual samples and stored in the soil archive for future analysis. Additionally, ATBs were subsampled annually and frozen for future analysis. However, not all years' samples were available; due to a fire on June 20th, 2018, many samples thawed and were discarded. To analyse MP content, 10g of soil was subsampled from the soil archive for each plot, a portion of each ATB was thawed and dried, and 2g was subsampled.

4.2.3 Experimental Design

<table>
<tr><td>37
S
14</td><td>38
S
42</td><td>39
S
0</td><td>40
S
7</td><td>41
S
Lime</td><td>42
S
28</td><td>43
A
14</td><td>44
A
Lime</td><td>45
A
7</td><td>46
A
0</td><td>47
A
28</td><td>48
A
42</td></tr>
<tr><td colspan="12">**Buffer**</td></tr>
<tr><td>25
A
Lime</td><td>26
A
14</td><td>27
A
28</td><td>28
A
42</td><td>29
A
0</td><td>30
A
7</td><td>31
S
Lime</td><td>32
S
42</td><td>33
S
14</td><td>34
S
28</td><td>35
S
7</td><td>36
S
0</td></tr>
<tr><td colspan="12">**Buffer**</td></tr>
<tr><td>13
A
42</td><td>14
A
Lime</td><td>15
A
7</td><td>16
A
14</td><td>17
A
28</td><td>18
A
0</td><td>19
S
28</td><td>20
S
7</td><td>21
S
14</td><td>22
S
0</td><td>23
S
42</td><td>24
S
Lime</td></tr>
<tr><td colspan="12">**Buffer**</td></tr>
<tr><td>1
S
28</td><td>2
S
0</td><td>3
S
14</td><td>4
S
Lime</td><td>5
S
7</td><td>6
S
42</td><td>7
A
7</td><td>8
A
0</td><td>9
A
42</td><td>10
A
Lime</td><td>11
A
14</td><td>12
A
28</td></tr>
</table>

Figure 3. Split-plot randomised complete block design of the field site with treatment rates (2 tonnes ha^{-1} lime or 0, 7, 14, 28, 42 tonnes ha^{-1} ATBs (wet weight) indicated by the number of tonnes added or lime. Annual management practice plots (A) are shown in darker green, while single application plots (S) are represented in lighter green. Treatment plots that were sampled are indicated by bolded boxes.

To evaluate the number of MPs, their size, and shape in the soil surface over time from the addition of ATBs, a split-plot randomised complete block design with four blocks of six treatments was used (Fig 3). A repeated measures approach was taken using the years 2008, 2014, 2016, 2021, and 2023, subsampling the post-harvest soil samples for the treatment rates 0, 14, and 42 tonnes ATB (wet weight) ha^{-1} for both management practices. Three hypotheses were tested using a repeated-measures approach:

1. If ATBs are repeatedly land applied, then the number of MPs in the soil will increase;
2. If ATBs are land applied at higher treatment rates, then there will be an increased number of MPs in the soil with a higher application rate; and
3. If ATBs are land applied only once, then the number of MPs in the soil after a single application will persist over time.

To assess the number of MPs, their size, and shape vertically within the soil, the same split-plot randomised complete block design was used with the same treatment rates and management practices (Fig 3). Instead of a repeated measures design, a single sampling interval from 2021 using a deeper soil core separated into depths of 0-15, 15-30, 30-60, and > 60 up to 100 cm was used. Four hypotheses were tested:

1. If ATBs are land-applied, then MPs will move vertically within the soil;
2. If ATBs are land applied repeatedly and at increasing treatment rates, then there will be an increased number of MPs at deeper soil depths;
3. If there is MP vertical movement in the soil, then MP shape (fragment, fibre, and sphere) will be a significant factor; and
4. If there is MP vertical movement in the soil, then MP size will be a significant factor.

To investigate the number of MPs, their size, and their shape within the ATBs used in this study, a simple random sampling approach with two replicates was used. Archived ATB samples were subsampled from 2010, 2014, 2021, 2023, and 2024. This analysis was done to test the hypothesis that if the ATBs originate from the same facility, then the microplastic content will remain consistent over time.

4.2.4 Microplastic Extraction

The implementation of appropriate sample pre-treatment is essential for the effective extraction of MPs from environmental samples. MPs are highly variable in size, shape, and polymer type, which makes their extraction particularly challenging, especially when embedded within a complex soil matrix. SOM and plastic share similar densities (0.9 -1.6g cm^{-3}), and when density separation is performed first, the SOM is also extracted, obscuring the sample (Thomas et al., 2020). Notably, recovery rates of MPs decrease as the organic content of the sample matrix increases, and recovery efficiencies are consistently lower using organic-rich soils (Radford et al., 2021; Schütze et al., 2022). The variability in organic content and different grain sizes within soil presents challenges for obtaining clean MP samples suitable for analysis. To address these challenges, organic matter removal (i.) was performed as a critical first step to improve the efficiency of MP extraction and was followed by density separation (ii.) using a saturated saline solution to facilitate the floatation and extraction of MPs from the samples.

i. Organic Matter Removal

Organic matter removal was performed using 30% hydrogen peroxide (H_2O_2) from Fisher Scientific™. 30% H_2O_2 has been verified as an effective method of organic matter removal by demonstrating 96.3% +/- 14.9% removal rates at 60ºC by Hurley et al. (2018) and ~93% at 50ºC by Radford et al. (2021). Further, H_2O_2 was chosen over other reagents to preserve MP morphological characteristics, with other reagents reaching temperatures that compromise plastic integrity, such as Fenton's reagent or acids that degrade plastics (Hurley et al., 2018; Tan et al., 2022). The overnight treatment using 30% H_2O_2 was not reported to have caused any damage to plastic particles (Liebezeit and Dubaish, 2012).

To each 10 g of sub-sampled soil, 30 mL of H_2O_2 was added in a 32 oz wide-mouth mason jar, which was then placed on an orbital mixer set to 145 RPM for 2 hours. At the halfway point, or when the reaction visibly slowed, an additional 20 mL of H_2O_2 was introduced. Samples with higher organic content elicited more vigorous reactions, necessitating periodic stirring with a glass stir rod to prevent overflow and sample loss. The stir rod was then rinsed with additional H_2O_2 to negate sample loss. After the reaction was complete, the sides of the jar were rinsed with deionised (DI) water, and the samples were incubated in a laboratory oven at 60°C for 24 hours to dry completely. Allowing the sample to dry in the same container eliminated the need for filtration and/or transfer to a different apparatus for the subsequent density separation, reducing the potential for contamination or MP loss during handling.

ii. Density Separation

Density separation of MPs was conducted using a saturated sodium bromide (NaBr) solution. Sodium bromide has demonstrated effectiveness in separating MPs from solid matrices, with spiked sample recovery rates of 94.7% ± 10% and 83-87% being reported by Schütze et al. (2022) and Quinn et al. (2017) using PE, PP, PVC, PET, PLA, PBS, MB, and PP, LDPE, HDPE, PE, PS, nylon, PVC, and PET respectively. NaBr also poses minimal environmental risk compared to other solutions. Further, NaBr can be reused up to five times with no adverse effect on plastic recovery rates, making it less wasteful (Li et al., 2021).

A saturated solution of NaBr was generated by combining ≤99.0% NaBr purchased from Fisher Scientific™ with DI water in a 4 L Erlenmeyer graduated flask. The mixture was stirred on a magnetic stirrer at 200 RPM at 25°C for 1 hour while more solute was periodically added until no more could be dissolved. 100 mL of the saturated NaBr solution was then added along with a stir bar to each dried sample. The mixture was stirred vigorously for at least 5 minutes on a magnetic stirrer to ensure thorough homogenisation. Any dried residue visibly adhering to the sides of the jar was scraped clean using a rubber-tipped glass stir rod, which was then rinsed with additional NaBr solution. Once the samples were well mixed, they were left to settle undisturbed for 24 hours. Upon settling, the surface layer of the sample, encompassing the floating MPs, was carefully skimmed using a 1 oz metal ladle. A NaBr-loaded wash bottle was used to rinse both the ladle and the jar sides, ensuring the maximum possible recovery of MPs.

The collected material was transferred onto a 0.45 µm PVDF filter paper using a vacuum filtration unit. The NaBr collected from the vacuum filtration unit was then reused up to five times. Between uses, the solution's density was tested using a sub-sample and plastic particles of varying polymer types (HDPE, LDPE, PP, PS, PET, and PVC). If not all polymers readily floated, the solution was re-saturated. The filtered MPs were then labelled and stored in 90 mm × 15 mm Petri dishes, providing secure separation and storage for further analysis.

4.2.5 Nile Red Staining

The addition of Nile Red (NR) to the extracted sample was implemented to aid in the subsequent identification of plastic particles. NR is lipophilic and behaves like a fluorochrome, favourably binding to hydrophobic substances such as plastics, causing them to fluoresce under specific wavelengths of light. Additionally, NR exhibits solvatochromic and metachromatic properties, meaning the fluorescence emission can vary depending on its surroundings' polarity and molecular environment (Ghoneim, 2000). This means that the fluorescence is impacted by the plastic type, size, and shape, greatly facilitating the visualisation of plastics under microscopy. NR has been used successfully as an aid in the identification of MPs in biological samples from both terrestrial and aquatic vertebrates and invertebrates (Nalbone et al., 2021; Prata et al., 2021; Süssmann et al., 2024) and is increasingly being adapted for use in a range of mediums, including crop plant tissues (Çelen Erdem et al., 2023), commercial salts (Vittal et al., 2024), freshwater sediments (Chanda et al., 2025), and more.

Invitrogen™ Nile Red and 99+% acetone purchased from Fisher Scientific™ were utilised by combining 0.001 g with 10mL of acetone to create a 100 mg/L stock solution. Acetone was chosen as the solvent based on its availability and capacity to enhance fluorescence intensity, as Tamminga et al. (2017) demonstrated. The stock solution was then kept in an amber dropper bottle in a fridge at 4ºC to limit degradation. When the extracted MP samples were ready to be dyed, the stock solution was diluted 1/10th to a 10 mg/L solution for use, similar to Maes et al. (2017) and Prasad et al. (2024). 1 ml of the 10 mg/L NR solution was pipetted onto the filtered samples and left to dry at room temperature in the dark for 24 hours before they were ready for visualisation.

4.2.6 Stereoscopic Analysis of Microplastics

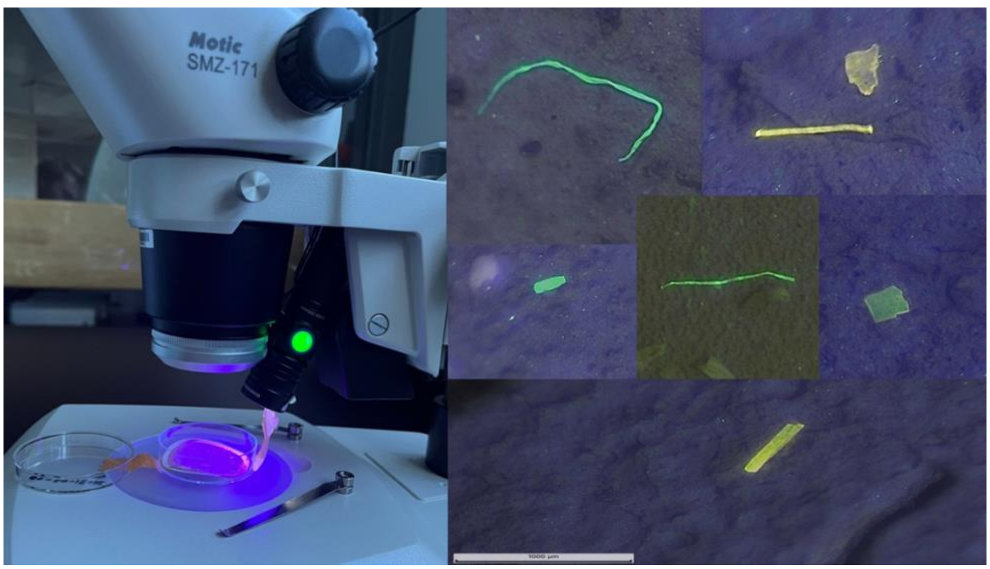

Figure 4. Left: Modified Motic SMZ-171 stereomicroscope equipped with a 300–395 nm wavelength UV flashlight for fluorescence excitation and a yellow gel light filter mounted on the objective lens to block blue light. Right: Visualisation achieved with a modified stereomicroscope demonstrating MPs of varying shapes and sizes in soil samples.

Stereomicroscopy is one of the most widely used and preferred methods for MP analysis, serving as the primary screening tool for the physical characterisation of particle size and shape. It has been applied across various matrices to identify MP particles, from aquatic environments and sediments to Antarctic snow (Blair et al., 2019; Aves et al., 2022; Kalaronis et al., 2022). The stereomicroscope provides a three-dimensional image by way of reflected light at different angles to obtain two images, generally between 3-50 times magnification (Mariano et al., 2021). Its ease of use, adaptability, and general availability make it an easily accessible entry point to fragmented polymer analysis.

To enhance fluorescence capabilities and visualise MP particles, a low-cost modification of a Motic SMZ-171 stereomicroscope was implemented (Fig 4). A 300-395nm wavelength UV flashlight served as the light source, inducing fluorescence in the NR-stained MP particles. Hengstmann & Fischer (2019) demonstrated that the use of a UV flashlight paired with NR is accurate, effective, and a faster alternative when compared to a fluorescent microscope, with over 90% identification accuracy of the stained particles, confirmed by μ-Raman spectroscopy. A yellow gel light filter was placed over the objective lens to block blue light, improving fluorescence contrast and reducing potential eye strain and damage while looking through the eyepiece. The entire filter paper was analysed using this setup.

4.2.7 Contamination Control

Measures were taken to minimise the contamination of samples with MPs throughout the duration of the study. Throughout the handling of samples, cotton clothing and Fisherbrand™ Nitrile gloves were worn to avoid the introduction of synthetic fibres and cross-contamination. All instruments and containers were thoroughly washed and rinsed with deionised (DI) water before use. Glass or metal instruments and containers were exclusively used to reduce contamination, and samples were covered with aluminium foil whenever possible to limit airborne contamination. Blank samples were included with every batch of analyses to monitor and account for potential contamination. On average, 4 MPs per blank were observed and consistently split between fibres and fragments. To correct this, 2 MPs were subtracted from both fibre and fragment counts in the results.

4.2.8 Limitations

This study was conducted using field-based samples in an uncontrolled environmental setting, which is inherently subject to unaccountable variables. For instance, weather events, which may significantly influence MP accumulation and vertical movement in soil, were not directly controlled. Furthermore, the open-system nature of the study introduces the possibility of MP fluxes, including contributions from atmospheric deposition or other sources.

During sample collection, drying, and storage, there was potential for contamination at various stages when the samples were handled. Moreover, the sieving of soils using a 2 mm mesh size during soil preparation may have excluded larger MPs up to 5 mm. Also, the prolonged storage of samples in a soil archive could have resulted in some changes to MP number, size, and shape through fragmentation. Despite meticulous precautions to minimise contamination during sub-sampling and analysis, its complete elimination cannot be guaranteed.

In the MP extraction workflow, organic matter removal left residual material in the sample, potentially reducing MP recovery and impeding identification. While the density separation process was effective, transferring separated MPs onto filter papers introduced opportunities for particle loss. Though effective in aiding MP identification, NR staining also has some limitations. The lipophilic dye can bind to non-polymeric substances, leading to false positives and reducing the accuracy of results. Lastly, the stereomicroscope-based visual analysis of MPs is inherently subjective. Although standardised operating procedures and consistent use of one operator mitigated variability, human error remains a limitation. The resolution and magnification constraints of stereomicroscopy also posed challenges, particularly for detecting smaller particles (<100μm).

This study highlights some areas in need of further optimisation of methodologies for isolating MPs from soil matrices. The lack of standardisation in MP analysis methods, particularly for soil, is a significant challenge. However, the approach presented in this study remains an accessible and cost-effective method capable of isolating and identifying MP particles.

4.3 STATISTICAL METHODS

4.3.1 Microplastics in Alkaline-Treated Biosolids

A one-way analysis of variance (ANOVA) was run in Minitab™ to test the null hypothesis that all means are equal ($\mu_1 = \mu_2 = \ldots = \mu a$) against the alternative hypothesis that at least one mean differs. The level of significance was set as $\alpha = 0.05$. The factor was year (5 levels), and the response was either the number of fragments, fibres, and spheres, the total number of MPs, or the size of fragments, fibres, and spheres. If the results of the ANOVA rejected the test of the null hypothesis (p-value $< \alpha$), then multiple means comparison was carried out using Fisher's least significant difference (LSD) with a 95%

confidence interval. Additionally, if no significance between years was determined, a one-sample t-test was performed for each response to obtain a population mean descriptive statistics.

4.3.2 Microplastics Over Time in Soil

A repeated measures analysis (RMA) was run using proc mixed ANOVA in SAS™ 9.4. The null hypothesis that all means are equal ($\mu_1 = \mu_2 = \ldots = \mu a$) was tested against the alternative hypothesis that at least one mean differs. The level of significance was set as $\alpha = 0.05$. The whole plot factor was management (2 levels), and the subplot factor was treatment (3 levels) and repeated over years (5 levels). Each plot (24 levels) was the subject of the repeated measure analysis, while the blocks (4 levels) were run as random effects. The response variables were the number of fragments, fibres, and spheres, the total number of MPs, or the size of fragments, fibres, and spheres. The most appropriate type of dependence was identified as compound symmetry (CS) using AIC values and incorporated into the model. If the results of the ANOVA reject the test of null hypothesis (p-value $< \alpha$), then multiple means comparison was carried out using Fisher's least significant difference (LSD) with a 95% confidence interval.

4.3.3 Microplastic Vertical Movement in Soil

A General Liner Model (GLM) in ANOVA using Minitab™ was run to test the null hypothesis that all means are equal ($\mu_1 = \mu_2 = \ldots = \mu a$) against the alternative hypothesis that at least one mean differs. The level of significance was set as $\alpha = 0.05$. The fixed effects were run as management (2 levels), the subplot factor was treatment (3 levels), and the sub-subplot factor was depth (4 levels). Plots and blocks were run as random effects. The response variables were the number of fragments, fibres, spheres, or the total number of MPs and the size of fragments, fibres, or spheres. If the results of the ANOVA reject the test of null hypothesis (p-value $< \alpha$), then multiple means comparison was carried out using Fisher's least significant difference (LSD) with a 95% confidence interval.

4.3.4 Assumptions

The assumptions of normality of the error terms, constant variance of the error terms, and independence of the error terms must be met to ensure the statistical validity of the results of the tests performed. A normal probability plot of the residuals is produced to ensure the normality of the error terms. When a pen is held up to the graph, if all points can be covered, and the p-value is greater than 0.100, then normality is assumed. To ensure constant variance of the error terms, a scatterplot of the residuals (on the y-axis) and fits (on the x-axis) is produced, and if there is an impression of a horizontal band, then constant variance is assumed. If the assumptions of normality and constant variance are not met, outliers are removed unless justifiable, and transformations must be performed to ensure the error terms meet the assumptions. Transformations are then back-transformed after the statistical analysis to ensure the results are relevant and understandable. Justifiable inclusion of outliers may be valid if they are believed to be representative of real-life phenomena and can reflect meaningful processes. However, their inclusion can increase variability in the results and reduce precision. Lastly, independence is assumed through the proper randomization of the experiment. However, the dependence assumption cannot be met through randomisation when using a RMA and the most appropriate type of dependence is identified using AIC values.

4.4 RESULTS

4.4.1 Microplastics in Alkaline-Treated Biosolids

The number of MPs in ATBs did not statistically significantly differ from 2010 to 2024, with a p-value of 0.586, and the null hypothesis that all means are equal is accepted. This suggests relatively consistent MP additions annually with ATB applications. On average, there were 138,600 ± 21,156 (117 444, 159 757) MP particles kg^{-1} of ATBs. The observed differences are shown in Figure 5 and likely reflect natural variability rather than systemic changes in the source material.

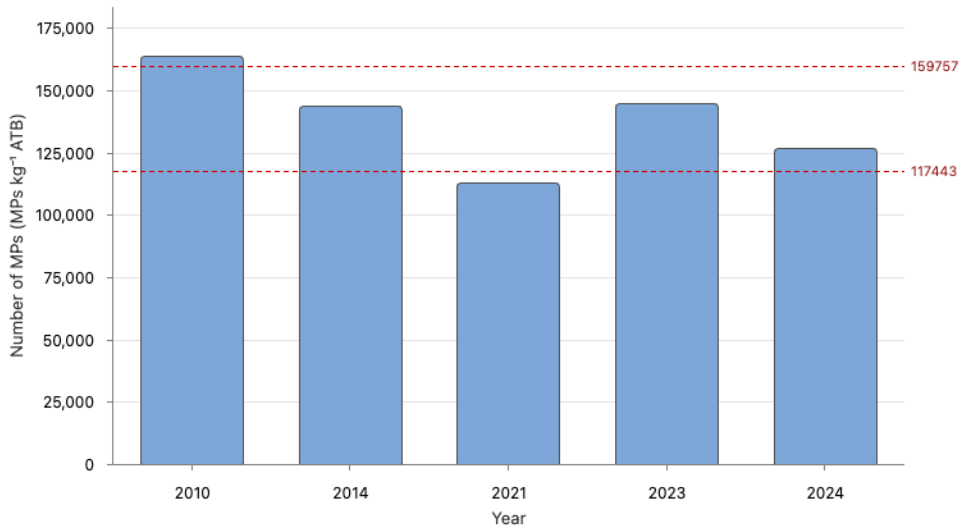

Figure 5. MP abundance (MPs kg^{-1}) in ATBs across years (2010, 2014, 2021, 2023, and 2024) with a pooled (N=10) 95% confidence interval (117443, 159757 MPs kg^{-1}ATB).

Fragments dominated the MP content in ATBs and comprised 84% (119 400 ± 25 889) of MPs observed, while fibres comprised 13% (18 444 ± 9098), and spheres 3% (4667 ± 2422), shown in Figure 6. There was no statistically significant difference in the number of fragments or spheres across years, with p-values of 0.779 and 0.694, respectively. In contrast, there was a difference in the number of fibres, with a p-value of 0.042. It was determined that 2010 was statistically significantly different from the rest of the years except for 2023. This difference likely reflects sampling and extraction variability rather than absolute changes, as no significant differences were observed among other years. It was then concluded that the null hypothesis that all means are equal holds true for fragments, fibres and spheres, as no statistically significant differences or trends in the number of MP particles were clearly observed and again, differences most likely reflect natural variability rather than alterations in the source material or processing technique. This suggests that the composition of MP within the ATBs was relatively consistent with annual additions. Supplemental interval plots of the number of MPs across years and the number of each MP shape across years are shown in Appendix B, Figures B1-4.

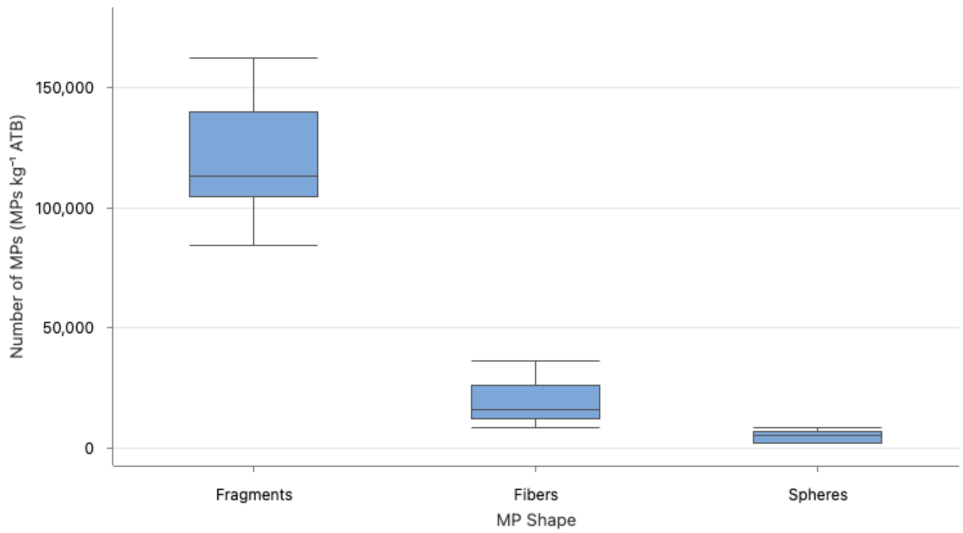

Figure 6. MP abundance (MPs kg^{-1}) in ATBs by shape (fragments, fibres, and spheres) with a 95% confidence interval (N=10).

Fragments had a median size of 127 µm, with a maximum of 175 µm and a minimum of 107 µm (Fig 7). Fibres dominated in size, having a median size of 596 µm, with a maximum of 692 µm and a minimum of 473 µm (Fig 7). Spheres were the smallest, having a median size of 71 µm, with a maximum of 90 µm and a minimum of 39 µm (Fig 7). There was no statistically significant difference in MP size within each shape category of fragments, fibres and spheres across years, with p-values of 0.214, 0.259, and 0.792, respectively. The null hypothesis was accepted that all means are equal, and the size of each MP shape observed did not statistically significantly differ across years. However, outliers and a larger spread in the size of fibres were observed and noted, suggesting larger variations in fibre size within the source material. These results suggest that the size dimensions of MP particles were relatively consistent with annual applications and, once again, that differences are most likely a reflection of natural variations rather than significant or systemic changes in the source material. Supplemental interval plots of MP size for each shape across years can be found in Appendix B, Figures B5-7.

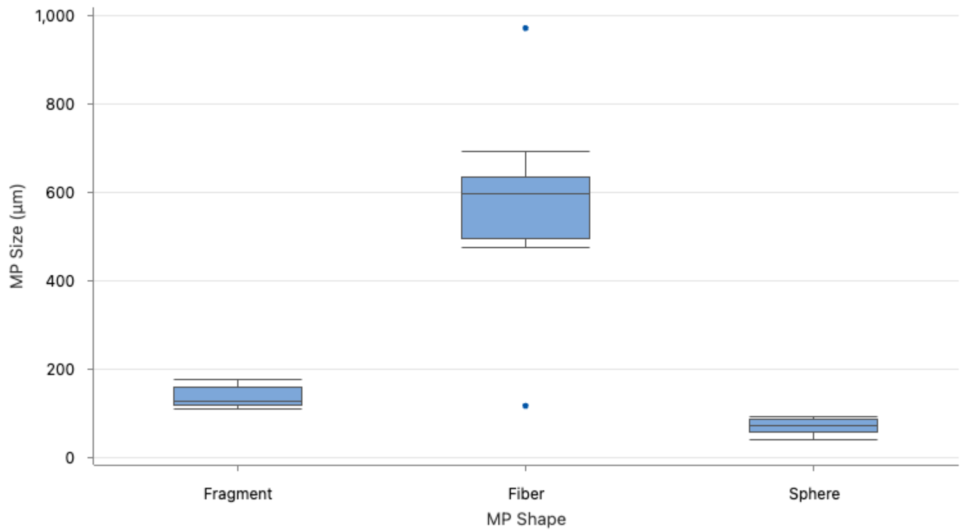

Figure 7. MP size (μm) by shape (fragment, fibre, and sphere) within ATBs with a 95% Confidence Interval (N=10).

4.4.2 Microplastics Over Time in Soil

During statistical analysis of soil MPs over time, outliers were consistently observed in plots with the highest treatment rate. These values were carefully considered and believed to reflect real-world phenomena, as the highest biosolid application rate logically results in substantially greater microplastic contamination. Removing these data points would risk underestimating the true impact of this treatment level. Retaining these values ensures that the analysis accurately represents soil MP responses to higher treatment rates, aligning with the study's objectives.

Abundance

The number of MPs over time, in the surface layer (0-15 cm) of the soil from the application of ATBs was significantly impacted by management practice (single vs annual), treatment rate (0, 14, and 42 tonnes ATB (wet weight) ha^{-1}), and year (2008, 2014, 2016, 2021, and 2023) with p-values of 0.0021, <0.0001, and <0.0001 respectively. The effect management practice and treatment rate had on the number of MPs is seen in Figure 8, highlighting that increased treatment rates of ATBs and an annual management strategy result in significantly more MP contamination; the effect management practice and years have on the number of MPs is seen in Figure 9 and calls attention to a cumulative effect time has on MP accumulation under different management practices; and the effect of treatment rate and years in Figure 10 denotes an ATB treatment intensity effect on MP contamination in soil over time. The three-way interaction of management strategy, treatment rate, and years had a p-value of 0.002, highlighting the complex and dynamic nature of MP contamination in soil. Fisher's LSD letter groupings for the 3-way interactions can be found in Appendix B, Table B1.

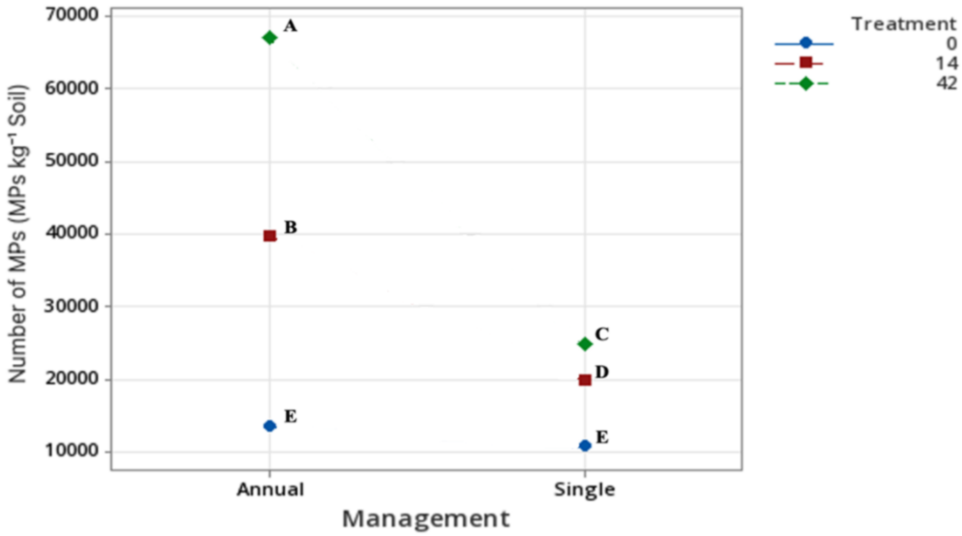

Figure 8. Effect of management practice (single vs annual) and treatment rate (0, 14, and 42 tonnes ATB (wet weight) ha^{-1}) on the number of MPs in soil (MPs kg^{-1}), based on means averaged across years. Data points that do not share a letter grouping (A, B, etc.) are statistically significantly different (p<0.05).

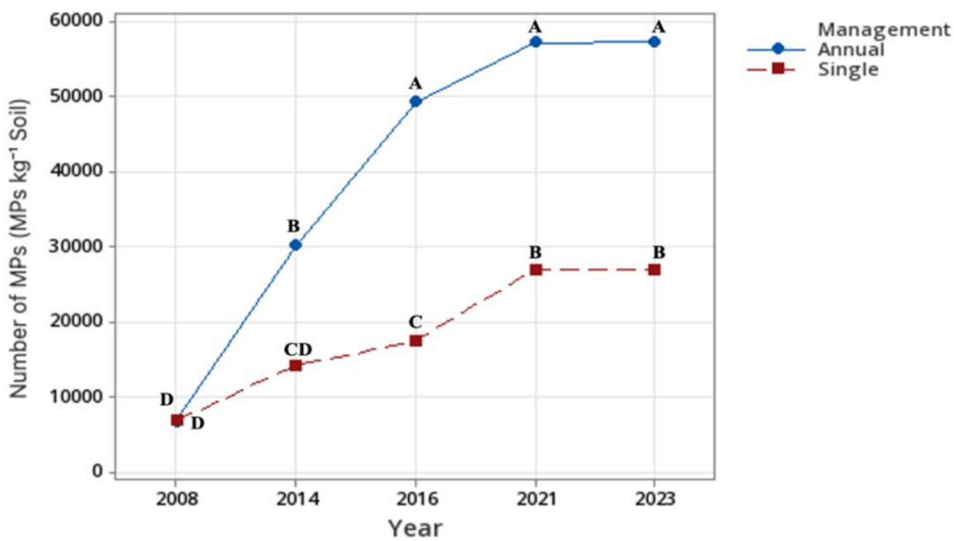

Figure 9. Effect of management practice (single vs annual) and years (2008, 2014, 2016, 2021, and 2023) on the number of MPs in soil (MPs kg^{-1}), based on means averaged across treatment rate. Data points that do not share a letter grouping (A, B, etc.) are statistically significantly different (p<0.05).

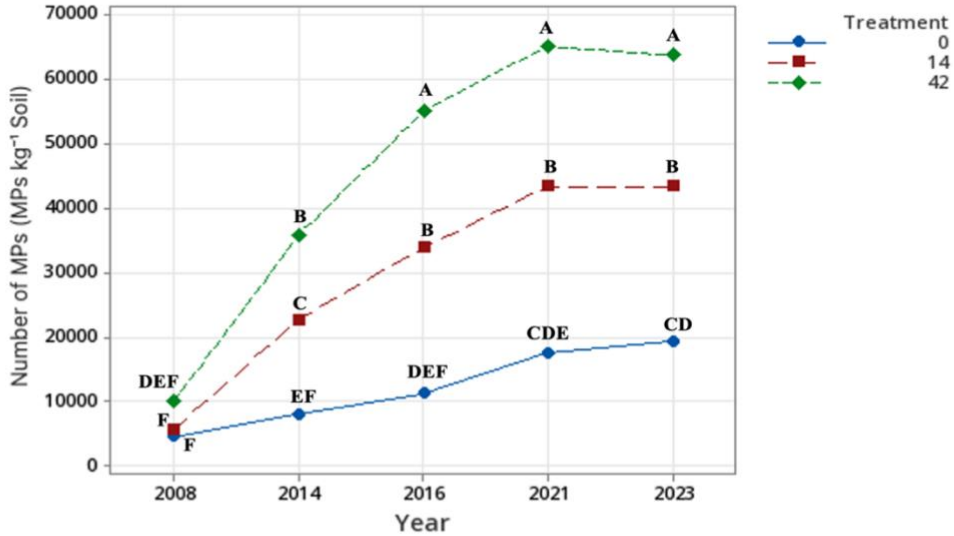

Figure 10. Effect of treatment rate (0, 14, and 42 tonnes ATB (wet weight) ha^{-1}) and year (2008, 2014, 2016, 2021, and 2023) on the number of MPs in soil (MPs kg^{-1}), based on means averaged across management practice. Data points that do not share a letter grouping (A, B, etc.) are statistically significantly different ($p<0.05$).

Post-biosolid application in the fall of 2008 showed no statistically significant differences in *the number of* MPs kg^{-1} soil between management practices when both had received the same amounts of ATBs, marking a baseline (Fig 8 and 9). Over time, annual applications of ATBs and at higher treatment rates resulted in significantly more MP contamination (Fig 8-11). Based on the agronomic recommendation for growing corn, the treatment rate of 14 tonnes ATB (wet weight) ha^{-1} had an 8.7-fold increase in MP presence from 6250 ± 5852 to 54 500 ± 9747 MPs kg^{-1} soil if annually applied over 15 years. When the treatment rate tripled to 42 tonnes ATB (wet weight) ha^{-1}, a 9.3-fold increase from 10 250 ± 8884 to 95 250 ± 28 745 MPs kg^{-1} soil was observed. A gradual increase in the number of MP kg^{-1} soil was also witnessed in the single application plots over time. At the rate of 14 tonnes ATB (wet weight) ha^{-1}, there was a 6.5-fold increase from 5000 ± 3830 to 32250 ± 8016 MPs kg^{-1} soil, which was seen 15 years after a single application of ATBs. Meanwhile, the triple rate of 42 tonnes ATB (wet weight) ha^{-1} saw a 3.2-fold increase from 10 000 ± 5354 to 32 250 ± 7805 MPs kg^{-1} soil after 15 years. A gradual increase in MP presence within control plots was also observed. The single application of ATBs controls had a 3-fold increase, while a 6-fold increase was seen in annual control plots after 15 years.

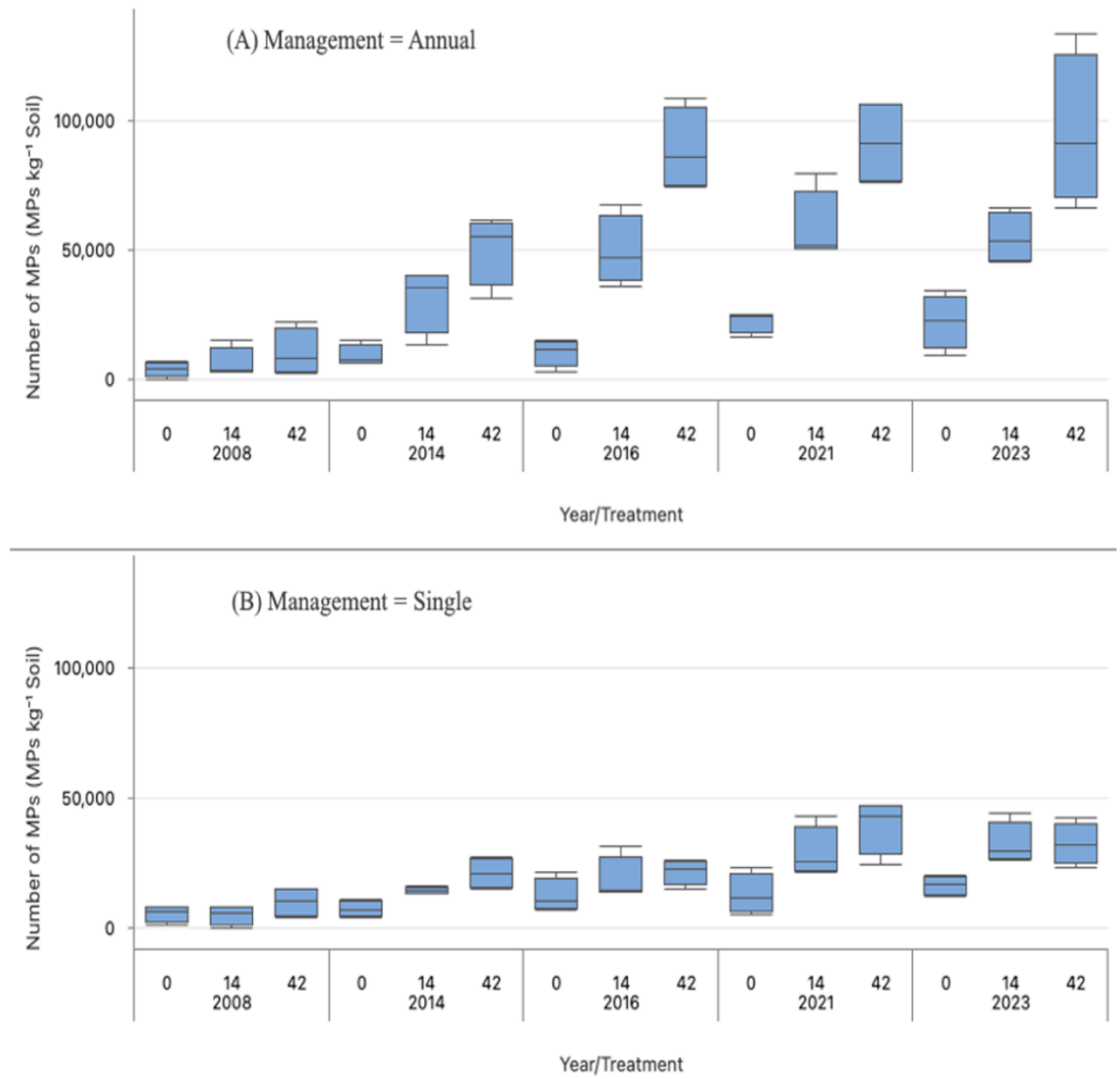

*Figure 11. Number of MPs (MPs kg^{-1}) in the surface (0-15 cm) soil over time in response to management practice ((**A**) annual represented in the top box plot vs (**B**) single represented in the bottom boxplot), treatment rate (0, 14, and 42 tonnes ATB (wet weight) ha^{-1}), and year (2008, 2014, 2016, 2021, and 2023).*

Size and Shape

The classification of MP contamination by size and shape (fragment, fibre, or sphere) in the surface (0-15 cm) of the soil consistently reflected the composition of the source material (ATBs). Fragments were the most abundant across all treatments and years, with percentages ranging from 55% to 95 %. Fibers were the second most common, with percentages varying between 4% and 45%. Meanwhile, spheres were the least observed, with percentages ranging from 0% to 22%. This distribution of MPs by shape aligns with the particle morphology of MPs originating from ATBs, where plastic fragments dominate.

The size of the MP particles by shape also reflected ATB as the source of contamination. Fragments, on average, ranged from 63.62 to 216.10 µm, fibres, 229.34 to 2168.53 µm, and spheres, 46.16 to 159.91 µm. These distributions in MP size by shape align with the particle morphology of MPs originating from ATBs, where fibres dominated in size. Over time, management practice, treatment rate, and years did not statistically significantly affect MP size in the soil's surface (0-15 cm) layer over the 15-year time frame. Supplemental boxplots of MP size by shape in response to management practice and years can be found in Appendix B, Figures B8-10.

4.4.3 Microplastic Vertical Movement in Soil

During statistical analysis, outliers were observed in the annual management plots at 15-30 cm soil depths. These values were carefully considered and believed to reflect real-world phenomena, as the annual application of biosolids logically results in more significant microplastic contamination. Removing these data points would risk underestimating the true impact of this management practice. Retaining these values ensures that the analysis accurately represents soil MP responses to long-term repeated applications of ATBs, aligning with the study's objectives.

Outliers were also observed during the statistical analysis of MP size at different soil depths and carefully considered. For transparency and consistency, these were retained, as they did not affect statistical significance. Notably, the presence of outliers likely reduced the size differences between soil depths rather than inflating significance. While contamination remains a possibility despite stringent precautions, these values may also reflect real-world variations. Removing them could risk overlooking environmentally relevant deviations. Retaining these values ensures a robust and transparent analysis, aligning with the study's objectives.

Abundance

The number of MP particles kg^{-1} soil was significantly impacted across soil depths (0-15, 15-30, 30-60, and 60-100 cm) by management practice, treatment rate, and depth, with p-values of 0.0068, 0.0002, and <0.0001 respectively. The effect management practice and depth had on the number of MPs is seen in Figure 12, highlighting greater abundances of MP in annual plots down to 30cm depth. The effect treatment rate and depth had on the number of MPs is seen in Figure 13, highlighting that increased treatment rates result in significantly more MPs down to 30 cm soil depth. The three-way interaction of management, treatment, and depth had a p-value of 0.0087. The Fisher's LSD letter groupings for three-way interactions can be found in Appendix B, Table B2.

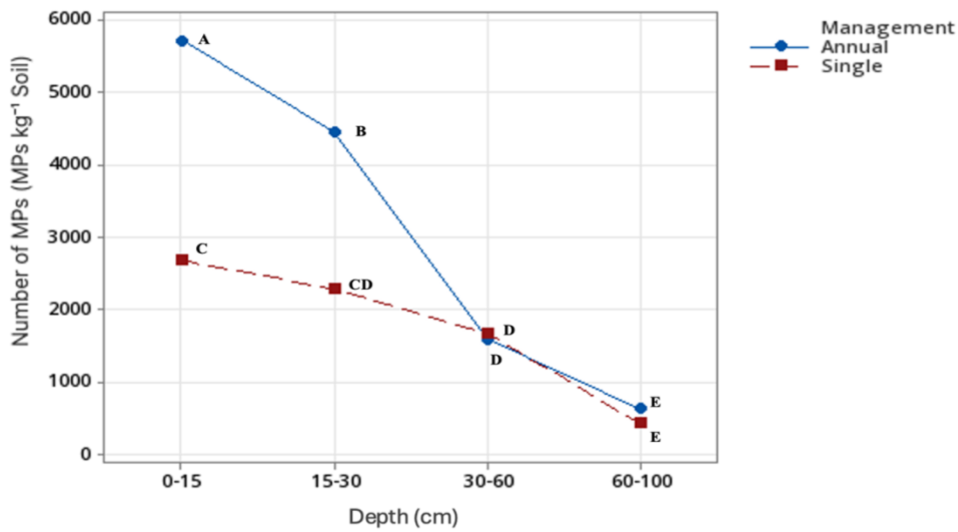

Figure 12. Effect of management practice (single vs annual) and soil depth (0-15, 15-30, 30-60, and 60-100 cm) on the number of MP particles (MPs kg^{-1}) in the soil, based on means averaged across treatment rates. Data points that do not share a letter grouping (A, B, etc.) are statistically significantly different (p<0.05).

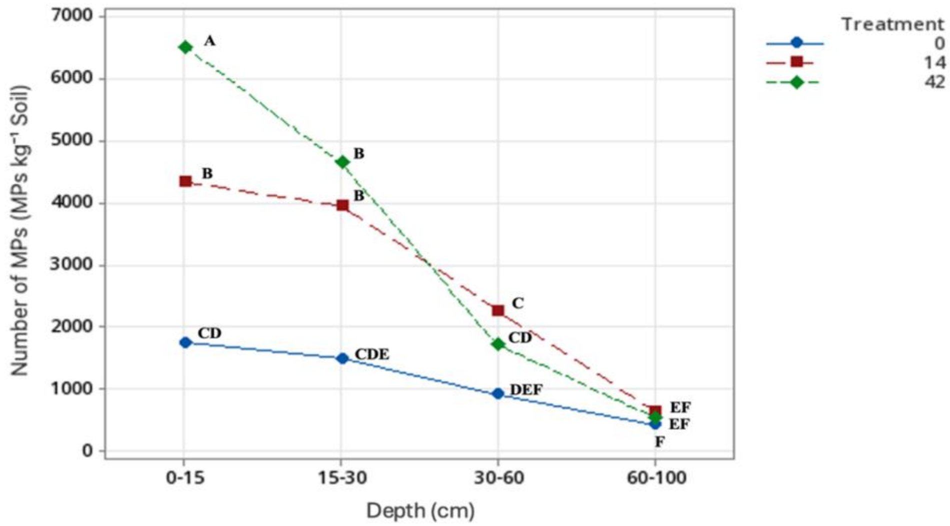

Figure 13. Effect of treatment rate (0, 14, and 42 tonnes ATB (wet weight) ha^{-1}) and soil depth (0-15, 15-30, 30-60, and 60-100 cm) on the number of MP particles (MPs kg^{-1}) in the soil, based on means averaged across management practice. Data points that do not share a letter grouping (A, B, etc.) are statistically significantly different ($p<0.05$).

The soil core, taken in 2021 after 13 years of ATB application, revealed the presence of MP contamination even at depths up to 100 cm. At the surface 0-15 cm soil depth, differences in management practice (Fig 12) and treatment rates (Fig 13) are the most pronounced. For example, the annual treatment rate of 14 tonnes ATB (wet weight) ha^{-1}, based on the agronomic recommendation for growing corn, resulted in 5800 ± 1407 MPs kg^{-1} soil at the 0-15 cm depth, whereas the single treatment resulted in 2875 ± 974 MPs kg^{-1} soil. At 15-30 cm depths, annual treatment applications resulted in 5350 ± 2336 MPs kg^{-1} soil, and the single treatment resulted in 2575 ± 727 MPs kg^{-1} soil. The triple rate of 42 tonnes ATB (wet weight) ha^{-1} followed the same trends but resulted in an even more significant disparity between single and annual plots in the surface 0-15 and 15-30 cm depths. For example, the annual application of 42 tonnes ATB (wet weight) ha^{-1} at the 0-15 cm depth resulted in 9100 ± 1675 MPs kg^{-1} soil, while the single application resulted in 3925 ± 1047 MPs kg^{-1} soil. At 15-30 cm depth, the annual application of ATBs resulted in 6500 ± 837 MPs kg^{-1} soil, and the single application resulted in 2800 ± 1364 MPs kg^{-1} soil. Moving down into the soil profile, the number of MP particles kg^{-1} consistently decreases as soil depth increases, regardless of management practice or treatment rate. For example, the annual application of 14 tonnes ATB (wet weight) ha^{-1} resulted in 5800 ± 1407 MPs kg^{-1} of soil at 0-15 cm, 5350 ± 2336 MPs kg^{-1} of soil at 15-30, 2150 ± 881 at 30-60 cm, and 850 ± 681 MPs kg^{-1} soil at 60-100 cm depths. A similar trend was observed in the single management practice plots and treatment rates. For both management practices and all treatment rates, when at soil depths below 30 cm, there was no significant difference in the number of MP particles kg^{-1} between treatment rates or management practice, indicating both vertical and lateral dispersion beyond 30 cm soil depths. Visualisation of these trends is seen in Figure 14.

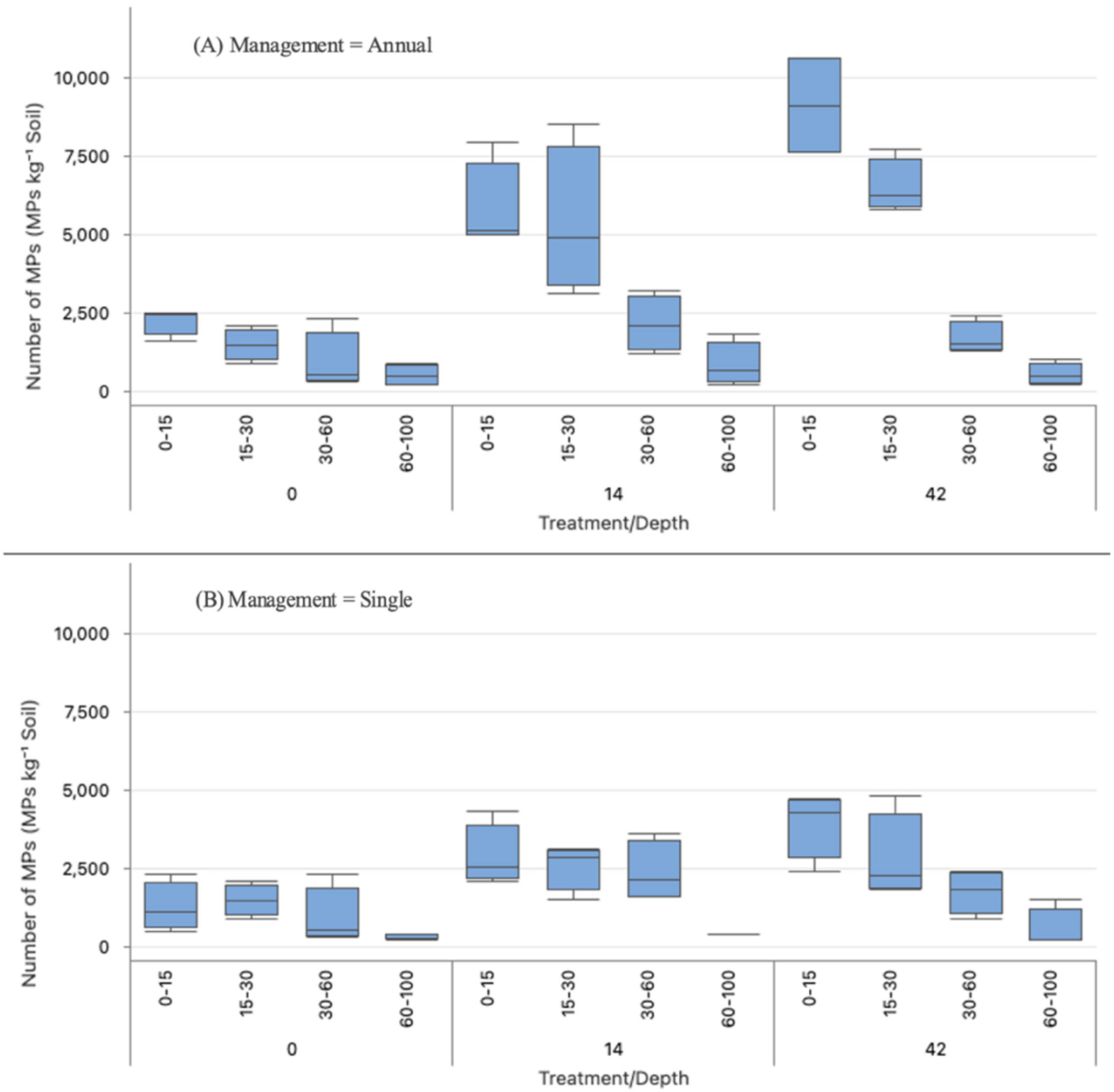

*Figure 14. Number of MP particles (MPs kg^{-1}) in response to management practice ((**A**) annual represented in the top box plot vs (**B**) single represented in the bottom boxplot), treatment rate (0, 14, and 42 tonnes ATB (wet weight) ha^{-1}), and soil depth (0-15, 15-30, 30-60, and 60-100 cm).*

Size and Shape

Fragments remained the most abundant form of MPs at all soil depths compared to fibres and spheres. The number of fragments also varied the most between each depth of 0-15, 15-30, 30-60, and 60-100 cm, each statistically significantly different from the other (Fig 15). In comparison, the number of fibres remained relatively consistent between 0-15, 15-30, and 30-60 cm depths, with only the 60-100 cm depth being significantly different with much lower numbers of MP particles kg^{-1} (Fig 16). Similarly, the number of spheres remained relatively consistent in the 0-15, 15-30, and 30-60 cm soil depths, while 60-100 cm depth was statistically significantly different with much lower numbers of MP particles kg^{-1} (Fig 17).

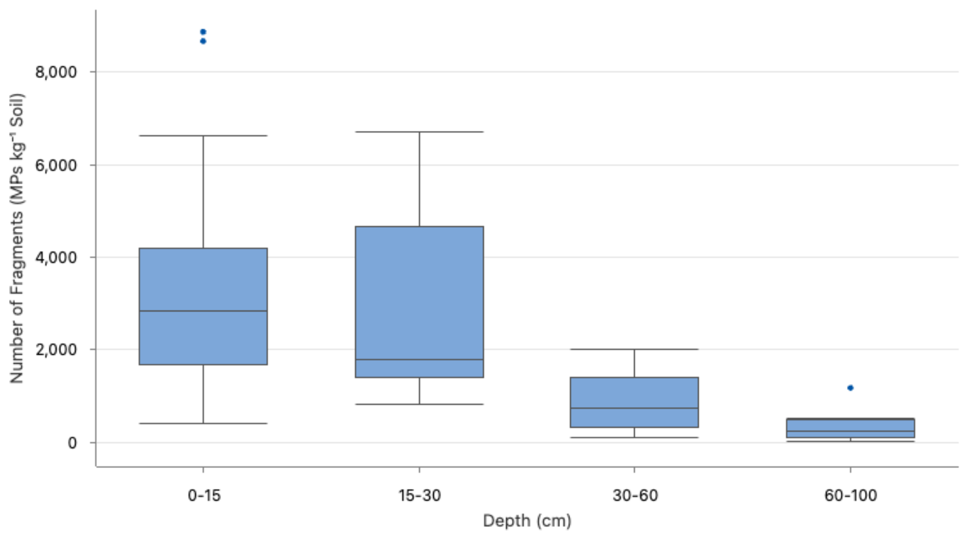

Figure 15. Number of MP fragments (MPs kg^{-1}) at different soil depths (0-15, 15-30, 30-60, and 60-100 cm).

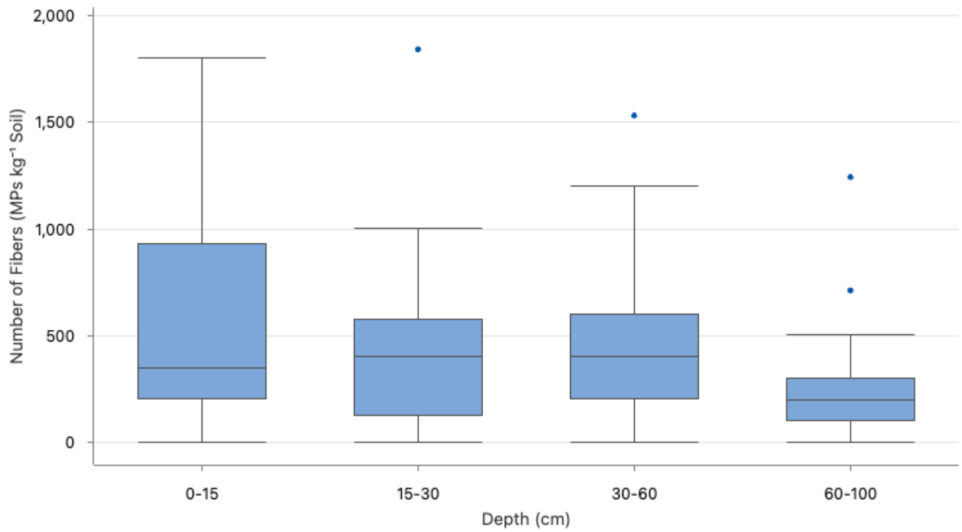

Figure 16. Number of fibres (MPs kg^{-1}) at different soil depths (0-15, 15-30, 30-60, and 60-100 cm).

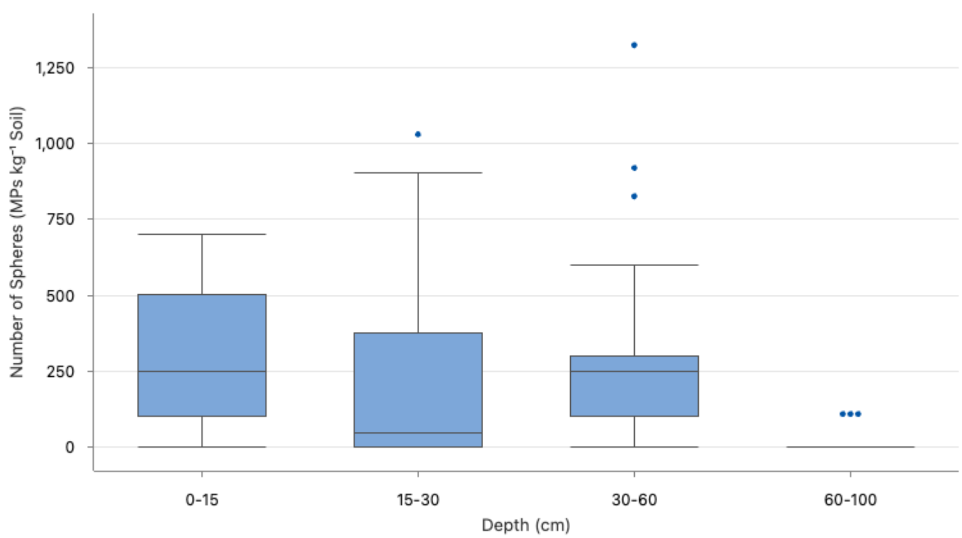

Figure 17. Number of spheres (MPs kg^{-1}) at different soil depths (0-15, 15-30, 30-60, and 60-100 cm).

The size of each MP shape (fragment, fibre, and sphere) all followed a general pattern of decreasing in size as soil depth increased while maintaining the pattern of fibres being the largest and spheres the smallest at all soil depths. Fibre size was not statistically significantly affected by any factor, but a slight size reduction can be seen (Fig 19). Fibres averaged 851 µm at 0-15 cm, 646 µm at 15-30 cm, 685 µm at 30-60 cm, and 558 µm at 60-100 cm depth. Fragment size was significantly affected by depth, with a p-value <0.001 (Fig 18). Fragments averaged 206 µm at 0-15 cm, 167 at 15-30 cm depth, 116 µm at 30-60 cm depth, and 140 µm at 60-100 cm depths. Sphere size was only affected by soil depth, with a p-value <0.001 (Fig 20). Spheres averaged 152 µm at 0-15 cm, 130 µm at 15-30 cm, 58 µm at 30-60 cm, and 48 µm at 60-100 cm depths.

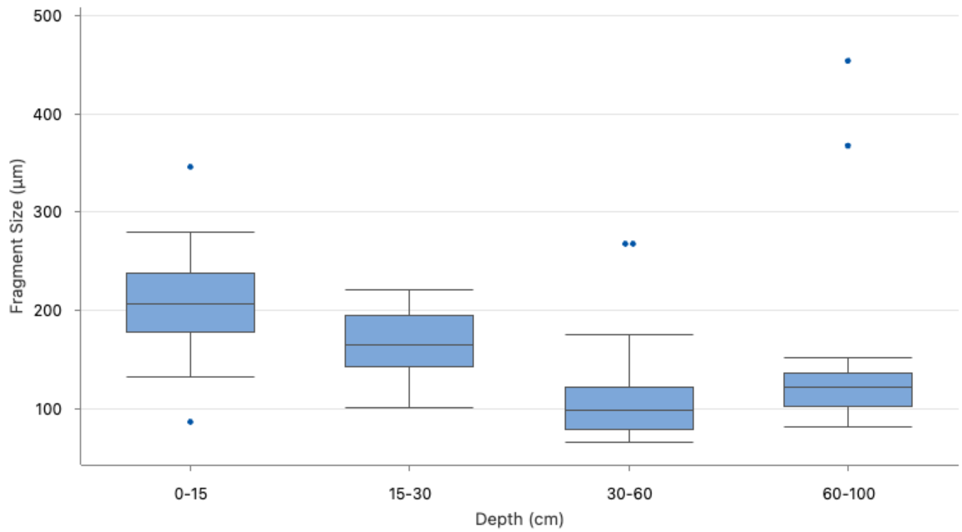

Figure 18. Fragment size (µm) at different soil depths (0-15, 15-30, 30-60, and 60-100 cm).

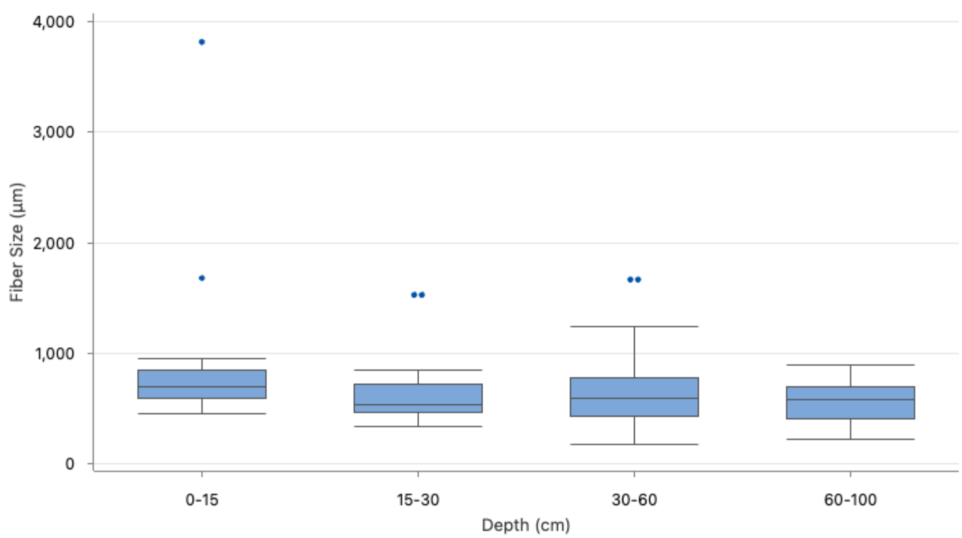

Figure 19. Fibre size (µm) at different soil depths (0-15, 15-30, 30-60, and 60-100 cm).

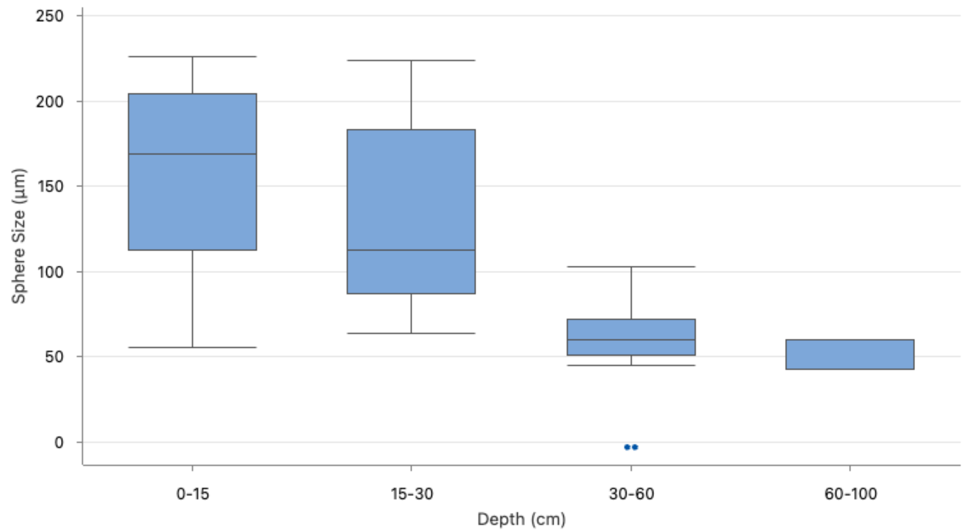

Figure 20. Sphere size (µm) at different soil depths (0-15, 15-30, 30-60, and 60-100 cm).

4.5 DISCUSSION

Biosolids inherently contain MPs due to their origin in wastewater streams contaminated from industrial and household sources. The ATB used for this study contained 138 600 ± 21 156 MPs kg^{-1}. These were comparable results to a study using a similar approach in southern Ontario, Canada, that also quantified the MPs within ATBs and found them to contain 206 800 (± 12 906) MPs kg^{-1} (Letwin et al., 2024). The ATB in this study is a Class A municipal biosolid generated by Halifax Regional Municipality and treated using the N-Viro™ patented process of alkaline stabilisation using cement kiln dust for alkalinity. This process mixes dewatered sewage sludge with the alkaline substance (cement kiln dust), which increases the pH above 12 and generates an exothermic reaction that can raise the temperature to 80ºC. The increased pH and temperature, as well as the material dilution with cement kiln dust, results in a biosolid that has fewer MPs than other processing techniques would generate. Supporting literature examining the number of MP particles in biosolids from 22 different WWTPs across nine provinces in Canada found that ATB had, on average, the least MPs with 299 000 MPs kg^{-1}, compared to anaerobic digestion with 812 000 MPs kg^{-1} which contained the most, followed by dewatering with 633 000 MPs kg^{-1}, then aerobic digestion with 589 000 MPs kg^{-1}, and pelletisation with 541 000 MPs kg^{-1} (Sivarajah et al., 2023). A similar trend with ATB containing fewer MPs than biosolids treated in other ways was observed by Letwin et al. (2024). It is then plausible that when other forms of biosolids are used, MP accumulation would be even more pronounced and result in more MP contamination, underscoring the need for standard monitoring.

This study found the composition of MPs within ATBs to be predominantly fragments, followed by fibres and then spheres. Similarly, Letwin et al. (2024) found ATBs to be predominantly comprised of fragments followed by fibres. This is contrary to other publications, which report fibres as being the most abundant, followed by fragments (Sivarajah et al., 2023; Ziajahromi et al., 2024). The alkaline treatment process may result in a reduced number of fibres because of the increased pH and heat while also causing larger plastic pieces to fragment further, inflating fragment counts. Another important detail is that fibres and larger shapes may have been removed when the soil samples were sieved to 2 mm before being placed in a soil archive. The rationale is that fibres were found to be the largest MP shape and can form bundles, making their size even larger and more likely to be removed with sieving. Also, fibres may not have been the only shape of MP removed during sieving, and any particles larger than 2mm would have been lost, which could have resulted in the underestimation of MP accumulation in agricultural soil.

MP accumulation and long-term persistence in the soil after receiving ATB application(s) were demonstrated in this study. This suggests that significant contamination in agricultural soils, particularly with repeated applications and higher treatment rates, is not speculative but a strong likelihood. However, application frequency and treatment intensity effects were not as prominent as expected, making it evident that not all MPs were retained within the soil system and likely migrated to adjacent environmental matrices. Limited studies have been completed to assess the fate and migration of MPs once in the environment, and our understanding is minimal, especially in soil systems. One of the first studies to assess the fate of MPs concluded that likely >99% of MPs from biosolid application to soil end up migrating to the aquatic environment and that fragments are most likely to migrate but failed to account for vertical migration within the soil matrix (Crossman et al., 2020). Extrapolating from the observed 8.7-fold increase in MP number from the annual addition of 14 tonnes ATB (wet weight) ha^{-1} and then generating a theoretically expected 26-fold increase if the rate was tripled, but instead observing a 9.3-fold increase in the triple rate of 42 tonnes ATB (wet weight) ha^{-1}, it is estimated that approximately 48% of MPs were lost to dispersion. The dispersal of MPs from plots receiving annual applications of ATBs and at higher treatment rates may account for the increases in the number of MP particles kg^{-1} soil in single management plots and control plots despite large buffer zones. Further, MPs are likely dispersing into adjacent environmental matrices, which raises concerns about broader ecological impacts. Long-term studies across multiple environmental matrices are needed to fully understand MP transport and transformation pathways originating from ATBs in agricultural soil.

Plastics' incredible durability and resistance to degradation was the logical first conclusion when no differences were seen in MP size in the surface soil (0-15 cm) over 15 years. MP resistance to degradation is also underscored by the persistence shown in single management practice plots over 15 years. It is not unusual to observe limited changes in plastic size and shape over such a relatively short period, as plastics are resistant to degradation and can persist for centuries once in the environment. The estimated half-lives of everyday plastic items buried in soil range from approximately 250 years for a HDPE plastic bottle, >2500 years for a PET single-use bottle, >2500 years for PS packaging, 5000 years for HDPE pipes, >2500 years for PVC pipes, and 5 years for LDPE bags (Chamas et al., 2020). This resistance to degradation is why they are so persistent and partially why they are so prevalent in environmental matrices. Currently, literature on the degradation of plastics in environmental conditions is also limited. Additional research is greatly needed to begin to understand a timeline for plastics degradation, what the degradation pathways are, and what factors affect the degradation process in a soil matrix.

This study also observed the vertical movement of MPs within the soil matrix, noting that most MPs are retained in the upper soil layers (0-15 and 15-30 cm), with significantly lower numbers of MPs kg^{-1} soil at deeper soil depths (30-60 and 60-100 cm). Significantly lower numbers of MPs do not diminish the fact that MPs are still present at deeper soil depths and may still pose significant ecological risks. It is also notable that MP size decreased with soil depth, likely attributed to the increased mobility of smaller particles compared to larger ones. Another study also found comparable results of MP particle size decreases with soil depth (Qiu et al., 2023). How soil characteristics, such as texture and OM content, impact the vertical movement of MPs in soil and what role MP shape plays are currently unknown. This study found that fragments potentially moved vertically the easiest in a dominantly sandy-silty textured soil, maintaining the highest numbers of MPs kg^{-1} soil at all soil depths. However, further studies assessing the interactions of MP size and shape with alternative soil textures and characteristics are needed to begin to understand MP vertical movement in a soil matrix.

4.6 CONCLUSION

The findings of this research identify agricultural soil as a significant MP sink, retaining substantial numbers of MPs, but also as a source to surrounding environments, with many MPs lost to dispersion. These findings also recognise ATBs as a major source of MP contamination in agricultural soil, emphasising the importance of considering application frequency and intensity to manage contamination. The research site was not developed to illustrate recommended agronomic practice but to highlight the role of high-intensity applications of organic amendments, in this case, a biosolid, in introducing contaminants and subsequent impacts on soil ecology. The purpose of this study was not to villainize the recycling of organic wastes in the form of biosolids but to increase our understanding of MP presence in ATBs and soils that have received ATB application (s) to improve upon ATB quality and safety for the longevity of agricultural practices. Quantifying MP presence in biosolids and their accumulation and persistence in agricultural soils is an important first step to generating evidence-based policy decisions that curb and safeguard further MP contamination. Currently, there are no guidelines or regulations concerning MP presence in biosolids, and WWTPs do not monitor them. WWTPs should be encouraged to monitor and even go so far as to implement strategies to reduce the number of MPs in sludge and biosolid applications. Legislations should also be revised to incorporate MP management strategies to limit contamination and safeguard agricultural soils and food and nutritional security.

CHAPTER 5: THERMOGRAVIMETRIC (TGA) AND DIFFERENTIAL SCANNING CALORIMETRY (DSC) PAIRED WITH FOURIER TRANSFORMED INFRARED (FTIR) SPECTROSCOPY FOR THE EXAMINATION OF MICROPLASTICS IN ALKALINE TREATED BIOSOLIDS AND SOIL

ABSTRACT

Microplastics (MPs) are pervasive and persistent environmental contaminants; however, analytical approaches for MPs in complex matrices like soils remain underdeveloped, limiting our understanding of their composition and potential impact. This study employs thermogravimetric analysis (TGA) paired with differential scanning calorimetry (DSC) and Fourier-transformed infrared (FTIR) spectroscopy for the chemical identification of MPs in alkaline-treated biosolids (ATBs) and agricultural soils receiving ATB applications. Prior to TGA-DSC-FTIR analysis, samples underwent organic matter removal (H_2O_2) and density separation (NaBr) to concentrate MPs in the samples. Results demonstrate that TGA-DSC-FTIR is a powerful tool that can effectively identify MP chemical type, distinguishing polypropylene (PP), polyethene (PE), and polystyrene (PS) in both ATBs and soils that had received large amounts of ATB applications (42 tonnes ha^{-1} ATB (wet weight) annually for 15 years). However, this study only begins to explore the possibilities of TGA-DSC-FTIR analysis; significant opportunities remain for method refinement and broader application. Developing diverse gas-phase spectral libraries for polymer identification and implementing machine learning algorithms could facilitate automation towards widespread adoption, methodological standardisation, and routine monitoring of MP contamination in a range of environmental matrices.

KEYWORDS

Microplastics; Alkaline-Treated Biosolids (ATBs); Agricultural Soil; Polymer Identification

HIGHLIGHTS

- TGA-DSC-FTIR was successfully used to chemically identify PP, PE, and PS MPs in ATBs and soil that had received long-term additions of ATBs.
- There is a critical need for the development of evolved gas spectral libraries to enhance polymer identification.
- Automation through machine learning could facilitate the adoption and standardisation for routine MP monitoring.

5.1 INTRODUCTION

Microplastics (MPs) are a persistent and ubiquitous pollutant that can be found in agricultural soils through atmospheric deposition (Allen et al., 2019; Welsh et al., 2022), the application of soil amendments (Crossman et al., 2020; Hao et al., 2024; Iswahyudi et al., 2024; Pérez-Reverón et al., 2022; Sheriff et al., 2023; Wang et al., 2024a) and other anthropogenic activities (Accinelli et al., 2019; Guo et al., 2023). However, analytical techniques equipped to handle MPs in soil environments remain underdeveloped, particularly with the chemical identification of MP polymer type. There is a strong need for more advanced characterisation techniques that simplify MP analysis and establish standardised protocols, enhancing comparability across soil MP studies.

Soil environments are a dynamic and highly heterogeneous mixture of inorganic and organic components that may obscure MPs, complicating extraction and identification (Canadian Council of Ministers of the Environment, 2012; Thomas et al., 2020). As a result, there is a lack of method standardisation and harmony within the study of MPs in complex matrices. Many current analytical techniques incorporate extensive sample processing, such as organic matter removal and density separation to extract MPs from soil samples, leading to incongruencies between studies and an inability to cross-validate methods (Iswahyudi et al., 2024; Tan et al., 2022; Thomas et al., 2020). Currently, the most abundantly utilised method of MP analysis is visual, using various forms of microscopy, but this approach lacks chemical identification of the material and is limited by particle size. Smaller particles are consistently reported as being challenging to capture and analyse (Blair et al., 2019; Harley-Nyang et al., 2022; Wang et al., 2024b). Thermal and spectroscopic techniques may complement visual analysis by providing chemical identification and addressing analytical challenges, such as particle size limitations for MPs in complex matrices such as soil.

Thermal analysis methods uniquely track materials' mass loss and decomposition patterns under controlled heating conditions, offering insights into MPs thermal stability and peak decomposition (Td) temperatures. Thermogravimetry (TGA) is a typical thermal instrument that can measure the mass lost from the sample as a function of temperature (Mariano et al., 2021). Further, polymers are known to degrade beginning with enthalpy changes, and it has been suggested that TGA be paired with differential scanning calorimetry (DSC) to measure these enthalpy changes in addition to mass loss (Golebiewski & Galeski, 2007; Majewsky et al., 2016). DSC measures temperature and heat flux during phase transitions, identifying thermal events such as melting (Tm), crystallisation (Tc), and glass transition (Tg) temperatures (Mariano et al., 2021). To advance the chemical identification of polymers, thermal decomposition products generated through TGA-DSC can be analysed using spectroscopic techniques, such as Fourier-transform infrared spectroscopy (FTIR) (Cho et al., 2023; Goedecke et al., 2020).

FTIR is a vibrational spectroscopic technique that detects molecular absorbance. When a molecule absorbs an infrared photon, it changes from its ground to an excited state, producing a measurable response. The infrared spectra are produced from the induced dipole moment of the chemical bonds (Elert et al., 2017). FTIR uses an interferometer so that all the generated wavelength frequencies from the sample can be scanned to create an intensity over time series that is transformed into a spectrum using the Fourier transform (Smith, 2011). The evolved gasses from thermal decomposition are analysed using FTIR, producing characteristic spectra by which the material can be identified. Each material has a unique spectral 'fingerprint' found within the 600 to 1700 cm^{-1} region that can be used for identification (Paterova et al., 2022; Ramírez-Hernández et al., 2019). When two spectra match within the fingerprint region, it strongly suggests that they correspond to the same material.

The objective of this Chapter is to chemically identify MP polymer types in ATBs and soils in Chapter 4 using TGA-DSC-FTIR. This analysis aims to identify the presence of specific polymer types and provide additional characterisation of MPs detected in prior chapters. Given the complexity of MP decomposition and the lack of comprehensive evolved gas reference libraries, this study focuses on qualitative polymer identification rather than quantification.

5.2 MATERIALS AND METHODS

5.2.1 Sample Collection

A total of 10 different polymer samples were collected to develop an initial polymer reference dataset: acrylonitrile butadiene styrene (ABS) fragment from a black pipe, polymethyl methacrylate (PMMA or acrylic) fragment from a display case, high-density polyethene (HDPE) fragment from a PEX pipe, low-density polyethene (LDPE) fragment from a plastic bag, polyethene fibres (PE) from an article of clothing, polyethene terephthalate (PETE) fragment from a single use water bottle, polypropylene (PP) opaque fragment from a single use cup, PP white fragment from a single use cup, and a polystyrene (PS) fragment from a takeout container. These reference polymers were collected from aged household items exposed to environmental conditions to represent environmentally weathered polymers and serve as comparative controls for MP identification.

Reference polymers ABS, PE, PP, and PS were also used to spike soil samples to provide qualitative context during the analysis of unknown samples. The soil was obtained from the parameter of the field site described from Chapter 4 and did not undergo MP extraction. These spiked soils are not presented as part of the results but are referenced in supplemental Appendix C.

In Chapter 4, samples that first underwent organic matter removal and density separation for stereoscopic analysis were used to analyse ATB and soil MPs. The extracted ATB samples from 2010, 2014, 2021, and 2023 were selected to assess the MP chemical composition within the source material. The extracted surface (0-15 cm) soil samples from the annual 42 tonnes ha^{-1} ATB (wet weight) plots in 2023, 15 years into the study, were selected to maximise potential MP identification. Samples were packaged and sent to the Soil Organic Matter Dynamics and Analysis Lab within the School of Environmental Sciences at the University of Guelph, ON, Canada, for thermal and spectroscopic characterisation of MP chemical composition.

5.2.2 Sample Analysis

Ruthenium (Ru) crucibles were rinsed with deionised water and heated to 1000ºC to dry and remove any residual material that could contaminate the analysis. Each cleaned and dried crucible was loaded with 15 - 25mg of sample and placed onto an automated sampler that could house 20 samples. Each run included an empty Ru crucible in the first slot as a baseline correction and another in the last as a reference.

Thermogravimetric analysis (TGA) was conducted using a Netzsch Jupiter STA449F3 simultaneous thermal analyser, which also recorded DCS data (TGA-DSC). The system was externally coupled via a heated gas transfer line to a Bruker Invenio FTIR spectrometer equipped with a gas cell for evolved gas analysis. Samples were heated from 20ºC up to 800ºC at a rate of 10ºC/min in an argon atmosphere (50 mL/min). FTIR spectra were recorded at 13.5-second intervals, generating over 300 spectra. Thermograms were processed and analysed using Netzsch Proteus thermal analysis software (8.0.3). FTIR spectra were extracted and interpreted using OPUS 3D (8.5).

5.2.3 Limitations

TGA-DSC-FTIR analysis has a maximum sample size of 2g, including the crucible weighing approximately 160mg. This leaves a maximum sample weight of 1.8g. In environmental studies, small sample sizes may not accurately reflect the heterogeneity of the matrix and contamination of MPs. It is recommended that larger sample sizes be concentrated using MP extraction techniques. However, a lack of method standardisation for MP extraction in soil limits the comparability and cross-validation of studies.

Detecting and characterising trace MPs in soil is challenging, and samples are consumed during thermal analysis, which limits reproducibility, cross-validation, and the ability to re-analyse samples. Reproducibility also requires the conditions to be as controlled as possible: size and shape of the sample, the type of atmosphere in which the sample is heated, and the heating rate (Mariano et al., 2021). While analytical conditions are controllable, the MP particles and the soils environment's heterogeneity present challenges.

For thermal analysis, polymer types can only be identified on the premise that their melting points are differentiated and do not overlap, which may not be ideal for environmental samples. For evolved gas analysis, polymer identification requires at least one unique or specific thermal decomposition product, which can be challenging to identify. Lastly, reference spectral libraries are critical for polymer identification using spectroscopy, yet their availability for evolved gas analysis is currently limited.

5.2.4 Workflow

Data generated from thermal and evolved gas analysis below 200ºC was excluded, as it primarily corresponds to moisture loss and volatile organic matter decomposition (Iswahyudi et al., 2024). Data above 600ºC was also excluded, as complete polymer decomposition occurred before reaching these temperatures. TG, DSC, and Gram-Schmidt profiles were manually inspected for unique decomposition properties and unique gas evolution temperatures. Spectra were then manually extracted at key temperatures identified using TG, DSC, and Gram-Schmidt profiles. In contrast, spectral matching for polymer identification was automated for the qualitative chemical identification of MPs in ATBs and soil. The following workflow was used:

I. Thermal Analysis

Thermogravimetric Analysis (TGA)

- TG profiles were plotted and overlaid with derivative thermogravimetric (DTG) curves to highlight the rate of mass loss as a function of temperature.
- Curves were smoothed to the seventh order to reduce noise while maintaining key peaks.
- Degradation onset (To) and peak degradation (Td) temperatures were identified.

Differential Scanning Calorimetry (DSC) Analysis

- DSC profiles were plotted alongside derivative DSC (DDSC) curves to assess polymer phase transitions.
- Curves were smoothed to the seventh order to reduce noise while maintaining key peaks.
- Prominent endothermic peak(s) were identified to distinguish volatilisation events.

II. Evolved Gas Analysis

Gram-Schmidt Analysis

- Gram-Schmidt profiles were plotted with derivative (d(GS)/dt) curves to assess the total infrared absorbance of evolved gasses as a function of temperature.
- Curves were smoothed to the third order to reduce noise while maintaining peak intensity.
- Temperatures where abrupt increases in gas evolution occurred were identified.

Extraction of Fourier-transform-infrared (FTIR) spectra

- Spectra were extracted at temperatures where peak degradation, prominent exothermic peaks, and peak gas evolution occurred based on TGA, DSC, and Gram-Schmidt profiles.

III. Compilation of Reference Library

- Extracted reference polymer spectra were vector-normalised to eliminate intensity variability between samples.
- Normalisation was performed by calculating the average y-value of the spectrum and subtracting it from the total spectrum.
- Normalisation is critical for standardising the dataset and ensuring intensity-independent comparison.
- Normalised spectra of reference polymers were then compiled into a gas-phase spectral reference library.

IV. Extracted ATBs and Soil Samples

- The above steps, I (Thermal Analysis) and II (Evolved Gas Analysis) were repeated.
- Spectra were also extracted at peak degradation, prominent exothermic peaks, and peak gas evolution temperatures of reference polymers.

Spectral Matching and Identification

- Extracted spectra from ATB and soil were vector normalised.
- Normalised spectra were cross-referenced with the above-generated gas-phase reference library using the ‘spectra fingerprint’ region of ~1700-600cm^{-1}.
- A minimum hit quality index (HQI) of 500 was set as the threshold for spectral identification.

5.3 RESULTS AND DISCUSSION

5.3.1 Reference Polymers

Thermal Analysis

The observed thermal stability and decomposition characteristics of the reference polymers from TG and DTG curves are shown in Figure 21. Many of the polymers are difficult to distinguish from one another, exhibiting overlapping thermal decompositions. Polymers such as ABS, acrylic, and PS display similar degradation behaviour, with overlapping degradation onset and peak degradation temperatures. Similarly, the PE variants (PE, PET, and PETE) are indistinguishable. HDPE and LDPE alter slightly from one another, with higher degradation values for HDPE, but are too similar to reliably differentiate using TGA alone. In contrast, PP stands out as the most thermally distinct polymer, with the lowest onset and highest peak degradation temperatures. ABS, PE, PP, and PS spiked soil TG profiles can be seen in Appendix C, Figure C1. Table 1 below summarises the degradation onset (To) and peak degradation temperatures (Td) observed for each reference polymer.

Table 4. Observed temperatures of reference polymer degradation onset (To) and peak decomposition (Td) using TGA and DSC.

Polymer	Structure	To (ºC)	Td (ºC)
ABS	Amorphous	350 - 370	~ 418
Acrylic	Semicrystalline	370 - 390	~ 416
HDPE	Semicrystalline	420 - 440	~ 481
LDPE	Semicrystalline	400 - 420	~ 473
PE	Semicrystalline	360 - 380	~ 434
PET	Semicrystalline	355 - 375	~ 438
PETE	Semicrystalline	360 - 380	~ 438
PP opaque	Semicrystalline	330 - 350	~ 462
PP White	Semicrystalline	340 - 360	~ 468
PS	Amorphous	330 - 350	~ 414

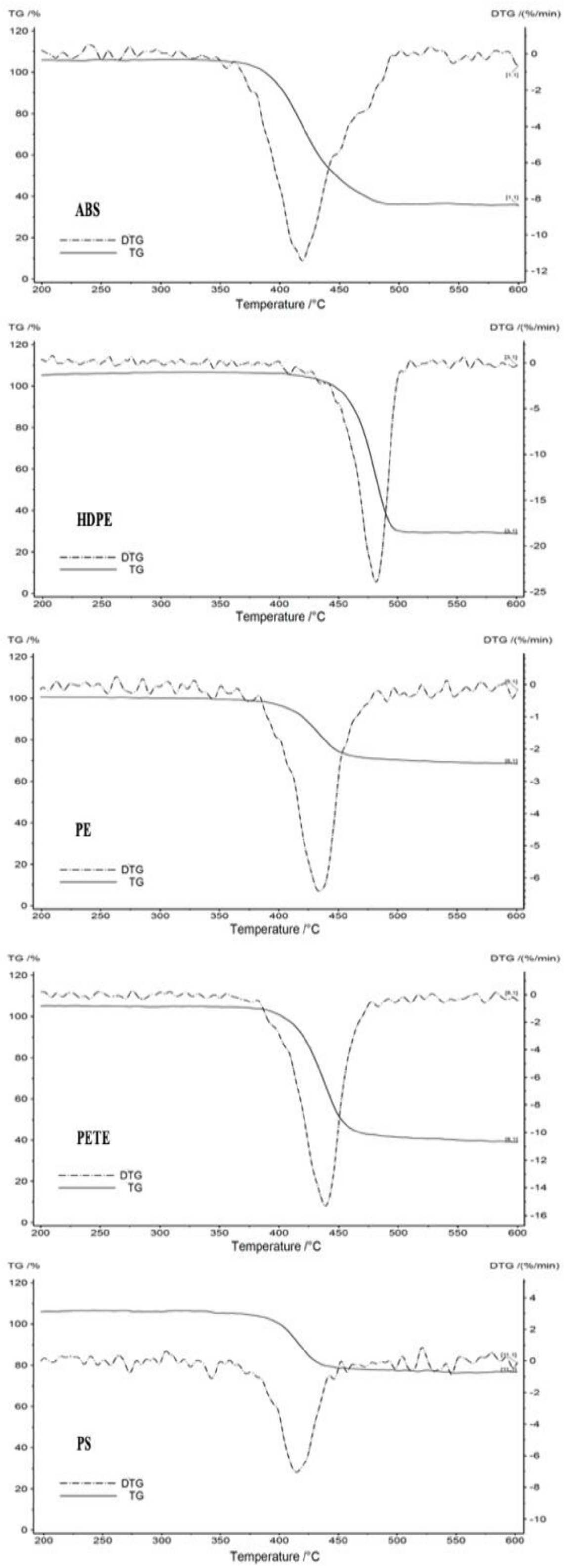

Figure 21. TG curve (solid line) shows the mass loss (%) as temperature increases. DTG curve (dashed line) indicates the rate (%/min) of mass loss as a function of temperature.

The DSC and DDSC curves in Figure 22 provide further insight into polymer phase transitions and decomposition behaviour within the parameters of this study. ABS and PS did not exhibit strong melting transitions like other polymers; instead, they gradually softened as heated. This is expected because they are amorphous polymers lacking well-defined crystalline structures (Sorolla-Rosario et al., 2022; Yang et al., 2004; Zhao & Fan, 2001). Meanwhile, semicrystalline polymers, such as PE, PET, and PETE, showed signs of multi-step decomposition, which may indicate an initial molecular rearrangement or recrystallisation at lower temperatures, followed by decomposition at higher temperatures. While acrylic, HDPE, and LDPE all display single-step decompositions, indicating minimal structural changes before complete decomposition. Lastly, PP shows a more complex multi-stage decomposition, potentially blurred by the degradation of additives adjacent to the polymer structure or a gradual softening. ABS, PE, PP, and PS spiked soil DSC profiles can be seen in Appendix C, Figure C2. While the combination of TG and DSC analysis provides essential thermal stability data, many polymers have overlapping decomposition temperatures, which makes their identification difficult and limits the application of TGA-DSC in multicomponent environmental matrices. The integration of subsequent evolved gas analysis to complement TG-DSC may be useful in providing a more refined analysis.

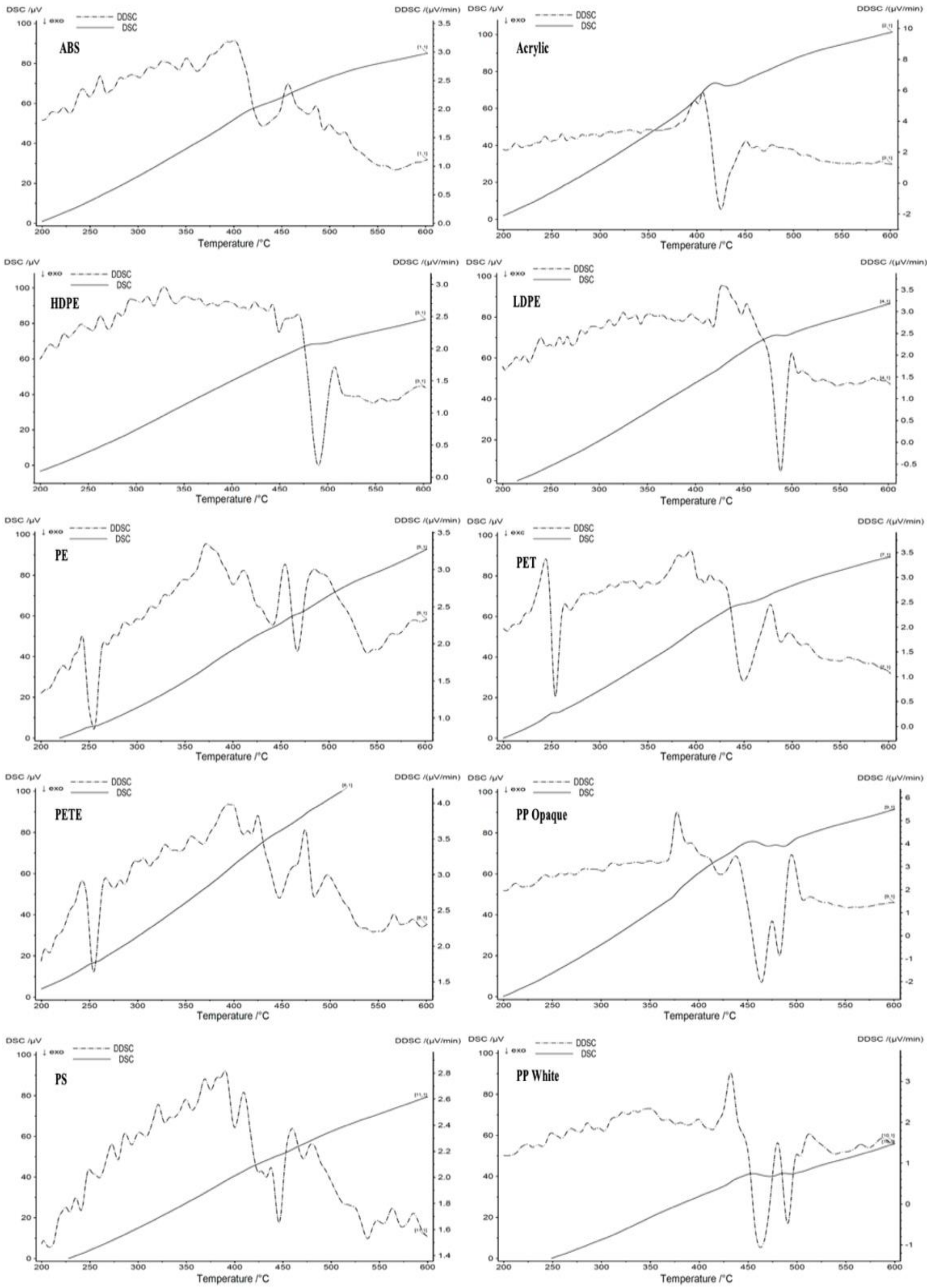

Figure 22. DSC curve (solid line) shows enthalpy changes as temperature increases (µV). DDSC curve (dashed line) represents the rate (µV/min) of heat flow change as a function of temperature.

Evolved Gas Analysis

The total infrared absorbance of the evolved gases from Gram-Schmidt curves and d(GS)/dt) curves are shown in Figure 23. Volatile decomposition products are all perceived to coincide with both TGA and DSC observations, correlating mass loss events with the volatilisation of decomposition products. A slight delay between mass loss detection (TG/DSC) and gas evolution detection is expected, as the gasses must pass through a heated transfer line, but it is minimal, as the heating rates were all kept to a consistent 10ºC/ min.

The addition of evolved gas analysis did not directly increase the distinguishability of each polymer type, and overlaps in phase transitions remain. However, using Gram-Schmidt gas evolution curves, further differences in decomposition behaviour are slightly more discernible. Acrylic is now distinguished by a single intense volatilisation event at approximately 420ºC. In comparison, ABS has a peak gasification at approximately 425ºC and PS at 390 and 450ºC. The previously observed two-step decomposition of PET and PETE based on TGA and DSC was not supported by evolved gas analysis as only a single volatilisation event was observed at approximately 440ºC. PE displayed multiple endothermic peaks at approximately 250, 420, and 510ºC. The multiple evolved gas peaks may be caused by the sample being in the form of fibres and not a single fragment, providing inconsistencies with results as they depend on consistent sample size and shape. This inconsistency highlights the urgency for MP studies that assess all shapes and sizes of MP particles. HDPE and LDPE exhibit a single strong gasification peak at approximately 440 and 430ºC, respectively, and remain hard to distinguish. Lastly, PP exhibits a single intense gasification event at approximately 425ºC. ABS, PE, PP, and PS spiked soil Gram-Schmidt's profiles can be seen in Appendix C, Figure C3. Adding Gram-Schmidt peaks proved valuable for assessing whether each polymer undergoes multi- or single-stage decomposition patterns. However, it is most beneficial for identifying distinct gas evolution peaks, indicating when spectra should be extracted to complete the chemical identification of polymers. Spectra extracted from Gram-Schmidt peaks for each reference polymer can be seen in Appendix C Figures C4-13, and ABS, PE, PP, and PS spiked soils in Figure C14.

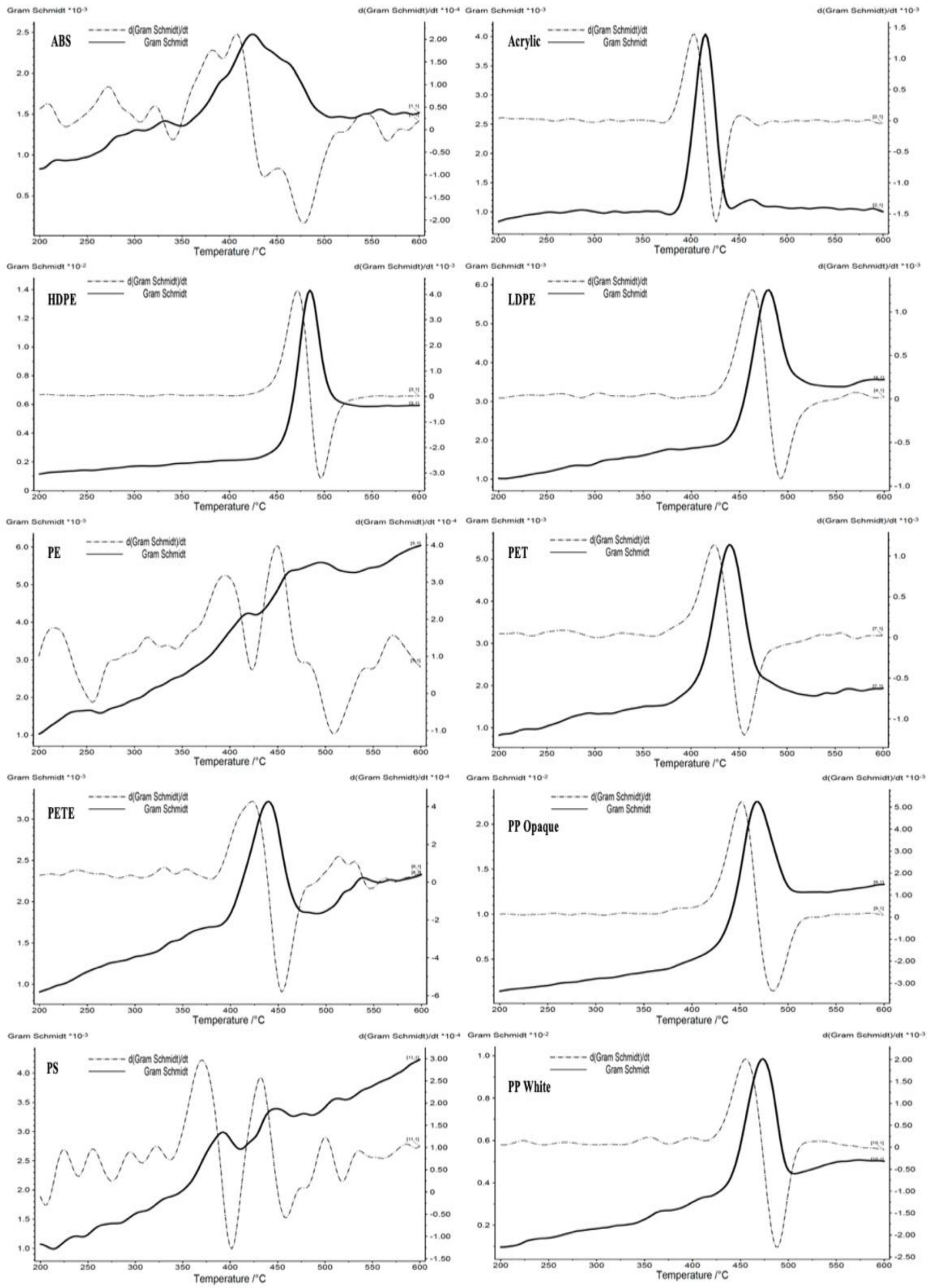

Figure 23. Gram-Schmidt curve (solid line) represents the total infrared absorbance of evolved gasses as a function of temperature. The d(Gram Schmidt/dt) curve (dashed line) indicates changes in the rate of gas evolution as a function of temperature.

5.3.2 Alkaline-Treated Biosolids

Thermal Analysis

The observed thermal stability and decomposition characteristics of ATBs from 2010, 2014, 2021, and 2023 used as replicates are shown in Figure 24 a). A main degradation event with an onset of approximately 250ºC and a peak mass loss event between 325 and 345ºC can be seen. Then, another degradation onset around 400ºC with a peak mass loss between 450 and 500ºC is visible. The first could more closely indicate biomass degradation, such as cellulose, which typically displays peak mass loss between 315 to 400ºC (Mironova et al., 2019; Yang et al., 2007). Solid wastes from wastewater treatment plants contain large amounts of biomass, and similarly to MPs, they can be concentrated in the sludge, are resistant to organic matter removal steps, and can lead to false identifications of MPs (Lares et al., 2018; Letwin et al., 2024). However, there is minimal literature on the TGA profile of ATBs, an area of study that could greatly benefit from future exploration. The second mass loss event more closely indicates MP presence, coinciding with PP, LDPE, and HDPE, but other polymer types cannot be ruled out.

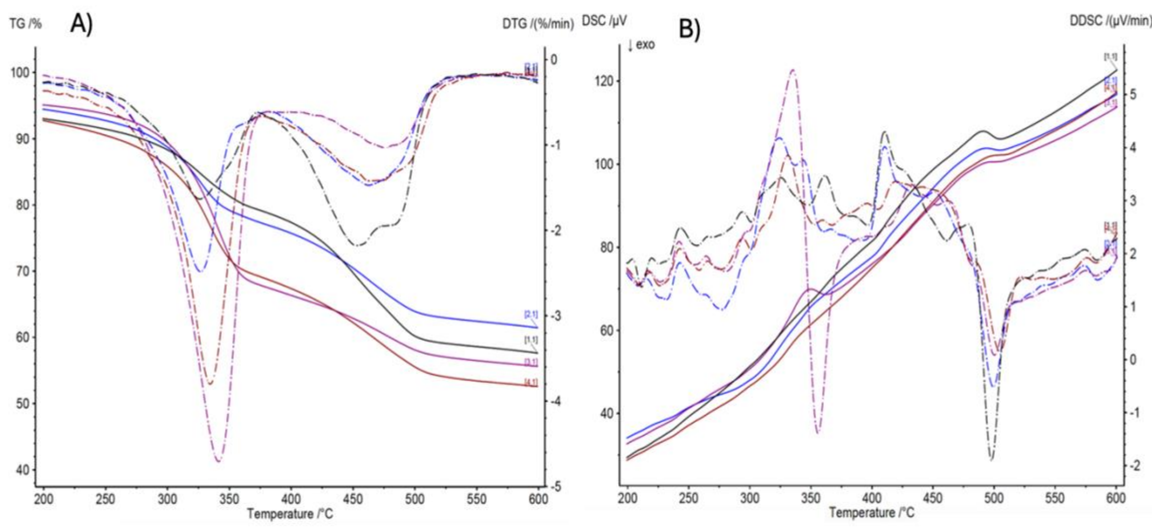

*Figure 24. TGA and DSC profiles of ATB samples with years as replicates (black:2010, blue:2014, purple:2021, brown:2023). **A)** TG curves (solid line) depict the mass loss (%) as the sample is heated, and DTG (dashed line) indicates the rate (%/min) of mass loss as a function of temperature. **B)** DSC curve (solid line) displays enthalpy changes (µV) as the sample is heated, and the DDSC (dashed line) shows the rate (µV/min) of heat flow changes as a function of temperature.*

The ATB phase transitions in response to heating are shown in Figure 24 b) above and confirm the complex multi-stage decomposition of ATBs within the parameters of this study. The first exothermic heat flux event is gradual, peaking between 350 and 400ºC, which more strongly aligns with biomass decomposition (Yang et al., 2007). The second exothermic heat flow event begins at approximately 425ºC and then occurs more sharply around 500ºC and aligns more similarly with reference polymers PP, LDPE, HDPE, PE, and potentially PS.

Evolved Gas Analysis

The evolved gasses from the decomposition of ATBs are shown in Figure 25. The two decomposition events perceived with the TGA and DSC curves are even more distinct. Spectra were extracted from the peak volatilisation event occurring between 325 and 350ºC and again from the second event between 450 and 500ºC. At the initial peak, spectra were matched to PS and PE, and at the second peak, PS and PP. The extracted gas-phase spectra from ATBs can be seen in Appendix C Figure C15. Additionally, an example of Spectral matching can be seen in Appendix C Figure C17. Using solid-state ATR-µFTIR, Letwin et al. (2023) found the MP composition of ATBs to be primarily polyamide (PA), PP, PET, and polyacrylamide (PAM). Also, PET, PP, PE, and ABS have been identified by Chen et al. (2024) in municipal biosolids using TGA-FTIR. In this study, a wider variety of reference samples would be needed to positively identify a broader range of polymer types.

Despite organic matter removal, some organic matter was present, and polymers were not the most abundant material in the heterogeneous ATB samples. Thus, the extracted MPs within the sample may not coincide with each peak volatilisation event and be overlooked if only major events are examined. To test this, spectra were also extracted at temperatures where the gas evolution peaks of polymers were expected based on reference peaks, but no additional polymer types were identified.

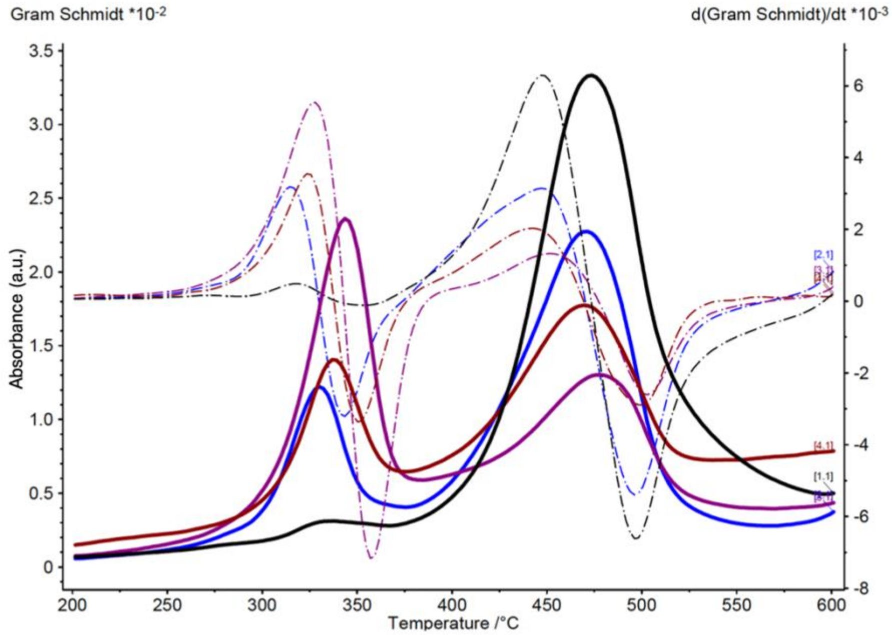

Figure 25. Gram-Schmidt profile of ATBs with years as replicates (black:2010, blue:2014, purple:2021, brown:2023). The solid line represents the total infrared absorbance of evolved gasses, and the dashed line indicates changes in the rate of gas evolution as a function of temperature.

5.3.3 Soil

Thermal Analysis

The observed decomposition and thermal stability characteristics of soil samples that had received 15 years of 42 tonnes ha^{-1} ATB (wet weight) applications are shown in Figure 26 a). A distinguishable sharp mass loss event is observed with an onset at approximately 430ºC and a mass loss peak between 465 and 475ºC. This coincides most closely with the reference polymers HDPE, LDPE, and PP. Some residual mass loss is detected above 500ºC and could be from inorganic residues such as minerals (Fernández et al., 2012). A study by Chen et al. (2024) using TGA on MP spiked soils observed two mass loss events, the first at ~200-400ºC that was attributed to cellulose, and again at ~400 – 500º attributed to MPs, aligning with the results of this study.

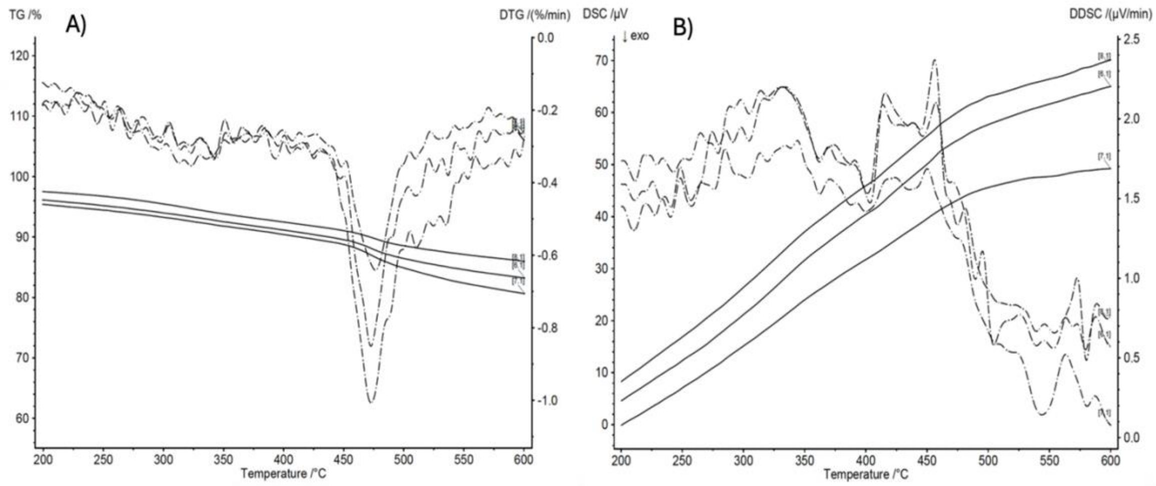

Figure 26. TGA and DSC profiles of soil (in triplicate) that has received 15 years of 42 tonnes ha^{-1} ATBs (wet weight). ***A)*** *TG curves (solid line) depict the mass loss (%) as the sample is heated, and DTG (dashed line) indicates the rate (%/min) of mass loss as a function of temperature.* ***B)*** *DSC curves (solids line) display enthalpy changes (µV) as the sample is heated, and DDSC (dashed line) shows the rate (µV/min) of heat flow changes as a function of temperature.*

Soil phase transitions in response to heating are shown in Figure 26 b) above, exposing a more complex decomposition than the TGA analysis alone. Gradual heat fluxes are perceived and potentially arise from the heterogeneous soil samples and residual mineral content that persists despite sample pre-processing. A gradual decomposition can be seen with exothermic heat fluxes between 330 and 400ºC, 420 and 440ºC, and the largest one continuing beyond approximately 460ºC. The gradual exothermic fluxes present beyond 460ºC may coincide with inorganic soil fractions rather than polymers (Fernández et al., 2012). It is too difficult to distinguish specific polymer types from the heat fluxes at lower temperatures, with overlapping phase transitions.

Evolved Gas Analysis

The evolved gasses from the decomposition of soil are shown in Figure 27 and display a prominent decomposition event between approximately 460 and 480ºC, most closely resembling PP, HDPE, and LDPE. Spectra extracted at the Gram-Schmidt peak and tested against the reference samples had matches with PE, aligning with one of the polymer types identified in the ATBs. Despite organic matter removal, some organic matter persisted, and polymers were not the most abundant material in the heterogeneous sample. Variations can be seen along the curve leading up to the largest gasification event. While these samples have undergone pre-sample processing to concentrate and extract MPs, they are still dominated by soil inorganic components. Consequently, polymers within the soil samples may not coincide with main volatilisation events and get overlooked if spectra are only extracted from these peak events. Thenceforth, spectra were also extracted at temperatures where reference polymers were expected to gasify based on reference polymer TG, DSC, and Gram-Schmidt results. This approach improved MP chemical identification to include PP and PS in addition to PE. Examples of extracted gas-phase spectra can be seen in Appendix C Figure C16 and an example of spectral matching in Figure C18.

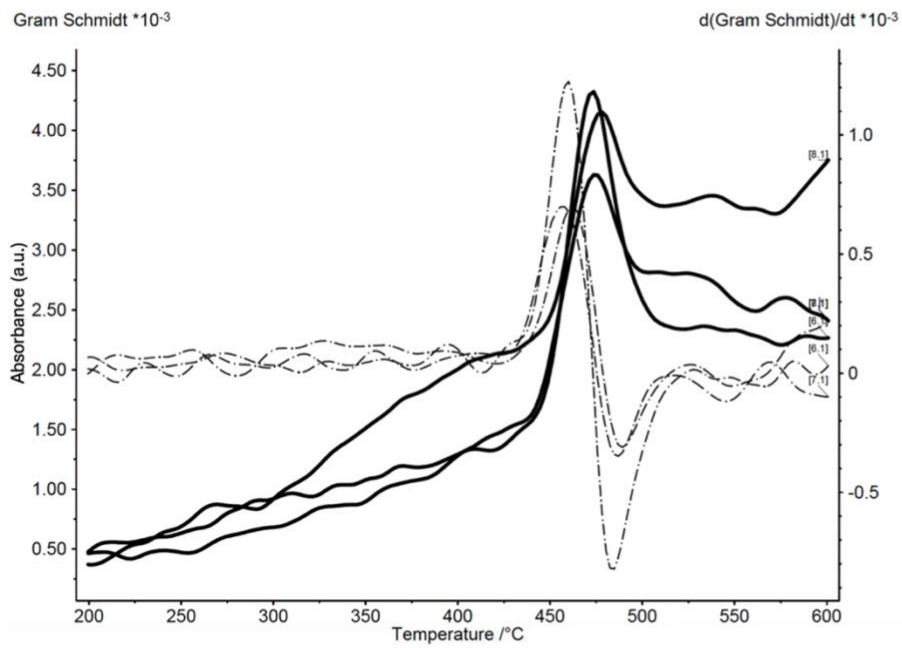

Figure 27. Gram-Schmidt profile of soil (in triplicate) that has received 15 years of 42 tonnes ha^{-1} ATBs (wet weight). The solid line represents the total infrared absorbance of evolved gasses as a function of temperature. The dashed line indicates changes in the rate of gas evolution as a function of temperature.

5.4 FUTURE CONSIDERATIONS

There is currently no standard methodology for sample preparation, temperature settings, spectral matching, or data interpretation for TGA-DSC-FTIR analysis of MPs extracted from different environmental matrices, such as soils, ATBs, or other forms of biosolids or composts. While this Chapter demonstrates the potential of TGA-DSC-FTIR, it only begins to explore its capabilities. This technique could be implemented for more advanced MP analysis, including polymer mass quantification using calibration curves, identifying specific pyrolysis products for each polymer type, identifying intermediate degradation products of polymers, assessing how weathered and pristine polymer degradations differ, and much more. However, an optimised method to implement TGA-DSC-FTIR must first be developed.

Firstly, tackling sample pre-treatment and instrument protocols to create a single optimised method would greatly benefit this area of study. MPs comprise only small percentages of the total mass of samples tested for their presence, leaving this form of analysis vulnerable with such small sample sizes. Optimising sample pre-treatment to extract and concentrate MPs and enhancing instrument calibration and signal processing to improve detection limits could significantly increase the identification of MPs. In complex matrices, such as soils, this study found that MP polymer gas evolution signals can be masked by other more abundant materials, and spectra should also be extracted from expected polymer decomposition temperatures. Establishing more consistent guidelines for future use will improve this form of analysis's credibility, comparability, and reproducibility.

Next, a lack of spectra reference libraries, particularly for evolved gas analysis, presents a significant obstacle for routine analysis. Most established libraries are designed for solid-state polymer analysis using μFTIR or Raman spectroscopy rather than for evolved gasses generated during thermal decomposition. Without comprehensive reference spectra for MP gaseous byproducts, polymer identification based on thermal decomposition remains a labour-intensive and challenging manual process. Future studies should focus on identifying gaseous byproducts from MP thermal decomposition and developing corresponding spectral reference libraries. Gas-phase analysis should follow the progress made in solid-state MP identification and develop open-source reference libraries similar to Open Specy (Cowger et al., 2020) and FLOPP or FLOPP-e (De Frond et al., 2021). Open-source libraries offer a unique opportunity for mass collaboration, enabling the creation of extensive spectral libraries that contain diverse polymer types, particle morphologies, and environmental weathering conditions. The creation of such a resource would significantly aid the advancement of MP identification in many matrices, including but not limited to soil.

Lastly, TGA-DSC-FTIR analysis is time-consuming, and data interpretation is complex. Integrating machine learning algorithms could automate this form of analysis, improving accuracy and facilitating method standardisation. This study did not implement machine learning due to limitations in dataset availability, computational expertise, and the absence of standardised spectral libraries for evolved gas analysis. However, future research should explore automated data processing techniques to enhance the efficiency and applicability of TGA-DSC-FTIR for routine MP monitoring in ATBs, soils, and other MP-contaminated matrices. Doing so could expand the implementation of this method into real-world applications for the routine monitoring of MPs in ATBs and soils.

5.5 CONCLUSION

This chapter applied TGA-DSC-FTIR for the chemical identification of MP polymer types in ATBs and soils amended with ATBs. Polyethene (PE), polypropylene (PP), and polystyrene (PS) were successfully identified in both ATB samples and agricultural soils subjected to 15 years of 42 tonnes ha^{-1} (wet weight) ATB applications, further reinforcing ATBs as a significant source of MP contamination. While TGA and DSC provided insights into polymer presence, their specificity was limited due to overlapping phase transitions, emphasizing the necessity of evolved gas analysis via FTIR for enhanced polymer identification in complex matrices.

Despite these successes, challenges remain in optimizing this approach for broader environmental applications. The lack of comprehensive evolved gas spectral libraries and standardised workflows currently limits its reproducibility and quantitative potential. Future research should focus on improving reference databases and refining analytical protocols to strengthen the reliability of TGA-DSC-FTIR as a tool for routine MP characterisation in environmental matrices.

CHAPTER 6: OVERALL CONCLUSIONS

This research provides strong evidence of MPs long-term accumulation, persistence, and vertical movement in agricultural soils receiving long-term applications of ATBs, directly addressing the study's objectives. ATBs were identified as the predominant source of MP contamination at the long-term research site, containing on average 138,600 (117,444, 159,757) MP particles kg^{-1} (dry weight), predominantly composed of fragments (84%), followed by fibres (13%) and spheres (3%), with median sizes of 127 µm, 596 µm, and 71 µm, respectively. The composition of MPs in soils receiving ATB applications mirrored that of ATBs, reinforcing their role as the primary source of contamination. Further solidifying this, polymers were chemically identified as PS, PP, and PE in ATB and soil samples using TGA-DSC-FTIR.

Long-term soil monitoring over 15 years demonstrated significant MP accumulation in surface soils, which increased with repeated ATB applications. Even a single application of ATBs resulted in long-term persistence, with no significant changes in particle size over time, reinforcing their long-term resistance to degradation. Annual application plots showed an 8.7x increase in MP abundance receiving 14 tonnes ha^{-1} (wet weight) ATBs and a 9.3x increase in plots receiving 42 tonnes ha^{-1} (wet weight) ATBs. However, a tripling of the application rate did not result in a tripling in MP accumulation and indicates the redistribution of MPs within the soil and possible migration to surrounding environmental matrices.

MPs demonstrated vertical mobility, with smaller MPs migrating to deeper soil layers, reinforcing concerns about MP movement and retention within agricultural soils. Increased application rates of ATBs resulted in significantly more MP accumulation in the surface soil layers of 0-15 and 15-30 cm depths but did not appear to impact vertical movement at deeper soil depts. This may indicate the horizontal and vertical dispersion of MPs in the soil and that high input pressure may not drive more vertical migration.

Overall, this study provides a foundational assessment of MP behaviour from a research site with high-frequency of biosolid-amended soils, provides a proof-of-concept on the application of TGA-DSC-FTIR for MP identification in complex matrices, and highlights the urgent need for continued research on the long-term environmental implications of MP contamination in agricultural soils. Ensuring sustainable agricultural practices, soil health, and global food security requires a better understanding of MP persistence and mobility. This study reinforces the necessity for stricter biosolid treatment regulations, improved waste management strategies, and enhanced MP monitoring protocols. As the global reliance on plastic continues, proactive measures are essential to mitigate MP pollution and its cascading effects on soil function and ecosystem stability. Addressing these challenges demands a collaborative effort between scientists, policymakers, and agricultural stakeholders to develop science-based solutions and regulatory frameworks that minimize the long-term risks of MP contamination in terrestrial environments and protect soil health, agricultural productivity, and food security.

6.1 OUTLOOK

Environmental plastic contamination is one of the most significant challenges the planet is currently facing, with mounting evidence of its far-reaching consequences on ecosystems, biodiversity, and human health. This study demonstrates that MPs in biosolid-amended soils persist long-term, accumulate with repeated applications, and exhibit vertical mobility within the soil profile. These findings reinforce the urgent need to address plastic contamination in agricultural systems.

The current “take-make-dispose” plastic economy, characterised by the widespread use of synthetic polymers with little concern for their end-of-life fate, is unsustainable. Agricultural amendments derived from waste streams, such as biosolids, are a valuable resource for improving soil health and nutrient availability and recycling organic wastes toward a circular economy. However, as demonstrated in this study, their use introduces MPs into the environment, potentially altering soil properties, contaminating crops, and threatening food security. A top-down approach is necessary to address these concerns, beginning with stricter oversight of plastic additives, improved waste management strategies, and greater transparency across the plastic value chain—including proprietary blends, degradation pathways, and environmental fate.

Scientific consensus is increasingly urging policymakers to categorize plastics as persistent, bioaccumulative, and toxic (PBT) contaminants (Alva et al., 2023). Classifying MPs under this framework would enable governments to establish enforceable regulations to control, limit, or eliminate the manufacture of harmful plastic products. Additionally, such measures would compel industrial sectors to report their contributions to environmental MP contamination. Some experts advocate for a global plastic treaty, incorporating six key pillars to address plastic pollution holistically: (1) reduction and simplification of plastic chemicals, (2) safe and sustainable polymer design, (3) economic incentives for change, (4) the development of alternative materials, (5) just and equitable interventions, and (6) centring human rights in plastic governance (Brander et al., 2024). The United Nations Environmental Programme (UNEP) Environment Assembly (2022) Resolution 5/14 aligns with this perspective, stating that international policies should aim to "prevent plastic pollution and its related risks to human health and adverse effects on human well-being and the environment."

Despite increasing awareness, significant knowledge gaps remain regarding MPs in agricultural systems. The long-term ecological consequences of MPs in soil ecosystems remain poorly understood. Future research should prioritize:

- Soil-MP interactions: How do MPs alter microbial communities, soil structure, and nutrient cycling?
- Plant uptake and trophic transfer: Do MPs absorbed by crops pose risks to food safety and human health?
- Transport mechanisms: How do MPs migrate through soil profiles, and what environmental conditions influence their persistence?
- Risk assessment and mitigation strategies: How can agricultural policies adapt to minimize MP contamination while maintaining soil fertility and productivity?

This study contributes to the growing body of literature emphasizing the need for science-based regulatory frameworks, technological advancements in plastic monitoring, and interdisciplinary collaboration among scientists, policymakers, and agricultural stakeholders. Addressing MP pollution requires a multi-pronged approach—from reducing plastic inputs at the source to developing effective waste management and remediation strategies. As plastic production continues to increase worldwide, the integration of scientific research into environmental policy will be critical in safeguarding soil health, food security, and ecosystem resilience for future generations.

REFERENCES

Abbasi, S., Jaafarzadeh, N., Zahedi, A., Ravanbakhsh, M., Abbaszadeh, S., & Turner, A. (2023). Microplastics in the atmosphere of Ahvaz City, Iran. *Journal of Environmental Sciences*, *126*, 95–102. https://doi.org/10.1016/j.jes.2022.02.044

Accinelli, C., Abbas, H. K., Shier, W. T., Vicari, A., Little, N. S., Aloise, M. R., & Giacomini, S. (2019). Degradation of microplastic seed film-coating fragments in soil. *Chemosphere*, *226*, 645–650. https://doi.org/10.1016/j.chemosphere.2019.03.161

Ahmad, M., & Bajahlan, A. S. (2007). Leaching of styrene and other aromatic compounds in drinking water from PS bottles. *Journal of Environmental Sciences*, *19*(4), 421–426. https://doi.org/10.1016/S1001-0742(07)60070-9

Alava, J. J., Jahnke, A., Bergmann, M., Aguirre-Martínez, G. V., Bendell, L., Calle, P., Domínguez, G. A., Faustman, E. M., Falman, J., Kazmiruk, T. N., Klasios, N., Maldonado, M. T., McMullen, K., Moreno-Báez, M., Öberg, G., Ota, Y., Price, D., Shim, W. J., Tirapé, A., … Weis, J. (2023). A Call to Include Plastics in the Global Environment in the Class of Persistent, Bioaccumulative, and Toxic (PBT) Pollutants. *Environmental Science & Technology*, *57*(22), 8185–8188. https://doi.org/10.1021/acs.est.3c02476

Allen, S., Allen, D., Phoenix, V. R., Le Roux, G., Durántez Jiménez, P., Simonneau, A., Binet, S., & Galop, D. (2019). Atmospheric transport and deposition of microplastics in a remote mountain catchment. *Nature Geoscience*, *12*(5), 339–344. https://doi.org/10.1038/s41561-019-0335-5

Al-Malack, M. H. (2001). Migration of lead from unplasticized polyvinyl chloride pipes. *Journal of Hazardous Materials*, *82*(3), 263–274. https://doi.org/10.1016/S0304-3894(00)00366-6

Almeida, M. P. de, Gaylarde, C., Pompermayer, F. C., Lima, L. da S., Delgado, J. de F., Scott, D., Neves, C. V., Vieira, K. S., Baptista Neto, J. A., & Fonseca, E. M. (2023). The Complex Dynamics of Microplastic Migration through Different Aquatic Environments: Subsidies for a Better Understanding of Its Environmental Dispersion. *Microplastics*, *2*(1), Article 1. https://doi.org/10.3390/microplastics2010005

Andjelković, T., Bogdanović, D., Kostić, I., Kocić, G., Nikolić, G., & Pavlović, R. (2021). Phthalates leaching from plastic food and pharmaceutical contact materials by FTIR and GC-MS. *Environmental Science and Pollution Research*, *28*(24), 31380–31390. https://doi.org/10.1007/s11356-021-12724-0

Andra, S. S., Makris, K. C., Shine, J. P., & Lu, C. (2012). Co-leaching of brominated compounds and antimony from bottled water. *Environment International*, *38*(1), 45–53. https://doi.org/10.1016/j.envint.2011.08.007

Andrady, A. L. (2017). The plastic in microplastics: A review. *Marine Pollution Bulletin*, *119*(1), 12–22. https://doi.org/10.1016/j.marpolbul.2017.01.082

Aquino, V. N., Plaul, F. E., Sanchez, A. D., Villagra, S., & Cappelletti, N. E. (2023). Microplastics and hydrocarbons in soils: Quantification as an anthropic carbon source. *Integrated Environmental Assessment and Management*, *19*(3), 698–705. https://doi.org/10.1002/ieam.4694

Aves, A. R., Revell, L. E., Gaw, S., Ruffell, H., Schuddeboom, A., Wotherspoon, N. E., LaRue, M., & McDonald, A. J. (2022). First evidence of microplastics in Antarctic snow. *The Cryosphere*, *16*(6), 2127–2145. https://doi.org/10.5194/tc-16-2127-2022

Baekeland, L. H. (1909). *Method of Making Insoluble Products of Phenol and Formaldehyde.* (Patent US942699A).

Bardgett, R. D., & van der Putten, W. H. (2014). Belowground biodiversity and ecosystem functioning. *Nature*, *515*(7528), 505–511. https://doi.org/10.1038/nature13855

Bertelsen, R. J., Carlsen, K. C. L., Calafat, A. M., Hoppin, J. A., Håland, G., Mowinckel, P., Carlsen, K.-H., & Løvik, M. (2013). Urinary Biomarkers for Phthalates Associated with Asthma in Norwegian Children. *Environmental Health Perspectives*, *121*(2), 251–256. https://doi.org/10.1289/ehp.1205256

Blair, R. M., Waldron, S., Phoenix, V. R., & Gauchotte-Lindsay, C. (2019). Microscopy and elemental analysis characterisation of microplastics in sediment of a freshwater urban river in Scotland, UK. *Environmental Science and Pollution Research*, *26*(12), 12491–12504. https://doi.org/10.1007/s11356-019-04678-1

Blume, H.-P., Brümmer, G. W., Fleige, H., Horn, R., Kandeler, E., Kögel-Knabner, I., Kretzschmar, R., Stahr, K., & Wilke, B.-M. (2016). *Scheffer/SchachtschabelSoil Science*. Springer Berlin Heidelberg. https://doi.org/10.1007/978-3-642-30942-7

Boots, B., Russell, C. W., & Green, D. S. (2019). Effects of Microplastics in Soil Ecosystems: Above and Below Ground. *Environmental Science & Technology*, *53*(19), 11496–11506. https://doi.org/10.1021/acs.est.9b03304

Boucher, J., & Friot, D. (2017). *Primary microplastics in the oceans: A global evaluation of sources*. IUCN International Union for Conservation of Nature. https://doi.org/10.2305/IUCN.CH.2017.01.en

Brander, S. M., Senathirajah, K., Fernandez, M. O., Weis, J. S., Kumar, E., Jahnke, A., Hartmann, N. B., Alava, J. J., Farrelly, T., Almroth, B. C., Groh, K. J., Syberg, K., Buerkert, J. S., Abeynayaka, A., Booth, A. M., Cousin, X., Herzke, D., Monclús, L., Morales-Caselles, C., … Wagner, M. (2024). The time for ambitious action is now: Science-based recommendations for plastic chemicals to inform an effective global plastic treaty. *Science of The Total Environment*, *949*, 174881. https://doi.org/10.1016/j.scitotenv.2024.174881

Canadian Council of Ministers of the Environment (CCME). (2012). Guidance Document for the Beneficial Use of Municipal Biosolids, Municipal Sludge and Treated Septage. *Government of Canada*.

Carr, S. A., Liu, J., & Tesoro, A. G. (2016). Transport and fate of microplastic particles in wastewater treatment plants. *Water Research*, *91*, 174–182. https://doi.org/10.1016/j.watres.2016.01.002

Çelen Erdem, İ., Ünek, C., Akkuş Süt, P., Karabıyık Acar, Ö., Yurtsever, M., & Şahin, F. (2023). Combined approaches for detecting polypropylene microplastics in crop plants. *Journal of Environmental Management*, *347*, 119258. https://doi.org/10.1016/j.jenvman.2023.119258

Chamas, A., Moon, H., Zheng, J., Qiu, Y., Tabassum, T., Jang, J. H., Abu-Omar, M., Scott, S. L., & Suh, S. (2020). Degradation Rates of Plastics in the Environment. *ACS Sustainable Chemistry & Engineering*, *8*(9), 3494–3511. https://doi.org/10.1021/acssuschemeng.9b06635

Chanda, M., Wright, L., Manning-Berg, A., Bhattacharyya, D., & Bathi, J. R. (2025). *Microplastics Pollution in Urban Freshwater Sediments: Impact of Land Use on Their Distribution Pattern* (SSRN Scholarly Paper 5122707). Social Science Research Network. https://doi.org/10.2139/ssrn.5122707

Chen, M., Coleman, B., Gaburici, L., Prezgot, D., Jakubek, Z. J., Sivarajah, B., Vermaire, J. C., Lapen, D. R., Velicogna, J. R., Princz, J. I., Provencher, J. F., & Zou, S. (2024). Identification of microplastics extracted from field soils amended with municipal biosolids. *Science of The Total Environment*, *907*, 168007. https://doi.org/10.1016/j.scitotenv.2023.168007

Cho, M.-H., Song, Y.-J., Rhu, C.-J., & Go, B.-R. (2023). Pyrolysis Process of Mixed Microplastics Using TG-FTIR and TED-GC-MS. *Polymers*, *15*(1), Article 1. https://doi.org/10.3390/polym15010241

Cole, M., Webb, H., Lindeque, P. K., Fileman, E. S., Halsband, C., & Galloway, T. S. (2014). Isolation of microplastics in biota-rich seawater samples and marine organisms. *Scientific Reports*, *4*(1), 4528. https://doi.org/10.1038/srep04528

Collivignarelli, M. C., Canato, M., Abbà, A., & Carnevale Miino, M. (2019). Biosolids: What are the different types of reuse? *Journal of Cleaner Production*, *238*, 117844. https://doi.org/10.1016/j.jclepro.2019.117844

Corradini, F., Meza, P., Eguiluz, R., Casado, F., Huerta-Lwanga, E., & Geissen, V. (2019). Evidence of microplastic accumulation in agricultural soils from sewage sludge disposal. *Science of The Total Environment*, *671*, 411–420. https://doi.org/10.1016/j.scitotenv.2019.03.368

Costa, J. P. da, Paço, A., Santos, P. S. M., Duarte, A. C., & Rocha-Santos, T. (2018). Microplastics in soils: Assessment, analytics and risks. *Environmental Chemistry*, *16*(1), 18–30. https://doi.org/10.1071/EN18150

Cowger, W., Gray, A., Rochman, C., Primpke, S., Lynch, J., Hapich, H., Munno, K., Frond, H. D., & Herodotou, O. (2020). *Open Specy*. https://doi.org/10.17605/OSF.IO/3UATF

Crossman, J., Hurley, R. R., Futter, M., & Nizzetto, L. (2020). Transfer and transport of microplastics from biosolids to agricultural soils and the wider environment. *Science of The Total Environment*, *724*, 138334. https://doi.org/10.1016/j.scitotenv.2020.138334

Cui, W., Gao, P., Zhang, M., Wang, L., Sun, H., & Liu, C. (2022). Adverse effects of microplastics on earthworms: A critical review. *Science of The Total Environment*, *850*, 158041. https://doi.org/10.1016/j.scitotenv.2022.158041

Dang, T. T., Sogut, E., Uysal-Unalan, I., & Corredig, M. (2024). Quantification of polystyrene microplastics in water, milk, and coffee using thermogravimetry coupled with Fourier transform infrared spectroscopy (TGA-FTIR). *Chemosphere*, *368*, 143777. https://doi.org/10.1016/j.chemosphere.2024.143777

De Frond, H., Rubinovitz, R., & Rochman, C. M. (2021). μATR-FTIR Spectral Libraries of Plastic Particles (FLOPP and FLOPP-e) for the Analysis of Microplastics. *Analytical Chemistry*, *93*(48), 15878–15885. https://doi.org/10.1021/acs.analchem.1c02549

de Souza Machado, A. A., Lau, C. W., Till, J., Kloas, W., Lehmann, A., Becker, R., & Rillig, M. C. (2018). Impacts of Microplastics on the Soil Biophysical Environment. *Environmental Science & Technology*, *52*(17), 9656–9665. https://doi.org/10.1021/acs.est.8b02212

Dierkes, G., Lauschke, T., & Földi, C. (2022). Analytical Methods for Plastic (Microplastic) Determination in Environmental Samples. In F. Stock, G. Reifferscheid, N. Brennholt, & E. Kostianaia (Eds.), *Plastics in the Aquatic Environment—Part I: Current Status and Challenges* (pp. 43–67). Springer International Publishing. https://doi.org/10.1007/698_2021_744

Dong, R., Liu, R., Xu, Y., Liu, W., Wang, L., Liang, X., Huang, Q., & Sun, Y. (2022). Single and joint toxicity of polymethyl methacrylate microplastics and As (V) on rapeseed (Brassia campestris L.). *Chemosphere*, *291*(Pt 3), 133066. https://doi.org/10.1016/j.chemosphere.2021.133066

Duty, S. M., Silva, M. J., Barr, D. B., Brock, J. W., Ryan, L., Chen, Z., Herrick, R. F., Christiani, D. C., & Hauser, R. (2003). Phthalate exposure and human semen parameters. *Epidemiology (Cambridge, Mass.)*, *14*(3), 269–277.

Edo, C., González-Pleiter, M., Leganés, F., Fernández-Piñas, F., & Rosal, R. (2020). Fate of microplastics in wastewater treatment plants and their environmental dispersion with effluent and sludge. *Environmental Pollution*, *259*, 113837. https://doi.org/10.1016/j.envpol.2019.113837

Elert, A. M., Becker, R., Duemichen, E., Eisentraut, P., Falkenhagen, J., Sturm, H., & Braun, U. (2017). Comparison of different methods for MP detection: What can we learn from them, and why asking the right question before measurements matters? *Environmental Pollution*, *231*, 1256–1264. https://doi.org/10.1016/j.envpol.2017.08.074

Environment and Climate Change Canada. (2015, July 8). *Microbeads – A Science Summary* [Assessments;research]. https://www.canada.ca/en/environment-climate-change/services/evaluating-existing-substances/microbeads-science-summary.html

Fajardo, C., Martín, C., Costa, G., Sánchez-Fortún, S., Rodríguez, C., de Lucas Burneo, J. J., Nande, M., Mengs, G., & Martín, M. (2022). Assessing the role of polyethylene microplastics as a vector for organic pollutants in soil: Ecotoxicological and molecular approaches. *Chemosphere*, *288*(Pt 1), 132460. https://doi.org/10.1016/j.chemosphere.2021.132460

Fang, X. Z., Fang, S. Q., Ding, Y., Ma, J. W., Ye, Z. Q., Liu, D., & Zhao, K. L. (2024). Microplastic exposure inhibits nitrate uptake and assimilation in wheat plants. *Environmental Pollution*, *360*, 124626. https://doi.org/10.1016/j.envpol.2024.124626

Fernández, J. M., Peltre, C., Craine, J. M., & Plante, A. F. (2012). Improved Characterization of Soil Organic Matter by Thermal Analysis Using CO2/H2O Evolved Gas Analysis. *Environmental Science & Technology*, *46*(16), 8921–8927. https://doi.org/10.1021/es301375d

Fitzmorris, K. B., Sarmiento, F., & O'Callaghan, P. (2009). Biosolids and Sludge Management. *Water Environment Research*, *81*(10), 1376–1393. https://doi.org/10.2175/106143009X12445568399730

Fließbach, A., Oberholzer, H.-R., Gunst, L., & Mäder, P. (2007). Soil organic matter and biological soil quality indicators after 21 years of organic and conventional farming. *Agriculture, Ecosystems & Environment*, *118*(1), 273–284. https://doi.org/10.1016/j.agee.2006.05.022

Gaylor, M. O., Harvey, E., & Hale, R. C. (2013). Polybrominated Diphenyl Ether (PBDE) Accumulation by Earthworms (Eisenia fetida) Exposed to Biosolids-, Polyurethane Foam Microparticle-, and Penta-BDE-Amended Soils. *Environmental Science & Technology*, *47*(23), 13831–13839. https://doi.org/10.1021/es403750a

Gerigny, O., Blanco, G., Lips, U., Buhhalko, N., Chouteau, L., Georges, E., Meyers, N., Vanavermaete, D., Galgani, F., Ourgaud, M., Papillon, L., Sempéré, R., & De Witte, B. (2024). Comparative analysis of microplastics detection methods applied to marine sediments: A case study in the Bay of Marseille. *Marine Pollution Bulletin*, *207*, 116787. https://doi.org/10.1016/j.marpolbul.2024.116787

Geyer, R., Jambeck, J. R., & Law, K. L. (2017). Production, use, and fate of all plastics ever made. *Science Advances*, *3*(7), e1700782. https://doi.org/10.1126/sciadv.1700782

Gies, E. A., LeNoble, J. L., Noël, M., Etemadifar, A., Bishay, F., Hall, E. R., & Ross, P. S. (2018). Retention of microplastics in a major secondary wastewater treatment plant in Vancouver, Canada. *Marine Pollution Bulletin*, *133*, 553–561. Scopus. https://doi.org/10.1016/j.marpolbul.2018.06.006

Goedecke, C., Dittmann, D., Eisentraut, P., Wiesner, Y., Schartel, B., Klack, P., & Braun, U. (2020). Evaluation of thermoanalytical methods equipped with evolved gas analysis for the detection of microplastic in environmental samples. *Journal of Analytical and Applied Pyrolysis*, *152*, 104961. https://doi.org/10.1016/j.jaap.2020.104961

Golebiewski, J., & Galeski, A. (2007). Thermal stability of nanoclay polypropylene composites by simultaneous DSC and TGA. *Composites Science and Technology*, *67*(15), 3442–3447. https://doi.org/10.1016/j.compscitech.2007.03.007

Government of Canada. (2023). *Lists of acceptable polymers for use in food packaging applications* [Guidance]. https://www.canada.ca/en/health-canada/services/food-nutrition/legislation-guidelines/guidance-documents/lists-acceptable-polymers-use-food-packaging-applications.html

Grause, G., Kuniyasu, Y., Chien, M.-F., & Inoue, C. (2022). Separation of microplastic from soil by centrifugation and its application to agricultural soil. *Chemosphere (Oxford)*, *288*(Pt 3), 132654–132654. https://doi.org/10.1016/j.chemosphere.2021.132654

Grigorescu, R., David, M. E., Iancu, Ghioca, P., & Ion, R.-M. (2019). Waste Electrical and Electronic Equipment: A Review on the Identification Methods for Polymeric Materials. *Recycling*, *4*, 32. https://doi.org/10.3390/recycling4030032

Groh, K. J., Backhaus, T., Carney-Almroth, B., Geueke, B., Inostroza, P. A., Lennquist, A., Leslie, H. A., Maffini, M., Slunge, D., Trasande, L., Warhurst, A. M., & Muncke, J. (2019). Overview of known plastic packaging-associated chemicals and their hazards. *Science of The Total Environment*, *651*, 3253–3268. https://doi.org/10.1016/j.scitotenv.2018.10.015

Guo, J.-J., Huang, X.-P., Xiang, L., Wang, Y.-Z., Li, Y.-W., Li, H., Cai, Q.-Y., Mo, C.-H., & Wong, M.-H. (2020). Source, migration and toxicology of microplastics in soil. *Environment International*, *137*, 105263. https://doi.org/10.1016/j.envint.2019.105263

Hahladakis, J. N., Velis, C. A., Weber, R., Iacovidou, E., & Purnell, P. (2018). An overview of chemical additives present in plastics: Migration, release, fate and environmental impact during their use, disposal and recycling. *Journal of Hazardous Materials*, *344*, 179–199. https://doi.org/10.1016/j.jhazmat.2017.10.014

Halliwell, S. M. (2002). *Polymers in building and construction*. Rapra Technology Ltd.

Han, C., Kim, H.-J., Lee, J.-S., Sakakura, Y., & Hagiwara, A. (2023). Differential modes of response to zinc chloride in the marine rotifers *Brachionus plicatilis* and *Brachionus rotundiformis*: Reproductive flexibility and stress-defensive activity. *Aquaculture*, *564*, 739081. https://doi.org/10.1016/j.aquaculture.2022.739081

Hao, Y., Min, J., Ju, S., Zeng, X., Xu, J., Li, J., Wang, H., Shaheen, S. M., Bolan, N., Rinklebe, J., & Shi, W. (2024). Possible hazards from biodegradation of soil plastic mulch: Increases in microplastics and CO2 emissions. *Journal of Hazardous Materials*, *467*, 133680–133680. https://doi.org/10.1016/j.jhazmat.2024.133680

Harley-Nyang, D., Memon, F. A., Jones, N., & Galloway, T. (2022). Investigation and analysis of microplastics in sewage sludge and biosolids: A case study from one wastewater treatment works in the UK. *Science of The Total Environment*, *823*, 153735. https://doi.org/10.1016/j.scitotenv.2022.153735

Harley-Nyang, D., Memon, F. A., Osorio Baquero, A., & Galloway, T. (2023). Variation in microplastic concentration, characteristics and distribution in sewage sludge & biosolids around the world. *Science of The Total Environment*, *891*, 164068. https://doi.org/10.1016/j.scitotenv.2023.164068

Hartmann, N. B., Hüffer, T., Thompson, R. C., Hassellöv, M., Verschoor, A., Daugaard, A. E., Rist, S., Karlsson, T., Brennholt, N., Cole, M., Herrling, M. P., Hess, M. C., Ivleva, N. P., Lusher, A. L., & Wagner, M. (2019). Are We Speaking the Same Language? Recommendations for a Definition and Categorization Framework for Plastic Debris. *Environmental Science & Technology*, *53*(3), 1039–1047. https://doi.org/10.1021/acs.est.8b05297

Hengstmann, E., & Fischer, E. K. (2019). Nile red staining in microplastic analysis—Proposal for a reliable and fast identification approach for large microplastics. *Environmental Monitoring and Assessment*, *191*(10), 1–9. https://doi.org/10.1007/s10661-019-7786-4

Horton, A. A., Cross, R. K., Read, D. S., Jürgens, M. D., Ball, H. L., Svendsen, C., Vollertsen, J., & Johnson, A. C. (2021). Semi-automated analysis of microplastics in complex wastewater samples. *Environmental Pollution*, *268*. Scopus. https://doi.org/10.1016/j.envpol.2020.115841

Hou, D. (2023). Soil health and ecosystem services. *Soil Use and Management*, *39*(4), 1259–1266. https://doi.org/10.1111/sum.12945

Huerta Lwanga, E., Gertsen, H., Gooren, H., Peters, P., Salánki, T., van der Ploeg, M., Besseling, E., Koelmans, A. A., & Geissen, V. (2016). Microplastics in the Terrestrial Ecosystem: Implications for Lumbricus terrestris (Oligochaeta, Lumbricidae). *Environmental Science & Technology*, *50*(5), 2685–2691. https://doi.org/10.1021/acs.est.5b05478

Hurley, R. R., Lusher, A. L., Olsen, M., & Nizzetto, L. (2018). Validation of a Method for Extracting Microplastics from Complex, Organic-Rich, Environmental Matrices. *Environmental Science & Technology*, *52*(13), 7409–7417. https://doi.org/10.1021/acs.est.8b01517

Iswahyudi, I., Widodo, W., Warkoyo, W., Sutanto, A., Garfansa, M. P., & Septia, E. D. (2024). Determination and quantification of microplastics in compost. *Environmental Quality Management*, *34*(1), e22184. https://doi.org/10.1002/tqem.22184

Jenner, L. C., Rotchell, J. M., Bennett, R. T., Cowen, M., Tentzeris, V., & Sadofsky, L. R. (2022). Detection of microplastics in human lung tissue using μFTIR spectroscopy. *Science of The Total Environment*, *831*, 154907. https://doi.org/10.1016/j.scitotenv.2022.154907

Jia, L., Liu, L., Zhang, Y., Fu, W., Liu, X., Wang, Q., Tanveer, M., & Huang, L. (2023). Microplastic stress in plants: Effects on plant growth and their remediations. *Frontiers in Plant Science*, *14*. https://doi.org/10.3389/fpls.2023.1226484

Kadac-Czapska, K., Trzebiatowska, P. J., Knez, E., Zaleska-Medynska, A., & Grembecka, M. (2023). Microplastics in food—A critical approach to definition, sample preparation, and characterisation. *Food Chemistry*, *418*, 135985. https://doi.org/10.1016/j.foodchem.2023.135985

Kalaronis, D., Ainali, N. M., Evgenidou, E., Kyzas, G. Z., Yang, X., Bikiaris, D. N., & Lambropoulou, D. A. (2022). Microscopic techniques as means for the determination of microplastics and nanoplastics in the aquatic environment: A concise review. *Green Analytical Chemistry*, *3*, 100036. https://doi.org/10.1016/j.greeac.2022.100036

Kim, S., Hyeon, Y., & Park, C. (2023). Microplastics' Shape and Morphology Analysis in the Presence of Natural Organic Matter Using Flow Imaging Microscopy. *Molecules (Basel, Switzerland)*, *28*(19), 6913-. https://doi.org/10.3390/molecules28196913

Kim, Y.-J., Osako, M., & Sakai, S. (2006). Leaching characteristics of polybrominated diphenyl ethers (PBDEs) from flame-retardant plastics. *Chemosphere*, *65*(3), 506–513. https://doi.org/10.1016/j.chemosphere.2006.01.019

Kirstein, I. V., Hensel, F., Gomiero, A., Iordachescu, L., Vianello, A., Wittgren, H. B., & Vollertsen, J. (2021). Drinking plastics? – Quantification and qualification of microplastics in drinking water distribution systems by µFTIR and Py-GCMS. *Water Research*, *188*, 116519. https://doi.org/10.1016/j.watres.2020.116519

Kumar, R., Manna, C., Padha, S., Verma, A., Sharma, P., Dhar, A., Ghosh, A., & Bhattacharya, P. (2022). Micro(nano)plastics pollution and human health: How plastics can induce carcinogenesis to humans? *Chemosphere*, *298*, 134267. https://doi.org/10.1016/j.chemosphere.2022.134267

Lares, M., Ncibi, M. C., Sillanpää, M., & Sillanpää, M. (2018). Occurrence, identification and removal of microplastic particles and fibers in conventional activated sludge process and advanced MBR technology. *Water Research*, *133*, 236–246. https://doi.org/10.1016/j.watres.2018.01.049

Latini, G., De Felice, C., Presta, G., Del Vecchio, A., Paris, I., Ruggieri, F., & Mazzeo, P. (2003). In utero exposure to di-(2-ethylhexyl) phthalate and duration of human pregnancy. *Environmental Health Perspectives*, *111*(14), 1783–1785. https://doi.org/10.1289/ehp.6202

Lebeau, B. (2023). *Sewage Biosolids – Managing Urban Nutrients Responsibly for Crop Production*.

Leslie, H. A., Van Velzen, M. J. M., Brandsma, S. H., Vethaak, A. D., Garcia-Vallejo, J. J., & Lamoree, M. H. (2022). Discovery and quantification of plastic particle pollution in human blood. *Environment International*, *163*, 107199. https://doi.org/10.1016/j.envint.2022.107199

Letwin, N. V., Gillespie, A. W., Ijzerman, M. M., Kudla, Y. M., Csajaghy, J. D., & Prosser, R. S. (2024). Characterizing the Microplastic Content of Biosolids in Southern Ontario, Canada. *Environmental Toxicology and Chemistry*, *43*(4), 793–806. https://doi.org/10.1002/etc.5813

Li, C., Cui, Q., Zhang, M., Vogt, R. D., & Lu, X. (2021). A commonly available and easily assembled device for extraction of bio/non-degradable microplastics from soil by flotation in NaBr solution. *Science of The Total Environment*, *759*, 143482. https://doi.org/10.1016/j.scitotenv.2020.143482

Li, J., Song, Y., & Cai, Y. (2020). Focus topics on microplastics in soil: Analytical methods, occurrence, transport, and ecological risks. *Environmental Pollution*, *257*, 113570. https://doi.org/10.1016/j.envpol.2019.113570

Li, Y., Hou, Y., Hou, Q., Long, M., Wang, Z., Rillig, M. C., Liao, Y., & Yong, T. (2023). Soil microbial community parameters affected by microplastics and other plastic residues. *Frontiers in Microbiology*, *14*, 1258606. https://doi.org/10.3389/fmicb.2023.1258606

Liebezeit, G., & Dubaish, F. (2012). Microplastics in Beaches of the East Frisian Islands Spiekeroog and Kachelotplate. *Bulletin of Environmental Contamination and Toxicology*, *89*(1), 213–217. https://doi.org/10.1007/s00128-012-0642-7

Lin, Y., Ye, G., Kuzyakov, Y., Liu, D., Fan, J., & Ding, W. (2019). Long-term manure application increases soil organic matter and aggregation, and alters microbial community structure and keystone taxa. *Soil Biology and Biochemistry*, *134*, 187–196. https://doi.org/10.1016/j.soilbio.2019.03.030

Lind, P. M., Roos, V., Rönn, M., Johansson, L., Ahlström, H., Kullberg, J., & Lind, L. (2012). Serum concentrations of phthalate metabolites are related to abdominal fat distribution two years later in elderly women. *Environmental Health*, *11*(1), 21. https://doi.org/10.1186/1476-069X-11-21

Liu, H., Pan, B., Zhang, J., Huang, Z., Li, P., & Shen, J. (2024). Determination of microplastics in agricultural soil by double-shot pyrolysis-gas chromatography combined with two-step extraction. *Journal of Separation Science*, *47*(1), 2300253. https://doi.org/10.1002/jssc.202300253

Luo, H., Liu, C., He, D., Sun, J., Li, J., & Pan, X. (2022a). Effects of aging on environmental behavior of plastic additives: Migration, leaching, and ecotoxicity. *Science of The Total Environment*, *849*, 157951. https://doi.org/10.1016/j.scitotenv.2022.157951

Luo, Y., Li, L., Feng, Y., Li, R., Yang, J., Peijnenburg, W. J. G. M., & Tu, C. (2022b). Quantitative tracing of uptake and transport of submicrometre plastics in crop plants using lanthanide chelates as a dual-functional tracer. *Nature Nanotechnology*, *17*(4), 424–431. https://doi.org/10.1038/s41565-021-01063-3

Lupton, J. M. (2010). Single-Molecule Spectroscopy for Plastic Electronics: Materials Analysis from the Bottom-Up. *Advanced Materials*, *22*(15), 1689–1721. https://doi.org/10.1002/adma.200902306

MacLean, J., Mayanna, S., Benning, L. G., Horn, F., Bartholomäus, A., Wiesner, Y., Wagner, D., & Liebner, S. (2021). The Terrestrial Plastisphere: Diversity and Polymer-Colonizing Potential of Plastic-Associated Microbial Communities in Soil. *Microorganisms*, *9*(9), Article 9. https://doi.org/10.3390/microorganisms9091876

Maes, T., Jessop, R., Wellner, N., Haupt, K., & Mayes, A. G. (2017). A rapid-screening approach to detect and quantify microplastics based on fluorescent tagging with Nile Red. *Scientific Reports*, *7*(1), 44501. https://doi.org/10.1038/srep44501

Majewsky, M., Bitter, H., Eiche, E., & Horn, H. (2016). Determination of microplastic polyethylene (PE) and polypropylene (PP) in environmental samples using thermal analysis (TGA-DSC). *The Science of the Total Environment*, *568*, 507–511. https://doi.org/10.1016/j.scitotenv.2016.06.017

Mansa, R., & Zou, S. (2021). Thermogravimetric analysis of microplastics: A mini review. *Environmental Advances*, *5*, 100117. https://doi.org/10.1016/j.envadv.2021.100117

Mariano, S., Tacconi, S., Fidaleo, M., Rossi, M., & Dini, L. (2021). Micro and Nanoplastics Identification: Classic Methods and Innovative Detection Techniques. *Frontiers in Toxicology*, *3*. https://doi.org/10.3389/ftox.2021.636640

Martin, C., Baalkhuyur, F., Valluzzi, L., Saderne, V., Cusack, M., Almahasheer, H., Krishnakumar, P. K., Rabaoui, L., Qurban, M. A., Arias-Ortiz, A., Masqué, P., & Duarte, C. M. (2020). Exponential increase of plastic burial in mangrove sediments as a major plastic sink. *Science Advances*, *6*(44), eaaz5593. https://doi.org/10.1126/sciadv.aaz5593

Martín de la Fuente, A., Marhuenda-Egea, F. C., Ros, M., Pascual, J. A., Saez-Tovar, J. A., Martinez-Sabater, E., & Peñalver, R. (2022). Thermogravimetry coupled with mass spectrometry successfully used to quantify polyethylene and polystyrene microplastics in organic amendments. *Environmental Research*, *213*, 113583. https://doi.org/10.1016/j.envres.2022.113583

Marturano, V., Cerruti, P., & Ambrogi, V. (2017). Polymer additives. *Physical Sciences Reviews*, *2*(6). https://doi.org/10.1515/psr-2016-0130

Mattsson, K., Ekstrand, E., Granberg, M., Hassellöv, M., & Magnusson, K. (2022). Comparison of pre-treatment methods and heavy density liquids to optimize microplastic extraction from natural marine sediments. *Scientific Reports*, *12*, 15459. https://doi.org/10.1038/s41598-022-19623-5

McKeen, L. W. (2014). *The effect of temperature and other factors on plastics and elastomers* (Fourth edition.). William Andrew.

Meng, F., Yang, X., Riksen, M., & Geissen, V. (2022). Effect of different polymers of microplastics on soil organic carbon and nitrogen – A mesocosm experiment. *Environmental Research*, *204*, 111938. https://doi.org/10.1016/j.envres.2021.111938

Mercy, F. T., Alam, A. K. M. R., & Akbor, M. A. (2023). Abundance and characteristics of microplastics in major urban lakes of Dhaka, Bangladesh. *Heliyon*, *9*(4). https://doi.org/10.1016/j.heliyon.2023.e14587

Mironova, M., Makarov, I., Golova, L., Vinogradov, M., Shandryuk, G., & Levin, I. (2019). Improvement in Carbonization Efficiency of Cellulosic Fibres Using Silylated Acetylene and Alkoxysilanes. *Fibers*, *7*(10), Article 10. https://doi.org/10.3390/fib7100084

Mohajerani, A., & Karabatak, B. (2020). Microplastics and pollutants in biosolids have contaminated agricultural soils: An analytical study and a proposal to cease the use of biosolids in farmlands and utilise them in sustainable bricks. *Waste Management*, *107*, 252–265. https://doi.org/10.1016/j.wasman.2020.04.021

Mutsuga, M., Kawamura, Y., Sugita-Konishi, Y., Hara-Kudo, Y., Takatori, K., & Tanamoto, K. (2006). Migration of formaldehyde and acetaldehyde into mineral water in polyethylene terephthalate (PET) bottles. *Food Additives & Contaminants*, *23*(2), 212–218. https://doi.org/10.1080/02652030500398361

Nalbone, L., Panebianco, A., Giarratana, F., & Russell, M. (2021). Nile Red staining for detecting microplastics in biota: Preliminary evidence. *Marine Pollution Bulletin*, *172*, 112888. https://doi.org/10.1016/j.marpolbul.2021.112888

Net, S., Sempéré, R., Delmont, A., Paluselli, A., & Ouddane, B. (2015). Occurrence, Fate, Behavior and Ecotoxicological State of Phthalates in Different Environmental Matrices. *Environmental Science & Technology*, *49*(7), 4019–4035. https://doi.org/10.1021/es505233b

OECD. (2022). *Global Plastics Outlook: Economic Drivers, Environmental Impacts and Policy Options*. OECD. https://doi.org/10.1787/de747aef-en

Osman, K. T. (2014). Physical Deterioration of Soil. In K. T. Osman (Ed.), *Soil Degradation, Conservation and Remediation* (pp. 45–67). Springer Netherlands. https://doi.org/10.1007/978-94-007-7590-9_2

Paterova, A. V., Toa, Z. S. D., Yang, H., & Krivitsky, L. A. (2022). Broadband Quantum Spectroscopy at the Fingerprint Mid-Infrared Region. *ACS Photonics*, *9*(6), 2151–2159. https://doi.org/10.1021/acsphotonics.2c00464

Paul, E., & Frey, S. (2023). *Soil Microbiology, Ecology and Biochemistry*. Elsevier.

Perez, C. N., Carré, F., Hoarau-Belkhiri, A., Joris, A., Leonards, P. E. G., & Lamoree, M. H. (2022). Innovations in analytical methods to assess the occurrence of microplastics in soil. *Journal of Environmental Chemical Engineering*, *10*(3), 107421. https://doi.org/10.1016/j.jece.2022.107421

Pérez-Reverón, R., González-Sálamo, J., Hernández-Sánchez, C., González-Pleiter, M., Hernández-Borges, J., & Díaz-Peña, F. J. (2022). Recycled wastewater as a potential source of microplastics in irrigated soils from an arid-insular territory (Fuerteventura, Spain). *Science of The Total Environment*, *817*, 152830. https://doi.org/10.1016/j.scitotenv.2021.152830

Pfohl, P., Wagner, M., Meyer, L., Domercq, P., Praetorius, A., Hüffer, T., Hofmann, T., & Wohlleben, W. (2022). Environmental Degradation of Microplastics: How to Measure Fragmentation Rates to Secondary Micro- and Nanoplastic Fragments and Dissociation into Dissolved Organics. *Environmental Science & Technology*, *56*(16), 11323–11334. https://doi.org/10.1021/acs.est.2c01228

Prasad, S., Bennett, A., & Triantafyllou, M. (2024). Characterization of Nile Red-Stained Microplastics through Fluorescence Spectroscopy. *Journal of Marine Science and Engineering*, *12*(8), 1403. https://doi.org/10.3390/jmse12081403

Prata, J. C., Sequeira, I. F., Monteiro, S. S., Silva, A. L. P., da Costa, J. P., Dias-Pereira, P., Fernandes, A. J. S., da Costa, F. M., Duarte, A. C., & Rocha-Santos, T. (2021). Preparation of biological samples for microplastic identification by Nile Red. *Science of The Total Environment*, *783*, 147065. https://doi.org/10.1016/j.scitotenv.2021.147065

Price, G. W., Astatkie, T., Gillis, J. D., & Liu, K. (2015). Long-term influences on nitrogen dynamics and pH in an acidic sandy soil after single and multi-year applications of alkaline treated biosolids. *Agriculture, Ecosystems & Environment*, *208*, 1–11. https://doi.org/10.1016/j.agee.2015.04.010

Qiu, Y., Zhou, S., Zhang, C., Chen, L., Qin, W., & Zhang, Q. (2023). Vertical distribution and weathering characteristic of microplastics in soil profile of different land use types. *Science of The Total Environment*, *905*, 166902. https://doi.org/10.1016/j.scitotenv.2023.166902

Quinn, B., Murphy, F., & Ewins, C. (2017). Validation of density separation for the rapid recovery of microplastics from sediment. *Analytical Methods*, *9*(9), 1491–1498. https://doi.org/10.1039/C6AY02542K

Radford, F., Horton, A., Hudson, M., Shaw, P., & Williams, I. (2023). Agricultural soils and microplastics: Are biosolids the problem? *Frontiers in Soil Science*, *2*. https://doi.org/10.3389/fsoil.2022.941837

Radford, F., M. Zapata-Restrepo, L., A. Horton, A., D. Hudson, M., J. Shaw, P., & D. Williams, I. (2021). Developing a systematic method for extraction of microplastics in soils. *Analytical Methods*, *13*(14), 1695–1705. https://doi.org/10.1039/D0AY02086A

Ragusa, A., Lelli, V., Fanelli, G., Svelato, A., D'Avino, S., Gevi, F., Santacroce, C., Catalano, P., Rongioletti, M. C. A., De Luca, C., Gulotta, A., Rinalducci, S., & Timperio, A. M. (2022). Plastic and Placenta: Identification of Polyethylene Glycol (PEG) Compounds in the Human Placenta by HPLC-MS/MS System. *International Journal of Molecular Sciences*, *23*(21), Article 21. https://doi.org/10.3390/ijms232112743

Ramírez-Hernández, A., Aguilar-Flores, C., & Aparicio-Saguilán, A. (2019). Fingerprint analysis of FTIR spectra of polymers containing vinyl acetate. *DYNA*, *86*(209), 198–205.

Rillig, M. C., Lehmann, A., Ryo, M., & Bergmann, J. (2019). Shaping Up: Toward Considering the Shape and Form of Pollutants. *Environmental Science & Technology*, *53*(14), 7925–7926. https://doi.org/10.1021/acs.est.9b03520

Sajiki, J., & Yonekubo, J. (2004). Leaching of bisphenol A (BPA) from polycarbonate plastic to water containing amino acids and its degradation by radical oxygen species. *Chemosphere*, *55*(6), 861–867. https://doi.org/10.1016/j.chemosphere.2003.11.065

Scarascia-Mugnozza, G., Sica, C., & Russo, G. (2011). PLASTIC MATERIALS IN EUROPEAN AGRICULTURE: ACTUAL USE AND PERSPECTIVES. *Journal of Agricultural Engineering*, *42*(3), Article 3. https://doi.org/10.4081/jae.2011.3.15

Schell, T., Hurley, R., Buenaventura, N. T., Mauri, P. V., Nizzetto, L., Rico, A., & Vighi, M. (2022). Fate of microplastics in agricultural soils amended with sewage sludge: Is surface water runoff a relevant environmental pathway? *Environmental Pollution*, *293*, 118520. https://doi.org/10.1016/j.envpol.2021.118520

Schütze, B., Thomas, D., Kraft, M., Brunotte, J., & Kreuzig, R. (2022). Comparison of different salt solutions for density separation of conventional and biodegradable microplastic from solid sample matrices. *Environmental Science and Pollution Research*, *29*(54), 81452–81467. https://doi.org/10.1007/s11356-022-21474-6

Sheriff, I., Yusoff, M. S., Manan, T. S. B. A., & Koroma, M. (2023). Microplastics in manure: Sources, analytical methods, toxicodynamic, and toxicokinetic endpoints in livestock and poultry. *Environmental Advances*, *12*, 100372. https://doi.org/10.1016/j.envadv.2023.100372

Shotyk, W., & Krachler, M. (2007). Contamination of Bottled Waters with Antimony Leaching from Polyethylene Terephthalate (PET) Increases upon Storage. *Environmental Science & Technology*, *41*(5), 1560–1563. https://doi.org/10.1021/es061511+

Sivarajah, B., Lapen, D. R., Gewurtz, S. B., Smyth, S. A., Provencher, J. F., & Vermaire, J. C. (2023). How many microplastic particles are present in Canadian biosolids? *Journal of Environmental Quality*, *52*(5), 1037–1048. https://doi.org/10.1002/jeq2.20497

Smith, B. C. (2011). *Fundamentals of Fourier Transform Infrared Spectroscopy*. CRC Press.

Soni, P., & Joseph, S. (2021). ECHA's Microplastics Use Restriction—Impact on Pharmaceuticals. *Pharmaceutical Technology Europe*, *33*(1), 21–24.

Sorolla-Rosario, D., Llorca-Porcel, J., Pérez-Martínez, M., Lozano-Castelló, D., & Bueno-López, A. (2022). Study of microplastics with semicrystalline and amorphous structure identification by TGA and DSC. *Journal of Environmental Chemical Engineering*, *10*(1), 106886. https://doi.org/10.1016/j.jece.2021.106886

Stapleton, M. J., Ansari, A. J., Ahmed, A., & Hai, F. I. (2023). Change in the chemical, mechanical and physical properties of plastics due to UVA degradation in different water matrices: A study on the recyclability of littered plastics. *Environmental Pollution (1987)*, *334*, 122226–122226. https://doi.org/10.1016/j.envpol.2023.122226

Sun, P., Liu, X., Zhang, M., Li, Z., Cao, C., Shi, H., Yang, Y., & Zhao, Y. (2021). Sorption and leaching behaviors between aged MPs and BPA in water: The role of BPA binding modes within plastic matrix. *Water Research*, *195*, 116956. https://doi.org/10.1016/j.watres.2021.116956

Süssmann, J., Fischer, E. K., Hildebrandt, L., Walz, E., Greiner, R., Rohn, S., & Fritsche, J. (2024). Nile red staining for rapid screening of plastic-suspect particles in edible seafood tissues. *Analytical and Bioanalytical Chemistry*, *416*(14), 3459–3471. https://doi.org/10.1007/s00216-024-05296-8

Tan, M., Sun, Y., Gui, J., Wang, J., Chen, X., & Wu, D. (2022). The Efficiency of Different Digestion and Separation Methods for Extracting Microplastics in Typical Organic Solid Waste. *International Journal of Environmental Research*, *16*(2), 16. https://doi.org/10.1007/s41742-022-00394-w

Telo da Gama, J. (2023). The Role of Soils in Sustainability, Climate Change, and Ecosystem Services: Challenges and Opportunities. *Ecologies*, *4*(3), Article 3. https://doi.org/10.3390/ecologies4030036

Thomas, D., Schütze, B., Heinze, W. M., & Steinmetz, Z. (2020). Sample Preparation Techniques for the Analysis of Microplastics in Soil—A Review. *Sustainability*, *12*(21), 9074. https://doi.org/10.3390/su12219074

Tian, G., Franzluebbers, A. J., Granato, T. C., Cox, A. E., & O'Connor, C. (2013). Stability of soil organic matter under long-term biosolids application. *Applied Soil Ecology : A Section of Agriculture, Ecosystems & Environment*, *64*, 223–227. https://doi.org/10.1016/j.apsoil.2012.12.001

UNEP. (2019). *Microplastics | UNEP - UN Environment Programme*. https://www.unep.org/resources/report/microplastics

UNEP. (2023). *Chemicals in Plastics—A Technical Report*. https://www.unep.org/resources/report/chemicals-plastics-technical-report

US EPA, O. (2022, April 22). *Microplastics Research* [Overviews and Factsheets]. https://www.epa.gov/water-research/microplastics-research

Vanhatalo, K., Maximova, N., Perander, A. M., Johansson, L. S., Haimi, E., & Dahl, O. (2016). Comparison of conventional and lignin-rich microcrystalline cellulose. *BioResources*, *11(2), 4037–4045*. https://doi.org/10.15376/biores.11.2.4037-4054

Vargas, R. (2022). *Soils, Where Food Begins*. United Nations; United Nations. https://www.un.org/en/un-chronicle/soils-where-food-begins

Vittal, R., Xavier, S., Mohan, M., Chakraborty, A., & Chakraborty, G. (2024). *Detection and Characterization of Microplastics in Commercial Salts in Indi*. https://doi.org/10.21203/rs.3.rs-3893146/v1

Waldman, W. R., & Rillig, M. C. (2020). Microplastic Research Should Embrace the Complexity of Secondary Particles. *Environmental Science & Technology*, *54*(13), 7751–7753. https://doi.org/10.1021/acs.est.0c02194

Wang, J., Li, J., Liu, W., Zeb, A., Wang, Q., Zheng, Z., Shi, R., Lian, Y., & Liu, L. (2023). Three typical microplastics affect the germination and growth of amaranth (Amaranthus mangostanus L.) seedlings. *Plant Physiology and Biochemistry: PPB*, *194*, 589–599. https://doi.org/10.1016/j.plaphy.2022.12.007

Wang, Y., Wang, Y., Shao, T., Wang, R., Dong, Z., & Xing, B. (2024). Antibiotics and microplastics in manure and surrounding soil of farms in the Loess Plateau: Occurrence and correlation. *Journal of Hazardous Materials*, *465*, 133434. https://doi.org/10.1016/j.jhazmat.2024.133434

Wang, Z., Wang, X., Hu, C., Ge, T., Wang, L., Xing, J., He, X., & Zhao, Y. (2024). Comparative Evaluation of Analytical Techniques for Quantifying and Characterizing Polyethylene Microplastics in Farmland Soil Samples. *Agriculture*, *14*(4), Article 4. https://doi.org/10.3390/agriculture14040554

Welsh, B., Aherne, J., Paterson, A. M., Yao, H., & McConnell, C. (2022). Atmospheric deposition of anthropogenic particles and microplastics in south-central Ontario, Canada. *The Science of the Total Environment*, *835*, 155426. https://doi.org/10.1016/j.scitotenv.2022.155426

Withana, P. A., Senadheera, S. S., He, D., Bank, M. S., Gu, C., Hwang, S. Y., & Ok, Y. S. (2024). Soil microplastic analysis: A harmonized methodology. *Critical Reviews in Environmental Science and Technology*. https://www.tandfonline.com/doi/abs/10.1080/10643389.2023.2301052

Wright, J., Kenner, S., & Lingwall, B. (2022). Utilization of Compost as a Soil Amendment to Increase Soil Health and to Improve Crop Yields. *Open Journal of Soil Science*, *12*(6), Article 6. https://doi.org/10.4236/ojss.2022.126009

Wu, C., Xiong, X., Hamidian, A. H., Zhang, Y., & Xu, X. (2022). A review on source, occurrence, and impacts of microplastics in freshwater aquaculture systems in China. *Water Biology and Security*, *1*(3). Scopus. https://doi.org/10.1016/j.watbs.2022.100040

Xiang, Y., Rillig, M. C., Peñuelas, J., Sardans, J., Liu, Y., Yao, B., & Li, Y. (2024). Global Responses of Soil Carbon Dynamics to Microplastic Exposure: A Data Synthesis of Laboratory Studies. *Environmental Science & Technology*, *58*(13), 5821–5831. https://doi.org/10.1021/acs.est.3c06177

Yang, H., Yan, R., Chen, H., Lee, D. H., & Zheng, C. (2007). Characteristics of hemicellulose, cellulose and lignin pyrolysis. *Fuel*, *86*(12), 1781–1788. https://doi.org/10.1016/j.fuel.2006.12.013

Yang, S., Rafael Castilleja, J., Barrera, E. V., & Lozano, K. (2004). Thermal analysis of an acrylonitrile–butadiene–styrene/SWNT composite. *Polymer Degradation and Stability*, *83*(3), 383–388. https://doi.org/10.1016/j.polymdegradstab.2003.08.002

Yu, J., Wang, P., Ni, F., Cizdziel, J., Wu, D., Zhao, Q., & Zhou, Y. (2019). Characterization of microplastics in environment by thermal gravimetric analysis coupled with Fourier transform infrared spectroscopy. *Marine Pollution Bulletin*, *145*, 153–160. https://doi.org/10.1016/j.marpolbul.2019.05.037

Yuan, Z., Nag, R., & Cummins, E. (2022). Human health concerns regarding microplastics in the aquatic environment—From marine to food systems. *Science of the Total Environment*, *823*. Scopus. https://doi.org/10.1016/j.scitotenv.2022.153730

Zhang, G. S., & Liu, Y. F. (2018). The distribution of microplastics in soil aggregate fractions in southwestern China. *The Science of the Total Environment*, *642*, 12–20. https://doi.org/10.1016/j.scitotenv.2018.06.004

Zhang, K., Hamidian, A. H., Tubić, A., Zhang, Y., Fang, J. K. H., Wu, C., & Lam, P. K. S. (2021). Understanding plastic degradation and microplastic formation in the environment: A review. *Environmental Pollution*, *274*, 116554. https://doi.org/10.1016/j.envpol.2021.116554

Zhang, L., Xie, Y., Liu, J., Zhong, S., Qian, Y., & Gao, P. (2020). An Overlooked Entry Pathway of Microplastics into Agricultural Soils from Application of Sludge-Based Fertilizers. *Environmental Science & Technology*, *54*(7), 4248–4255. https://doi.org/10.1021/acs.est.9b07905

Zhao, J., & Fan, Q. (2001). Amorphous phase in atactic polystyrene. *Polymer Bulletin*, *47*(1), 91–97. https://doi.org/10.1007/s002890170025

Ziajahromi, S., Lu, H.-C., Dwyer, J., Fernandes, M., Griffith, M., & Leusch, F. D. (2024). Transport and Accumulation of Microplastics from Biosolids to Australian Agricultural Soils: Detection of Microplastics Down to 1 µm. *Environmental Science & Technology*, *58*(38), 17048–17057. https://doi.org/10.1021/acs.est.4c04661

Zimmermann, L., Bartosova, Z., Braun, K., Oehlmann, J., Völker, C., & Wagner, M. (2021). Plastic Products Leach Chemicals That Induce In Vitro Toxicity under Realistic Use Conditions. *Environmental Science & Technology*, *55*(17), 11814–11823. https://doi.org/10.1021/acs.est.1c01103

APPENDIX A

PRELIMINARY METHODOLOGY TESTING

Testing Density Separation Process

The first set of experiments was to test the density separation process before implementing costly and hazardous saturated solutions. To do this, sand and soil were spiked with commercially ordered PP and separated using deionised (DI) H_2O. No prior organic matter removal was employed. Samples were shaken on a platform mixer for 10 minutes and left to settle for 12 hours.

Experiment #1

Group 1:

Table A1. Testing a decanting approach to extract MPs from sand and soil.

Treatment	Solution	Matrix	Spiking	Extracted
A	50ml DI H_2O (1.0g/cm^3)	25g Sand	2PP	2PP
B	50ml DI H_2O (1.0g/cm^3)	25g Soil	2PP	1PP
C	50ml DI H_2O (1.0g/cm^3)	50g Sand	2PP	2PP
D	50ml DI H_2O (1.0g/cm^3)	50g Soil	2PP	None

Observations: Decanting the samples was the fastest and easiest to implement but was not an efficient method of MP extraction. This method disturbed the settled substrate and significantly dirtied the vacuum filtration process, causing soil and sand to also be on the filter paper. Moreover, decanting resulted in MPs sticking to the sides of the jar rather than flowing out into the vacuum apparatus, significantly reducing extraction efficiency.

Group 2:

Table A2. Testing an overflow method to extract MPs from sand and soil.

Treatment	Solution	Matrix	Spiking	Extracted
A	500ml DI H_2O (1.0g/cm^3)	25g Sand	2PP	2PP
B	500ml DI H_2O (1.0g/cm^3)	25g Soil	2PP	2PP
C	500ml DI H_2O (1.0g/cm^3)	50g Sand	2PP	2PP
D	500ml DI H_2O (1.0g/cm^3)	50g Soil	2PP	2PP

Observations: Using a simple overflow method by overflowing the jar into another larger container successfully extracts MP particles and ensures no particles are stuck to the sides of the extraction jar. However, this method requires significantly more density separation solution and the transfer from one container to another, which could increase potential contamination and loss of MPs.

Group 3:

Table A3. Testing a ladling approach to extracting MPs from sand and soil.

Treatment	Solution	Matrix	Spiking	Extracted
A	50ml DI H_2O (1.0g/cm^3)	25g Sand	2PP	2PP
B	50ml DI H_2O (1.0g/cm^3)	25g Soil	2PP	2PP
C	50ml DI H_2O (1.0g/cm^3)	50g Sand	2PP	2PP
D	50ml DI H_2O (1.0g/cm^3)	50g Soil	2PP	2PP

Observations: All MPs could be successfully extracted, and the separation solution could be conserved. This method was more time-consuming and tedious but allowed for the sides of the jar to be rinsed, ensuring MPs were not stuck to the extraction jar, increasing effectiveness.

Testing Efficacy of Density Separation Solutions

No prior organic matter removal was implemented. Density separation solutions were tested by mixing with spiked soil and sand samples, shaken on a platform mixer for 10 min, left to settle for 12 hours, and then ladled and vacuum-filtered onto filter paper. Ultrasonication was also implemented in experiments 1 and 2 to test its ability to improve extraction. It was deemed that ultrasonication had no observable effect and did not significantly enhance efficiency. Instead, the use of this extra step only further complicated the procedure and made it more time-consuming.

Experiment #1

Figure A4. Using spiked sand and soil with commercially ordered PP and PE spheres and PS fragments from a coffee cup lid and separated using DI H2O.

Treatment	Solution	Matrix	Spiking	Extracted
A	50ml DI H_2O (1.0g/cm^3)	25g Sand	1PP+1PE+1PS	PP & PE
B	50ml DI H_2O (1.0g/cm^3)	25g Soil	1PP+1PE+1PS	PP & PE
C	50ml DI H_2O (1.0g/cm^3)	50g Sand	1PP+1PE+1PS	PP & PE
D	50ml DI H_2O (1.0g/cm^3)	50g Soil	1PP+1PE+1PS	PP & PE

Observations: Particles become trapped in the soil and sand matrices but resolved with shaking. PP and PE floated, while PS did not.

Experiment #2

Table A5. Using spiked sand and soil using commercially ordered PP and PE spheres and PS fragments from a coffee cup lid and separated using a saturated NaCl solution.

Treatment	**Solution**	**Matrix**	**Spiking**	**Extracted**
A	50ml NaCl (1.2g/cm^3)	25g Sand	1PP+1PE+1PS	PP, PE & PS
B	50ml NaCl (1.2g/cm^3)	25g Soil	1PP+1PE+1PS	PP, PE & PS
C	50ml NaCl (1.2g/cm^3)	50g Sand	1PP+1PE+1PS	PP, PE & PS
D	50ml NaCl (1.2g/cm^3)	50g Soil	1PP+1PE+1PS	PP, PE & PS

Observations: Particles were more frequently trapped in the soil matrix, but with shaking, they were easily extracted. Organic matter in soil clogs the filter and significantly hinders the visibility of MP particles.

Experiment #3

Table A6. Using spiked sand and soil using commercially ordered PP and PE spheres and PS fragments from a coffee cup lid and separated using a saturated NaBr solution.

Treatment	**Solution**	**Matrix**	**Spiking**	**Extracted**
A	50ml NaBr (1.5g/cm^3)	25g Sand	1PP+1PE+1PS	PP, PE & PS
B	50ml NaBr (1.5g/cm^3)	25g Soil	1PP+1PE+1PS	PP, PE & PS
C	50ml NaBr (1.5g/cm^3)	50g Sand	1PP+1PE+1PS	PP, PE & PS
D	50ml NaBr (1.5g/cm^3)	50g Soil	1PP+1PE+1PS	PP, PE & PS

Observations: Particles were more frequently trapped in the soil matrix and resolved with shaking. MPs appeared to float more readily than NaCl. However, with soil samples, more organic matter also floated, hindering vacuum filtration and obscuring MPs.

Experiment #4

Spiked soil with commercially ordered PP and PE spheres, HDPE fragments from a plastic cup, PS fragments from a coffee cup lid, and PET fragments from a water bottle. Canola oil in DI H_2O and saturated solutions NaCl, $CaCl_2$, NaBr, and $ZnCl_2$ were tested for density separation. This experiment had three replicates to get an average extraction efficiency.

Table A7. Using spiked soil with commercially ordered PP and PE spheres, HDPE fragments from a plastic cup, PS fragments from a coffee cup lid, and PET fragments from a water bottle and extracted Canola oil in DI H_2O or saturated solutions NaCl, $CaCl_2$, NaBr, and $ZnCl_2$.

Treatment	Solution	Matrix	Spiking	Extracted	Efficiency
A	50ml NaCl solution (1.2g/cm^3)	50g Soil	2PP+2PS+2PE+2PET+2HDPE	PP, PE, PE, PET	80-83%
B	50ml $CaCl_2$ solution (1.4g/cm^3)	50g Soil	2PP+2PS+2PE+2PET+2HDPE	All types	80-83%
C	50ml NaBr solution (1.50g/cm^3)	50g Soil	2PP+2PS+2PE+2PET+2HDPE	All types	84-87%
D	50ml $ZnCl_2$ solution (1.7g/cm^3)	50g Soil	2PP+2PS+2PE+2PET+2HDPE	All types	84-87%
E	50ml H_2O + 2.5ml Canola oil	50g Soil	2PP+2PS+2PE+2PET+2HDPE	All types	70-73%

Observations: Higher-density solutions (NaBr, $CaCl_2$, $ZnCl_2$) facilitated the floatation of all MP particles more rapidly and effortlessly, while lower-density solutions (NaCl) failed to extract high-density polymers. Canola oil was effective in floating MPs but was viscous, retaining MPs and causing them to become sticky, hindering extraction. $CaCl_2$ became discoloured (yellow). $ZnCl_2$ had biofilm formation, making it challenging and extremely slow to vacuum filter. Of the solutions tested, NaBr was effective in removing all polymer types tested with no unexpected observations and was easy to subsequently vacuum filter.

Testing Efficacy of Organic Matter Removal using H_2O_2

Experiment #1

Testing observable differences in organic removal using Fenton's reagent and 30 % H_2O_2 solutions. ATBs were tested but not spiked with MPs. In contrast, soil was spiked with commercially ordered PP and PE spheres, a HDPE fragment from a plastic cup, a PS fragment from a coffee cup lid, and a PET fragment from a water bottle.

Table A8. A comparison between 30 % H_2O_2 and Fenton's Reagent for soil and ATB organic matter removal.

Treatment	Solution	Matrix	Spiking
A	50ml 30 % H_2O_2	Soil	1PP+1PS+1PE+1PET+1HDPE
B	50ml 30 % H_2O_2	ATB	No spiking
C	50ml Fenton's Reagent	Soil	1PP+1PS+1PE+1PET+1HDPE
D	50ml Fenton's Reagent	ATB	No spiking

Observations: A marginally observable reduction of more organic matter using Fenton's reagent, particularly in ATB samples inundated with cellulose. However, reactions using Fenton's were more violent, bubbling over and reaching temperatures beyond 80ºC. In comparison, H_2O_2 reaction temperatures were lower. Further, after incubating for 24 hours, minimal degradation was observed under microscopy with Fenton's and no visible alterations using H_2O_2. Neither method removed all organic matter.

Experiment #2

Testing the effectiveness of organic matter removal (OMR) using 30% H_2O_2. Between 4 and 6 grams of soil was oven-dried until consistent dry weight was obtained. Once dry and weighed, 50ml of 30% H_2O_2 was added to samples and mixed on a platform mixer for 2 hours. Once mixed, samples were left to incubate for 24 hours. After 24-hour incubation, samples were vacuum-filtered onto dried and massed filter papers. Five replicate OMR soil samples were run and averaged. Two control samples were also run using DI H_2O and averaged. All masses were recorded to the fourth decimal, and oven drying was performed by massing and re-massing until no change in mass was observed, indicating the sample was truly dry. The following formula obtained a percentage mass loss, directly reflecting the OMR efficiency.

$$\text{Mass loss} = \frac{(Mass\ sample\ pre - (\ mass\ sample\ post - mass\ filter) - \ Mass\ loss\ control)}{(Mass\ sample\ pre - (Mass\ loss\ control)\ )} \text{ x } 100$$

The results indicated an approximate 85% removal efficiency.

Supplemental Research for Organic Matter Removal

Table A9. Comparison of common reagents for organic matter removal in soil using similar methodologies.

Reagent	Method	Polymers Evaluated	Polymers Degraded	Organic Removal Efficiency	Reference
30% H_2O_2	30 mL was added to 10g of soil at 60 ºC or 70ºC and an additional 5 mL was added as needed until no further reaction was observed.	PP, LDPE, HDPE, PS, PET, PA-6,6, PC, & PMMA.	60ºC: None 70ºC: PA-6-6, PS	60ºC: 96.3% +/- 14.9% 70ºC: 108% +/- 10.9%	Hurley et al., 2018
30% H_2O_2	50 mL was added to 10g of soil with either ‘high’ or ‘low’ organic matter and incubated at 100 rpm at either 40ºC or 50ºC for 24 hours.	PET, HDPE, PVC, LDPE, PP, & PS.	40ºC: None 50ºC: None	40ºC ‘high’: ~77% 40ºC ‘low’: ~ 88% 50ºC ‘high’: ~ 93% 50ºC ‘low’: ~ 81%	Radford et al., 2021
Fenton’s Reagent (30% H_2O_2 + Fe^{2+})	30 mL was added (1:1 ratio of H_2O_2 and Fe^{2+}) to 10g of soil and more was added until no further reaction was observed. An ice bath was used to modulate the temperature if it exceeded 40ºC.	PP, LDPE, HDPE, PS, PET, PA-6,6, PC, & PMMA.	None	106 % +/- 13.8%	Hurley et al., 2018
Fenton’s Reagent (30% H_2O_2 + Fe^{2+})	50 mL was added (1:1 ratio of H_2O_2 and Fe^{2+}) to 10g of soil with either ‘high’ or ‘low’ organic matter and an ice bath was used to modulate the temperature to a maximum temperature of either 40ºC or 50ºC until no reaction was visible.	PET, HDPE, PVC, LDPE, PP, & PS.	None	40ºC ‘high’: ~ 51% 40ºC ‘low’: ~ 87% 50ºC ‘high’: ~ 56% 50ºC ‘low’: ~ 85%	Radford et al., 2021
NaOH	50 ML of either a 1M solution or 10M solution at 60ºC to 10g of soil.	PP, LDPE, HDPE, PS, PET, PA-6,6, PC, & PMMA.	1M: None 10M: PC & PET	1M: 67.6% +/- 20.5% 10M: 64.4% +/- 42.7%	Hurley et al., 2018
10% KOH	50 mL was added to 10g of soil at 60ºC.	PP, LDPE, HDPE, PS, PET, PA-6,6, PC, & PMMA.	PC & PS	34.5% +/- 22.5%	Hurley et al., 2018
10% KOH	50 mL was added to 10g of soil with either ‘high’ or ‘low’ organic matter and incubated at 100 rpm at either 40ºC or 50ºC for 24 hours.	PET, HDPE, PVC, LDPE, PP, & PS.	40ºC: PVC 50ºC: PVC	40ºC ‘high’: ~ 20% 40ºC ‘low’: ~ 67% 50ºC ‘high’: ~ 65% 50ºC ‘low’: ~ 42%	Radford et al., 2021

Reagent	**Method**	**Polymers Evaluated**	**Polymers Degraded**	**Organic Removal Efficiency**	**Reference**
Reagent	Method	Polymers Evaluated	Polymers Degraded	Organic Removal Efficiency	Reference
30% H_2O_2	30 mL was added to 10g of soil at 60 ºC or 70ºC and an additional 5 mL was added as needed until no further reaction was observed.	PP, LDPE, HDPE, PS, PET, PA-6,6, PC, & PMMA.	60ºC: None 70ºC: PA-6-6, PS	60ºC: 96.3% +/- 14.9% 70ºC: 108% +/- 10.9%	Hurley et al., 2018

PP: polypropylene, LDPE: low-density polyethene, HDPE: high-density polyethene, PS: polystyrene, PET: polyethene terephthalate, PC: polycarbonate, PA: polyamide, PVC: polyvinyl chloride, PMMA: Poly methyl methacrylate.

Supplemental Research for Density Separation solutions

Table A10. Comparison of common saturated solutions using similar methodological techniques for density separation of MPs in soil samples.

Solution	Method	Polymers Used	Polymers Extracted	Extraction Efficiency	Reference
Water	200mL of solution was added to 66.66g soil spiked with 0.066g of MPs, stirred at 300 rpm for 3 minutes, left to settle for 10 minutes, and then vacuum filtered.	PP, LDPE, PE, HDPE, PS, Nylon, PVC, PET	All except PVC & PET	~ 60–78 %	Quinn et al., 2017
NaCl	300 mL of solution was added to 10 grams of soil either a 'high' or 'low' organic matter soil, shaken vigorously by hand for 30 seconds, and then left to settle overnight. The top layer was then removed with an overflow method, using an excess of the solution to overfill and spill the surface of the sample into a surrounding dish.	PET, HDPE, PVC, LDPE, PP, PS	All polymer types	'High': 33 ± 2.9% 'low': 59 ± 1.8 %	Radford et al., 2021
NaCl	200mL of solution was added to 66.66g soil spiked with 0.066g of MPs, stirred at 300 rpm for 3 minutes, left to settle for 10 minutes, and then vacuum filtered.	PP, LDPE, PE, HDPE, PS, Nylon, PVC, PET	All polymer types	~ 66-85%	Quinn et al., 2017
NaBr	An overflow apparatus was designed and implemented using an unspecified amount of solution with 30g of soil. The sample was stirred for 15-20 minutes and then left to settle for 3-18 hours before being overflown with the specially designed apparatus. The procedure was done 5 times, reusing the same solution.	PP, LDPE, PS, PVC, PBAT, PBS, PLA	All polymer types	96.5 ± 0.96% 93 ± 0.95% 94.1 ± 1.76% 95.9 ± 1.61% 95 ± 0.79 %	Li et al., 2021
NaBr	200mL of solution was added to 66.66g soil spiked with 0.066g of MPs, stirred at 300 rpm for 3 minutes, left to settle for 10 minutes, and then vacuum filtered.	PP, LDPE, PE, HDPE, PS, Nylon, PVC, PET	All polymer types	~ 83-87 %	Quinn et al., 2017
NaI	200mL of solution was added to 66.66g soil spiked with 0.066g of MPs, stirred at 300 rpm for 3 minutes, left to settle for 10 minutes, and then vacuum filtered.	PP, LDPE, PE, HDPE, PS, Nylon, PVC, PET	All polymer types	~ 88-94%	Quinn et al., 2017

Solution	Method	Polymers Used	Polymers Extracted	Extraction Efficiency	Reference
$CaCl_2$	An unknown amount of the solution was added to 10 g of sand spiked with 100mg of plastics. The sample was centrifuged at a speed of 3700min^{-1} for 10 minutes.	PET, PP, LDPE, PS, PVC	All polymer types	> 94%	Grause et al., 2022
$ZnCl_2$	300 mL of solution was added to 10 grams of soil either a 'high' or 'low' organic matter soil, shaken vigorously by hand for 30 seconds, and then left to settle overnight. The top layer was then removed with an overflow method, using an excess of the solution to overfill and spill the surface of the sample into a surrounding dish.	PET, HDPE, PVC, LDPE, PP, PS	All polymer types	'High': 53 ± 4% 'low': 80 ± 7%	Radford et al., 2021
$ZnBr_2$	200mL of solution was added to 66.66g soil spiked with 0.066g of MPs, stirred at 300 rpm for 3 minutes, left to settle for 10 minutes, and then vacuum filtered.	PP, LDPE, PE, HDPE, PS, Nylon, PVC, PET	All polymer types	> 95%	Quinn et al., 2017

PP: polypropylene, LDPE: low-density polyethene, HDPE: high-density polyethene, PS: polystyrene, PET: polyethene terephthalate, PC: polycarbonate, PA: polyamide, PVC: polyvinyl chloride, PMMA: Poly (methyl methacrylate), PBAT: polybutylene adipate terephthalate, PBC: polychlorinated biphenyl, PLA: polylactide, ABS: acrylonitrile butadien

Supplemental Research for MP Visual Analysis

Table A11. Overview of the advantages and limitation of microscopy techniques for MP analysis.

Identification Method	Information Obtained	Advantages	Limitations	Reference
Stereo-Microscopy	- Low Resolution - Size - Shape - Colour - Number	Easy and accessible immediate visualization of the sample. Identify Shape, Size, and colour. Non-destructive.	Only particles>100 µm. No polymer composition. Transparent particles are difficult to visualize. False identification of non-plastic particles. Very time-consuming.	Schell et al., 2022 Zhang et al., 2023
Fluorescence Microscopy	- Medium Resolution - Size - Shape - Number	Somewhat easy to perform. Immediate visualization and specificity of particles with dye. Transparent particles are easily visible. Non-destructive.	Chemical additives may interfere. Can falsely identify particles as plastic. The cost associated with the life of the light source. Additional sample preparation with dye.	Grause et al., 2022 Meyers et al., 2022
Scanning Electron Microscopy (SEM)	- High Resolution - Surface Morphology - EDS for Surface chemistry	Clear, high-resolution image. No sputter coating if ESEM mode. Non-destructive.	Expensive. Extensive sample preparation and sputter coating may limit subsequent analysis of particles.	Mahon et al., 2017 Stapleton et al., 2023
Atomic Force Microscopy (AFM)	- Very high Resolution - Surface Morphology - Stiffness - Hydrophobicity - Conductivity - Magnetization	3D mapping of the surface structure. Non-destructive but may damage the sample.	Expensive and time-consuming. The sample may be damaged from the tip of the instrument	Sullivan et al., 2019

APPENDIX B

SUPPLEMENTAL TO CHAPTER 4 RESULTS

Microplastics in Alkaline-Treated Biosolids

Abundance

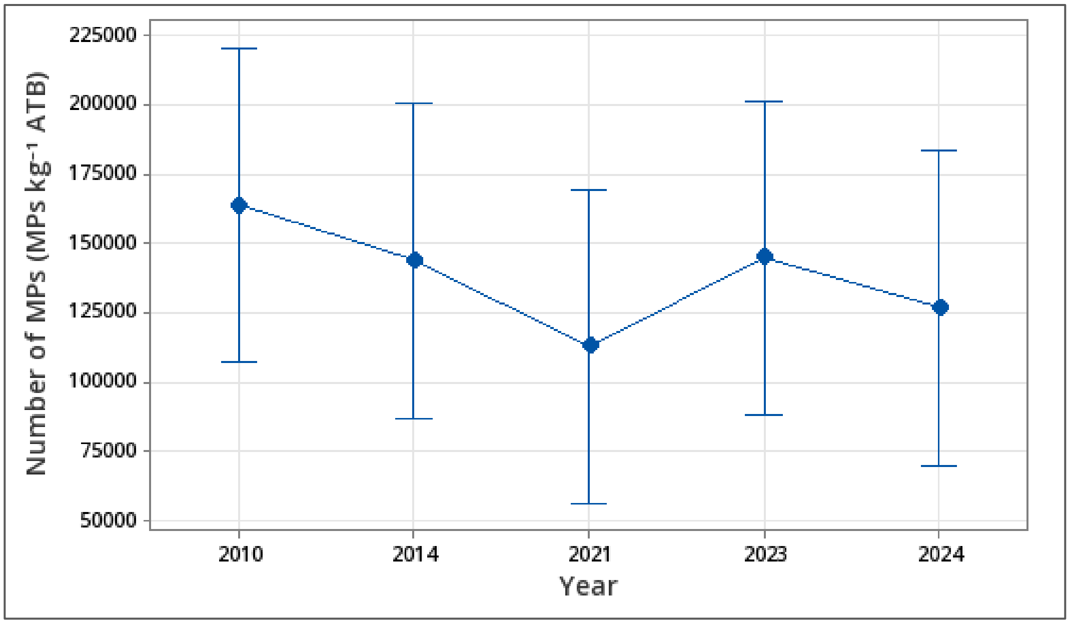

Figure B1. Mean number of MPs in ATBs (MPs kg^{-1}) each year (2010, 2014, 2021, 2023, 2024) using a pooled (N=10) 95 % Confidence Interval.

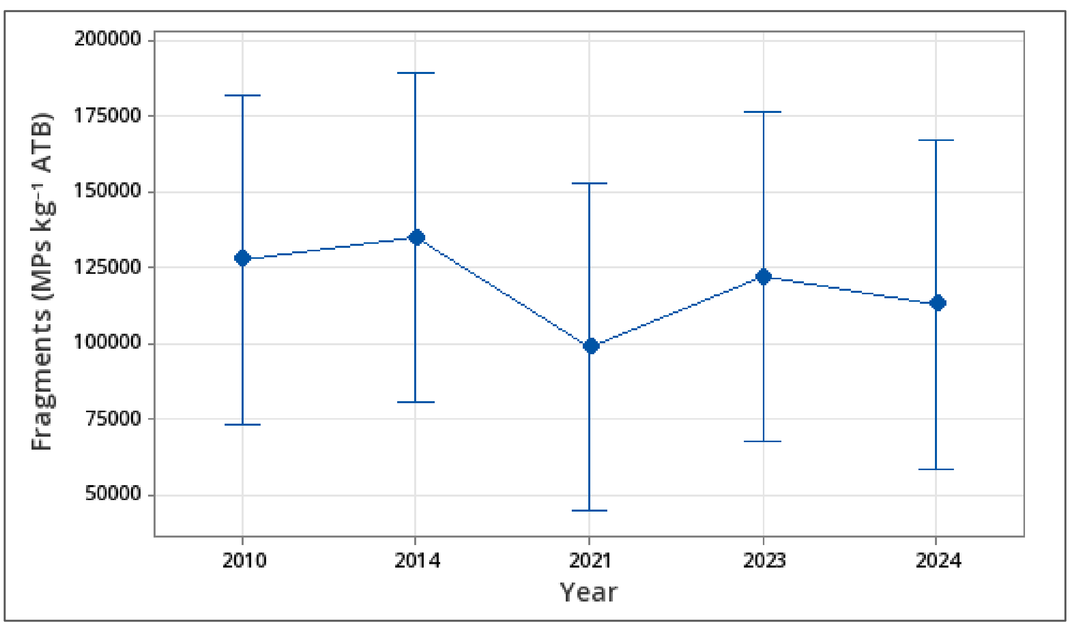

Figure B2. Mean number of fragments in ATBs (MPs kg^{-1}) each year (2010, 2014, 2021, 2023, 2024) using a pooled (N=10) 95 % Confidence Interval.

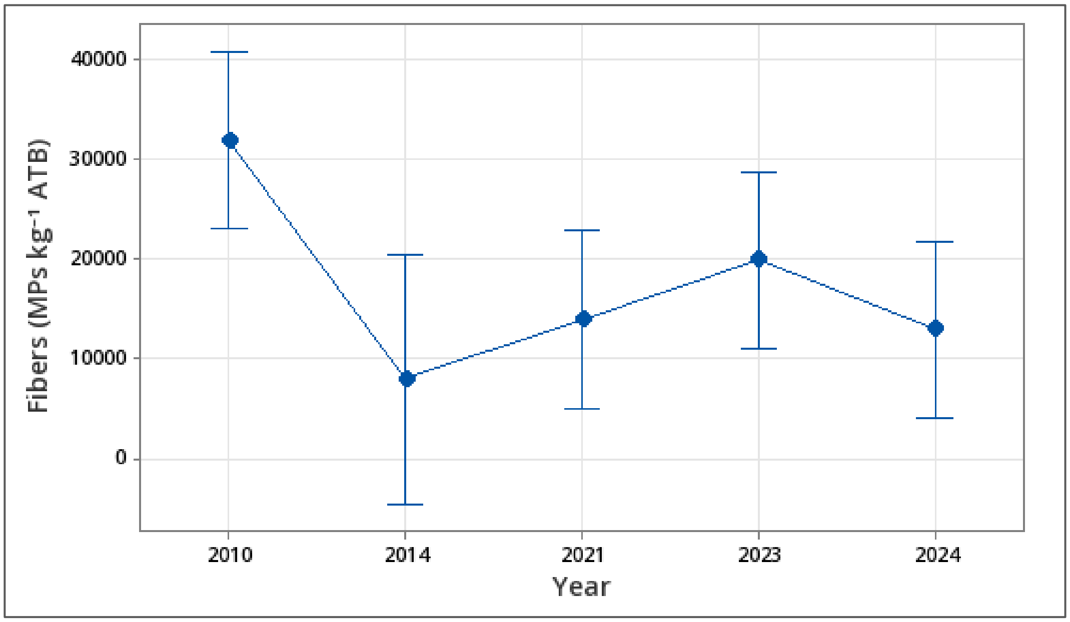

Figure B3. Mean number of fibres in ATBs (MPs kg^{-1}) each year (2010, 2014, 2021, 2023, 2024) using a pooled (N=10) 95 % Confidence Interval.

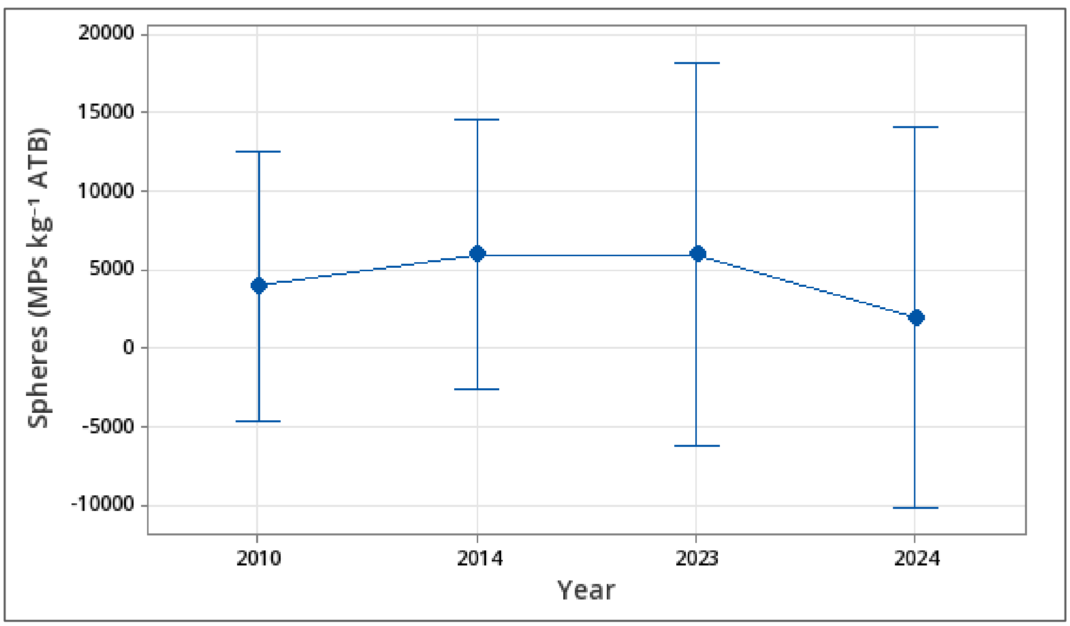

Figure B4. Mean number of spheres in ATBs (MPs kg^{-1}) each year (2010, 2014, 2021, 2023, 2024) using a pooled (N=8) 95 % Confidence Inte3rval

Size and Shape

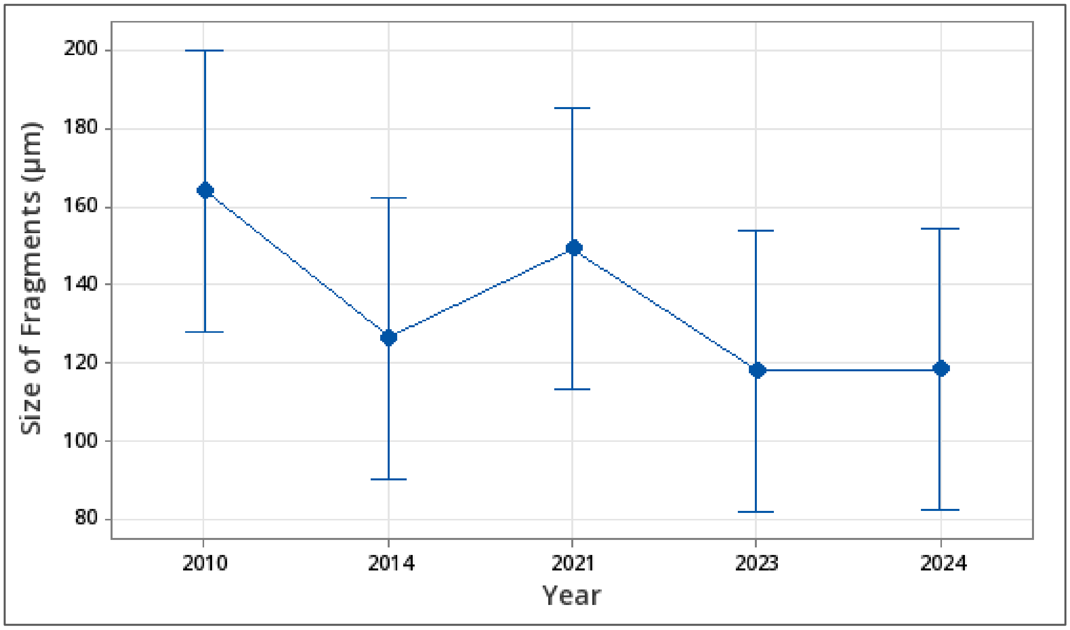

Figure B5. Mean size (µm) of fragments in ATBs across years with a pooled (N=10) 95% Confidence Interval.

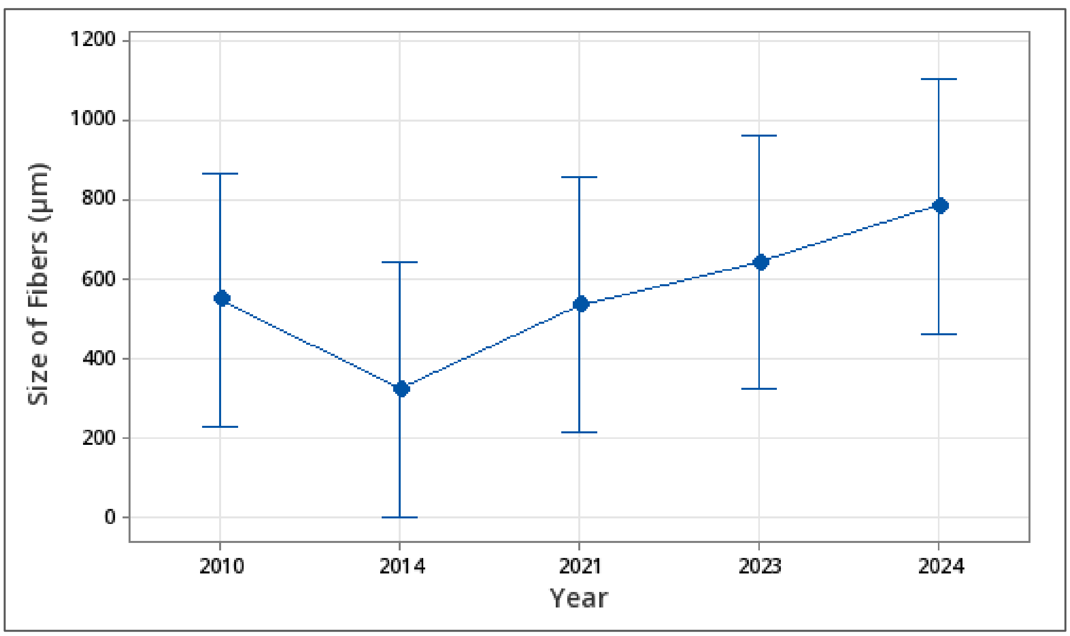

Figure B6. Mean size (µm) of fibres in ATBs across years with a pooled (N=10) 95% Confidence Interval.

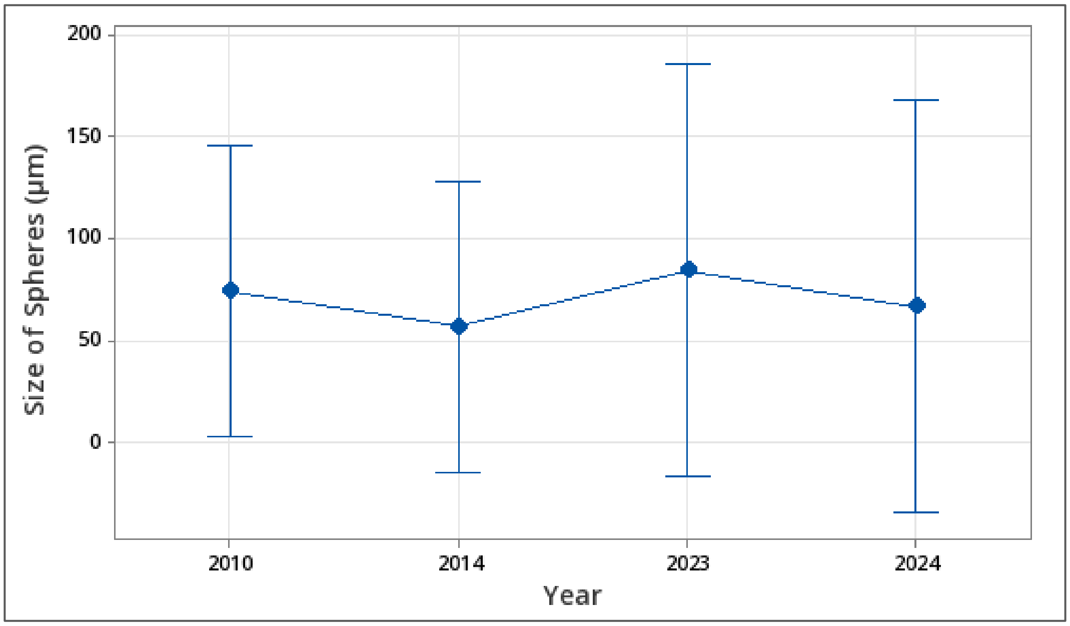

Figure B7. Mean size (µm) of spheres in ATBs across years with a pooled (N=8) 95% Confidence Interval.

Microplastics Over-Time in Soil

Abundance

Table B1. Fisher's LSD letter groupings for three-way interaction effects of management practice (single vs annual), treatment rate (0, 14, and 42 tonnes ATB (wet weight) ha^{-1}), and year (2008, 2014, 2016, 2021, and 2023) on the number of MPs (MPs kg^{-1} soil) over-time.

Management	Treatment	Year	Estimate	Standard Error	Letter Group
Annual	42	2023	95250	5074.30	A
Annual	42	2021	91000	5074.30	A
Annual	42	2016	88500	5074.30	A
Annual	14	2021	58000	5074.30	B
Annual	14	2023	54500	5074.30	B
Annual	42	2014	50500	5074.30	BC
Annual	14	2016	49250	5074.30	BC
Single	42	2021	39250	5074.30	CD
Single	14	2023	32250	5074.30	DE
Single	42	2023	32250	5074.30	DE
Annual	14	2014	31000	5074.30	DE
Single	14	2021	28750	5074.30	DEF
Annual	0	2021	22500	5074.30	EFG
Annual	0	2023	22250	5074.30	EFG
Single	42	2016	21500	5074.30	EFG
Single	42	2014	21000	5074.30	EFGH
Single	14	2016	18500	5074.30	EFGHI
Single	0	2023	16500	5074.30	FGHIJ
Single	14	2014	14500	5074.30	FGHIJ
Single	0	2021	12750	5074.30	GHIJ
Single	0	2016	12250	5074.30	GHIJ
Annual	0	2016	10250	5074.30	GHIJ
Annual	42	2008	10250	5074.30	GHIJ
Single	42	2008	10000	5074.30	GHIJ
Annual	0	2014	9000.00	5074.30	GHIJ
Single	0	2014	7250.00	5074.30	HIJ
Annual	14	2008	6250.00	5074.30	IJ
Single	0	2008	5500.00	5074.30	IJ
Single	14	2008	5000.00	5074.30	IJ
Annual	0	2008	3750.00	5074.30	J

Size and Shape

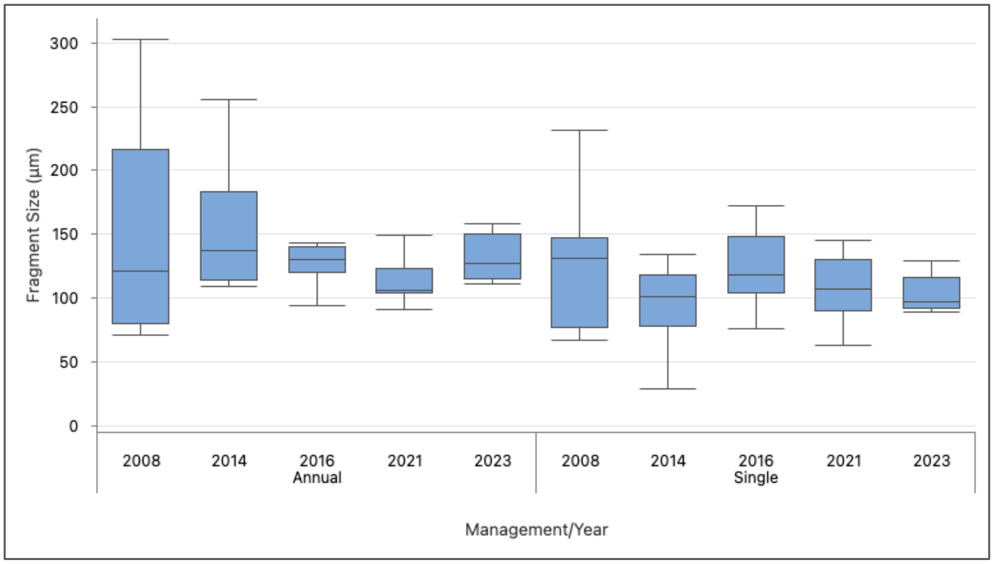

Figure B8. Size (µm) of fragments over time in response to management practice (single vs annual) and years (2008, 2014, 2016, 2021, 2023).

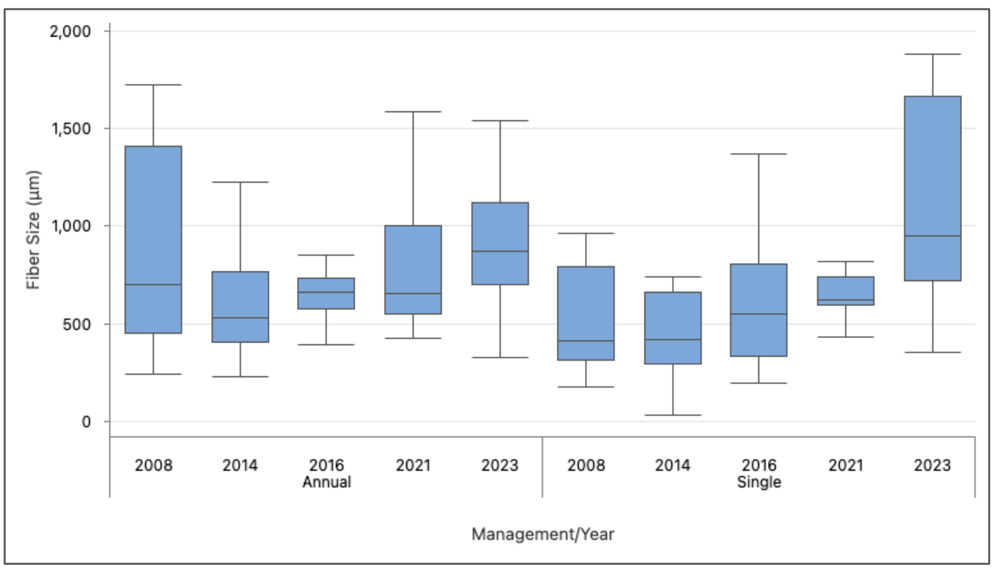

Figure B9. Size (µm) of fibres over time in response to management practice (single vs annual) and years (2008, 2014, 2016, 2021, 2023).

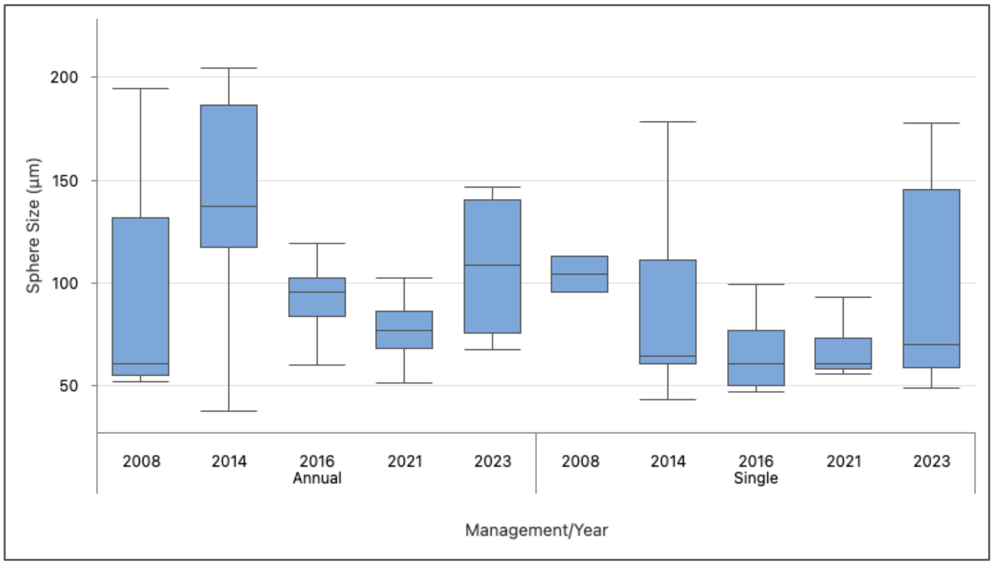

Figure B10. Size (µm) of spheres over time in response to management practice (single vs annual) and years (2008, 2014, 2016, 2021, 2023).

Microplastics Vertical Movement in Soil

Abundance

Table B2. Fisher's LSD letter groupings for three-way interaction effects of management practice (single vs annual), treatment rate (0, 14, and 42 tonnes ATB (wet weight) ha^{-1}), and depth (0-15, 15-30, 30-60 and 60-100 cm) on the number of MPs (MPs kg^{-1} soil) over-time.

Management	Treatment	Depth	Estimate	Standard Error	Letter Group
Annual	42	0-15	9100.00	480.68	A
Annual	42	15-30	6500.00	480.68	B
Annual	14	0-15	5800.00	480.68	B
Annual	14	15-30	5350.00	480.68	B
Single	42	0-15	3925.00	480.68	C
Single	14	0-15	2875.00	480.68	CD
Single	42	15-30	2800.00	480.68	CDE
Single	14	15-30	2575.00	480.68	CDEF
Single	14	30-60	2375.00	480.68	DEF
Annual	0	0-15	2250.00	480.68	DEFG
Annual	14	30-60	2150.00	480.68	DEFGH
Single	42	30-60	1750.00	480.68	DEFGHI
Annual	42	30-60	1700.00	480.68	DEFGHIJ
Annual	0	15-30	1500.00	480.68	EFGHIJ
Single	0	15-30	1500.00	480.68	EFGHIJ
Single	0	0-15	1275.00	480.68	FGHIJ
Annual	0	30-60	925.00	480.68	GHIJ
Single	0	30-60	925.00	480.68	GHIJ
Annual	14	60-100	850.00	480.68	HIJ
Single	42	60-100	550.00	480.68	IJ
Annual	42	60-100	550.00	480.68	IJ
Annual	0	60-100	525.00	480.68	IJ
Single	14	60-100	399.56	555.04	IJ
Single	0	60-100	350.00	480.68	J
Annual	42	0-15	9100.00	480.68	A
Annual	42	15-30	6500.00	480.68	B
Annual	14	0-15	5800.00	480.68	B
Annual	14	15-30	5350.00	480.68	B
Single	42	0-15	3925.00	480.68	C
Single	14	0-15	2875.00	480.68	CD

Table B3. Fisher's LSD letter groupings for three-way interaction effects of management practice (single vs annual), treatment rate (0, 14, and 42 tonnes ATB (wet weight) ha^{-1}), and depth (0-15, 15-30, 30-60 and 60-100 cm) on the number of fragments (MPs kg^{-1} soil) over-time.

Management	Treatment	Depth	Estimate	Standard Error	Letter Group
Annual	42	0-15	7400.00	370.51	A
Annual	42	15-30	5875.00	370.51	B
Annual	14	0-15	4350.00	370.51	C
Annual	14	15-30	3850.00	370.51	CD
Single	42	0-15	3075.00	370.51	DE
Single	14	0-15	2550.00	370.51	EF
Single	42	15-30	2300.00	370.51	EFG
Annual	0	0-15	2075.00	370.51	EFGH
Single	14	15-30	1900.00	370.51	FGHI
Annual	14	30-60	1375.00	370.51	GHIJ
Annual	0	15-30	1250.00	370.51	HIJK
Single	0	15-30	1250.00	370.51	HIJK
Annual	42	30-60	975.00	370.51	IJKL
Single	14	30-60	925.00	370.51	IJKL
Single	0	0-15	875.00	370.51	IJKL
Single	42	30-60	850.00	370.51	JKL
Single	0	30-60	550.00	370.51	JKL
Annual	0	30-60	550.00	370.51	JKL
Annual	14	60-100	500.00	370.51	JKL
Annual	42	60-100	400.00	370.51	JKL
Annual	0	60-100	300.00	370.51	KL
Single	14	60-100	233.33	427.83	KL
Single	0	60-100	125.00	370.51	L
Single	42	60-100	100.00	370.51	L

Table B4. Fisher's LSD letter groupings for three-way interaction effects of management practice (single vs annual), treatment rate (0, 14, and 42 tonnes ATB (wet weight) ha^{-1}), and depth (0-15, 15-30, 30-60 and 60-100 cm) on the number of fibres (MPs kg^{-1} soil) over-time.

Management	Treatment	Depth	Estimate	Standard Error	Letter Group
Annual	42	0-15	1300.00	167.77	A
Annual	14	15-30	1025.00	167.77	AB
Annual	14	0-15	900.00	167.77	ABC
Single	14	30-60	775.00	167.77	BCD
Single	42	30-60	600.00	167.77	BCDE
Single	42	0-15	525.00	167.77	CDEF
Annual	14	30-60	475.00	167.77	CDEF
Single	42	60-100	450.00	167.77	CDEF
Annual	42	15-30	450.00	167.77	CDEF
Annual	42	30-60	450.00	167.77	CDEF
Annual	14	60-100	350.00	167.77	DEF
Single	42	15-30	350.00	167.77	DEF
Single	14	15-30	325.00	167.77	DEF
Single	0	0-15	275.00	167.77	EF
Single	0	30-60	225.00	167.77	EF
Annual	0	60-100	225.00	167.77	EF
Single	0	15-30	225.00	167.77	EF
Annual	0	30-60	225.00	167.77	EF
Annual	0	15-30	225.00	167.77	EF
Single	0	60-100	175.00	167.77	EF
Single	14	0-15	150.00	167.77	EF
Annual	42	60-100	150.00	167.77	EF
Annual	0	0-15	125.00	167.77	F
Single	14	60-100	117.97	193.17	EF

Table B5. Fisher's LSD letter groupings for three-way interaction effects of management practice (single vs annual), treatment rate (0, 14, and 42 tonnes ATB (wet weight) ha^{-1}), and depth (0-15, 15-30, 30-60 and 60-100 cm) on the number of spheres (MPs kg^{-1} soil) over-time.

Management	Treatment	Depth	Estimate	Standard Error	Letter Group
Single	14	30-60	675.00	111.04	A
Annual	14	0-15	550.00	111.04	AB
Annual	14	15-30	475.00	111.04	ABC
Annual	42	0-15	400.00	111.04	ABCD
Single	14	15-30	350.00	111.04	BCDE
Single	42	0-15	325.00	111.04	BCDEF
Annual	14	30-60	300.00	111.04	BCDEFG
Single	42	30-60	300.00	111.04	BCDEFG
Annual	42	30-60	275.00	111.04	BCDEFG
Single	14	0-15	225.00	111.04	CDEFG
Annual	42	15-30	175.00	111.04	CDEFG
Single	0	30-60	150.00	111.04	DEFG
Single	42	15-30	150.00	111.04	DEFG
Annual	0	30-60	150.00	111.04	DEFG
Single	0	0-15	125.00	111.04	DEFG
Annual	0	0-15	75.0000	111.04	EFG
Single	0	60-100	50.0000	111.04	EFG
Single	14	60-100	33.3333	128.22	EFG
Single	0	15-30	25.0000	111.04	FG
Annual	0	15-30	25.0000	111.04	FG
Annual	0	60-100	2.13E-14	111.04	G
Annual	14	60-100	-995E-16	111.04	G
Annual	42	60-100	-171E-15	111.04	G
Single	42	60-100	-512E-15	111.04	G

APPENDIX C

SUPPLEMENTAL TO CHAPTER 5

Thermograms of Spiked Soil

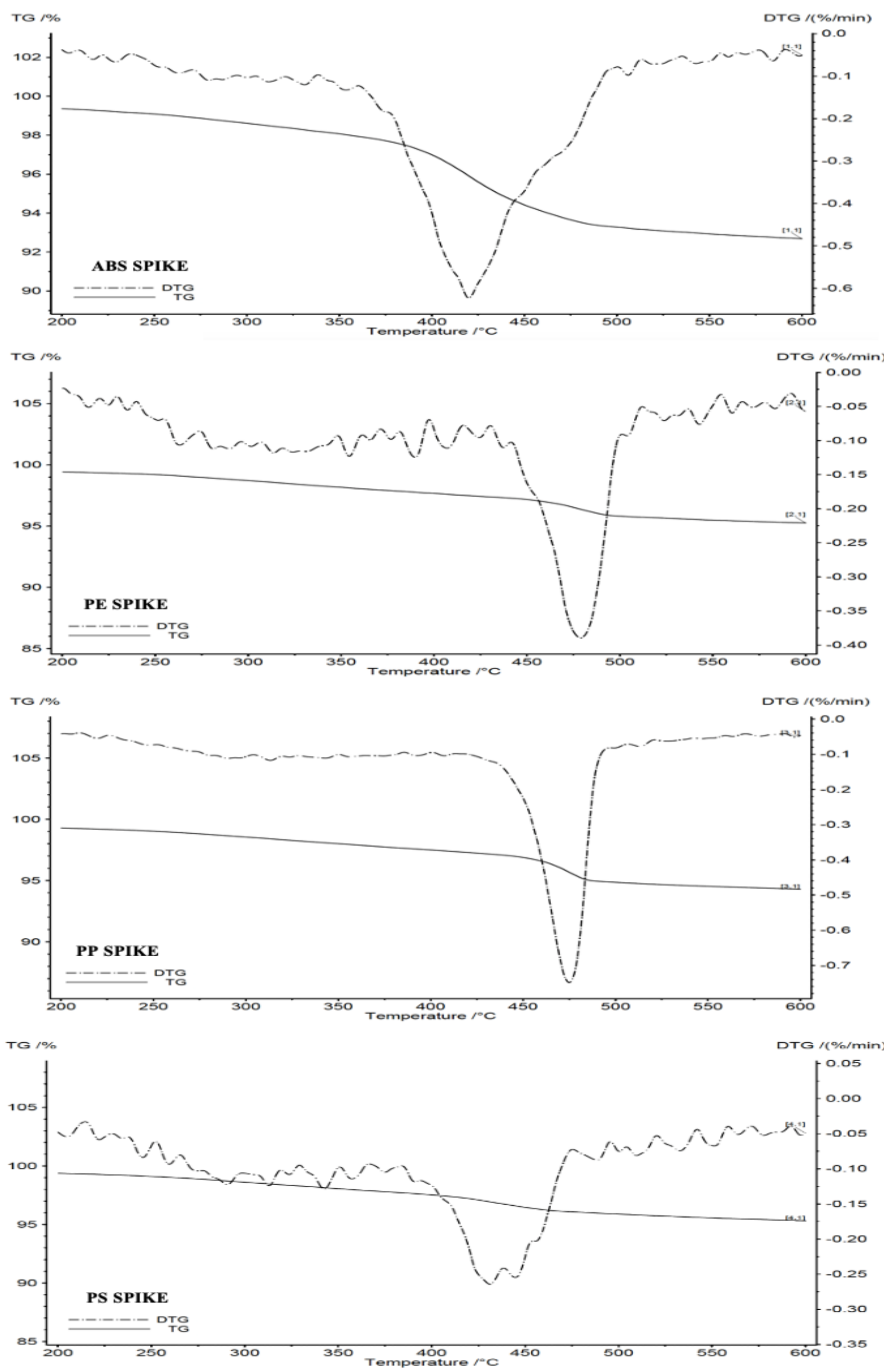

Figure C1. TG profiles of soil spiked with reference polymers ABS, PE, PP, and PS. TG curve (solid line) shows the mass loss (%) as temperature increases. DTG curve (dashed line) indicates the rate (%/min) of mass loss as a function of temperature.

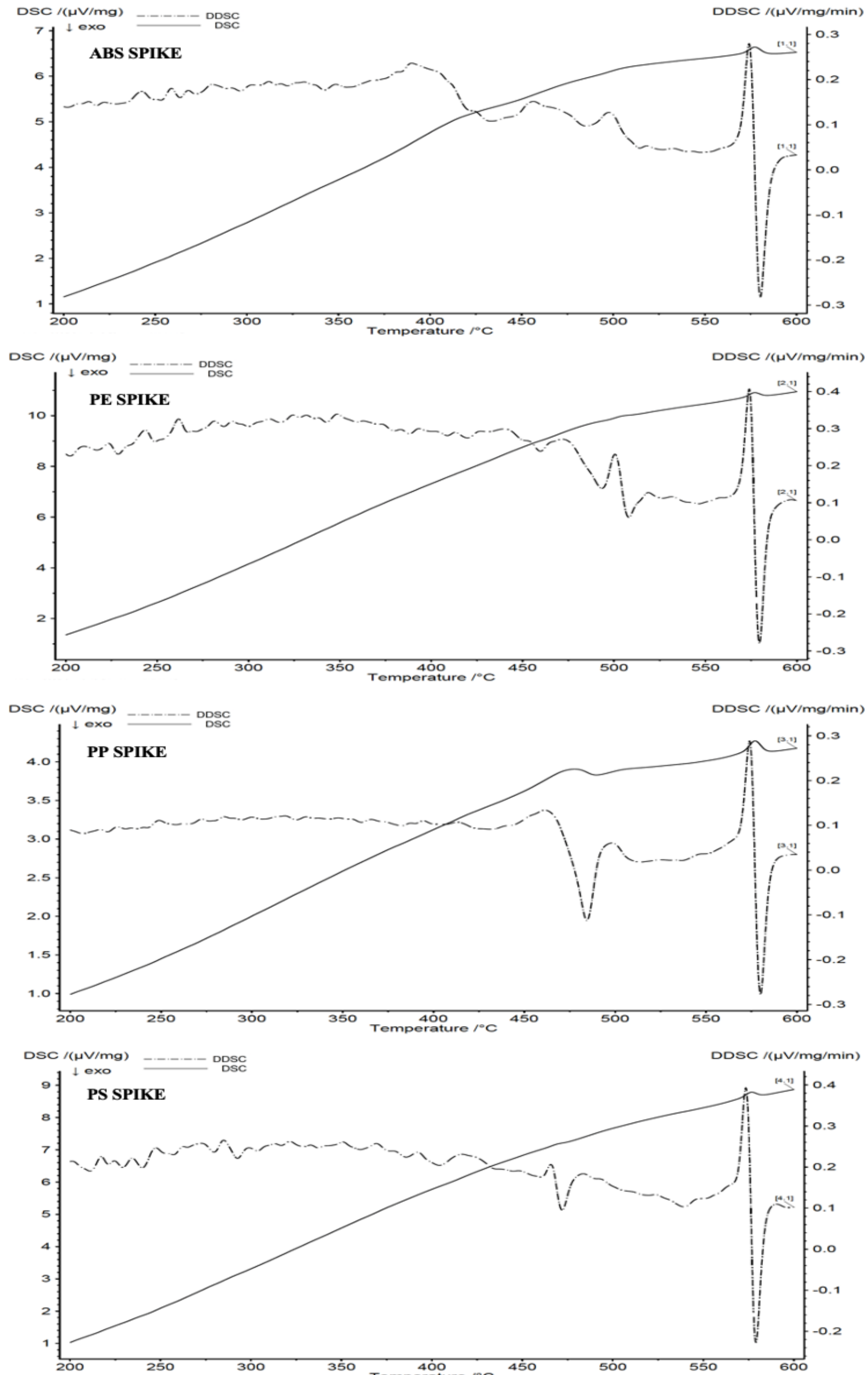

Figure C2. DSC profiles of soil spiked with reference polymers ABS, PE, PP, and PS. DSC curve (solid line) shows enthalpy changes as temperature increases (µV). DDSC curve (dashed line) represents the rate (µV/min) of heat flow change as a function of temperature.

Evolved Gas Profiles of Spiked Soil

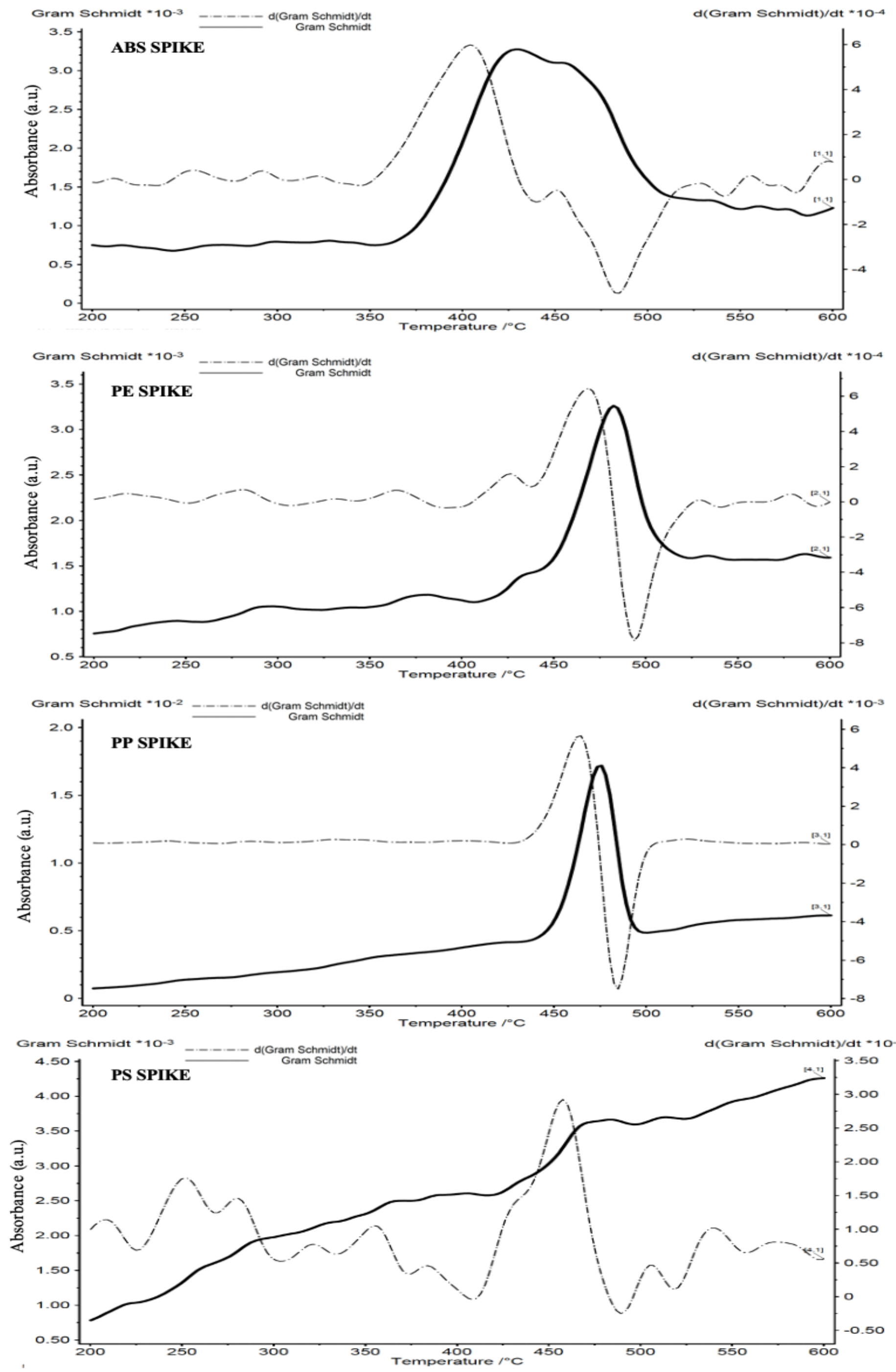

Figure C3. Gram-Schmidt profiles of soil spiked with ABS, PE, PP, and PS. Gram-Schmidt curve (solid line) represents the total infrared absorbance of evolved gasses as a function of temperature. The d(Gram Schmidt/dt) curve (dashed line) indicates changes in the rate of gas evolution as a function of temperature.

Extracted Spectra of Reference Polymers

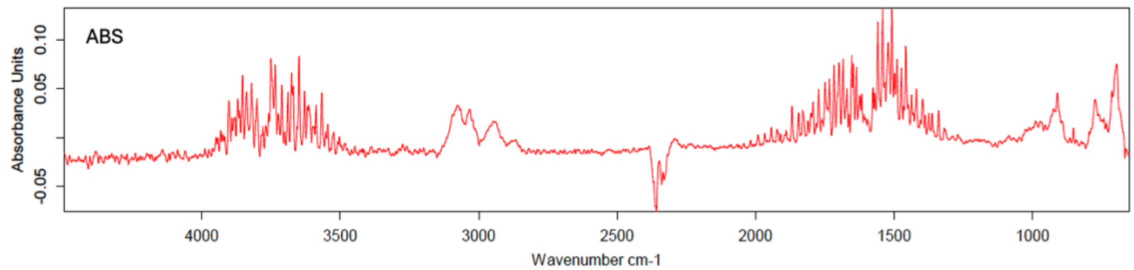

Figure C4. Spectra of evolved gasses from ABS at peak Gram-Schmidt temperature.

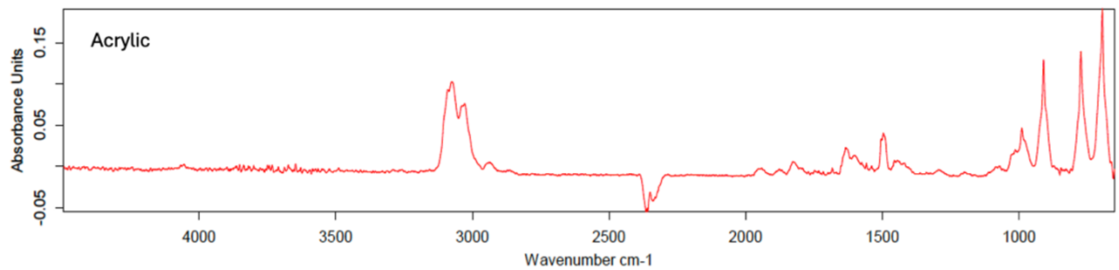

Figure C5. Spectra of evolved gasses from acrylic at peak Gram-Schmidt temperature.

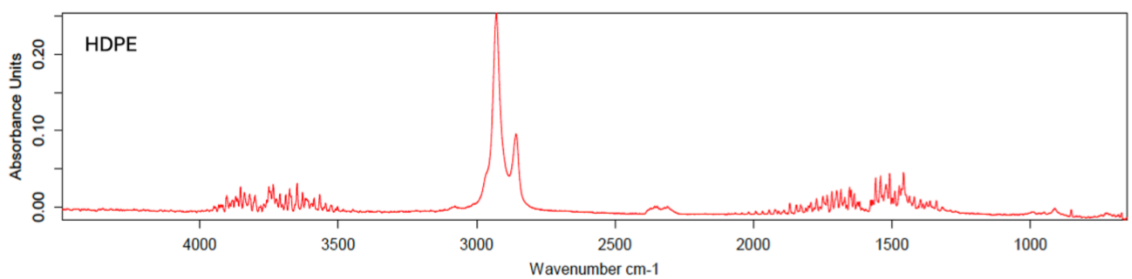

Figure C6. Spectra of evolved gasses from HDPE at peak Gram-Schmidt temperature.

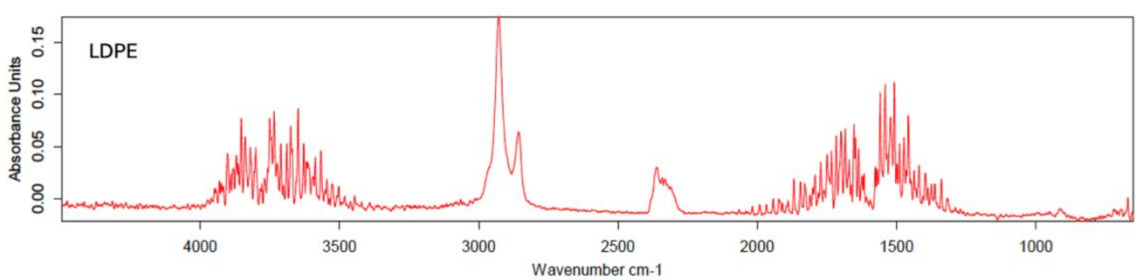

Figure C7. Spectra of evolved gasses from LDPE at peak Gram-Schmidt temperature.

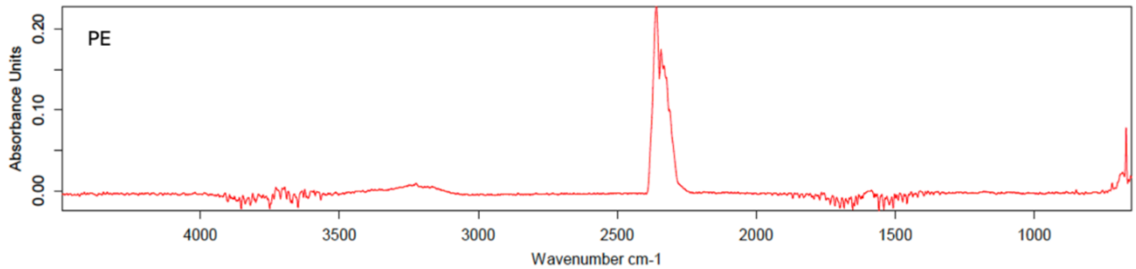

Figure C8. Spectra of evolved gasses from PE at peak Gram-Schmidt temperature.

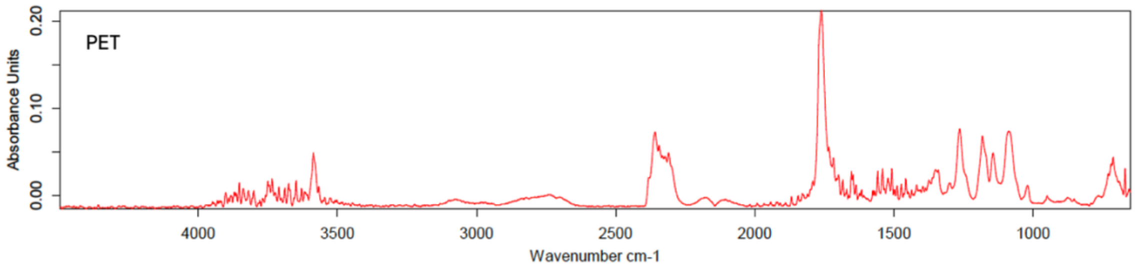

Figure C9. Spectra of evolved gasses from PET at peak Gram-Schmidt temperature.

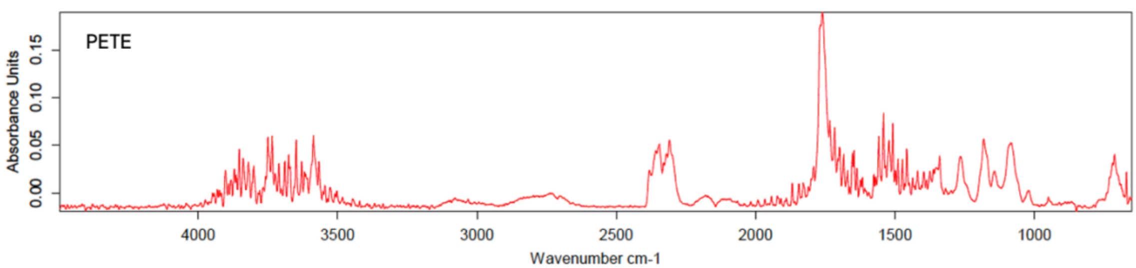

Figure C10. Spectra of evolved gasses from PETE at peak Gram-Schmidt temperature.

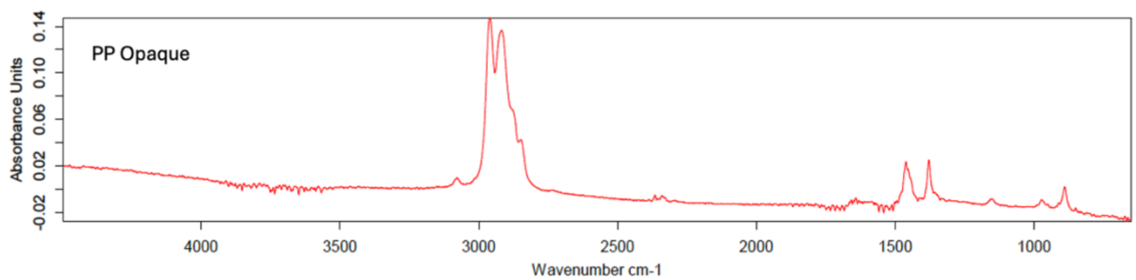

Figure C11. Spectra of evolved gasses from opaque PP at peak Gram-Schmidt temperature.

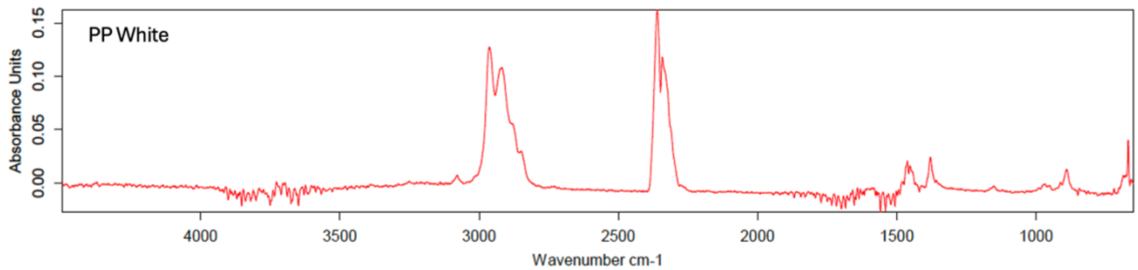

Figure C12. Spectra of evolved gasses from white PP at peak Gram-Schmidt temperature.

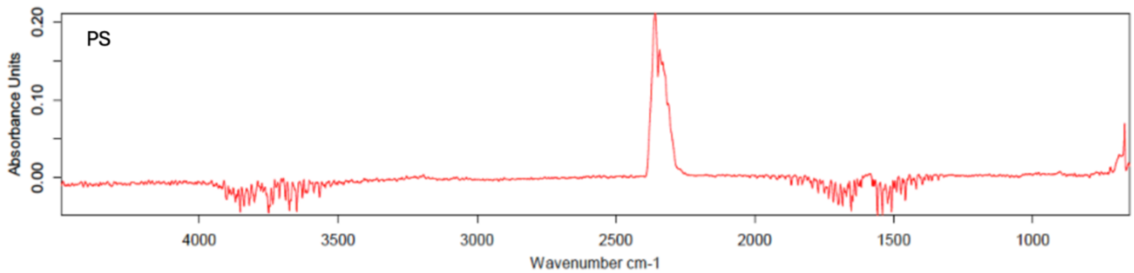

Figure C13. Spectra of evolved gasses from PS at peak Gram-Schmidt temperature.

Extracted Spectra of Soil Spiked with Reference Polymers

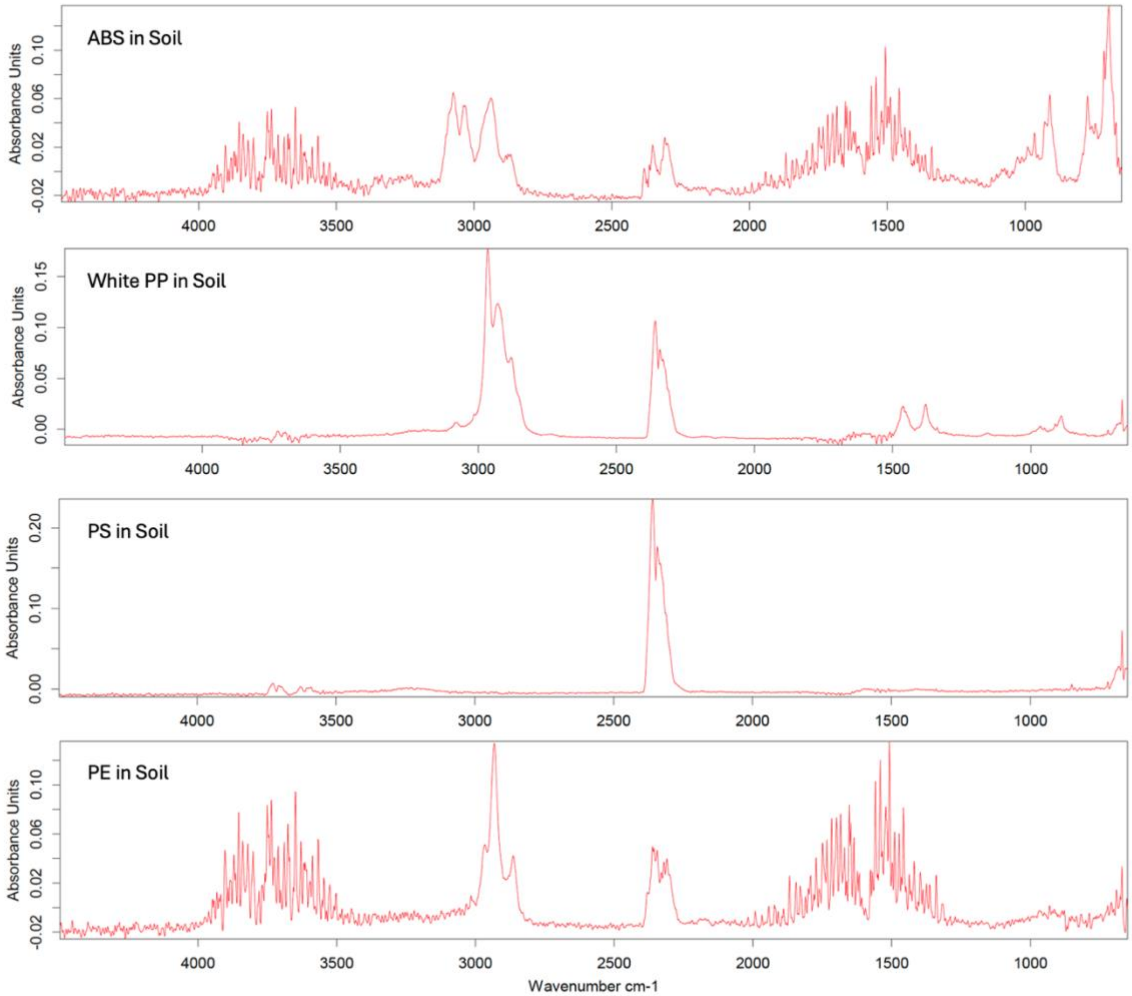

Figure C14. Spectra of evolved gasses from soil spiked with ABS, PP, PS, and PE, extracted at peak Gram-Schmidt temperatures.

Extracted Spectra of ATB Samples

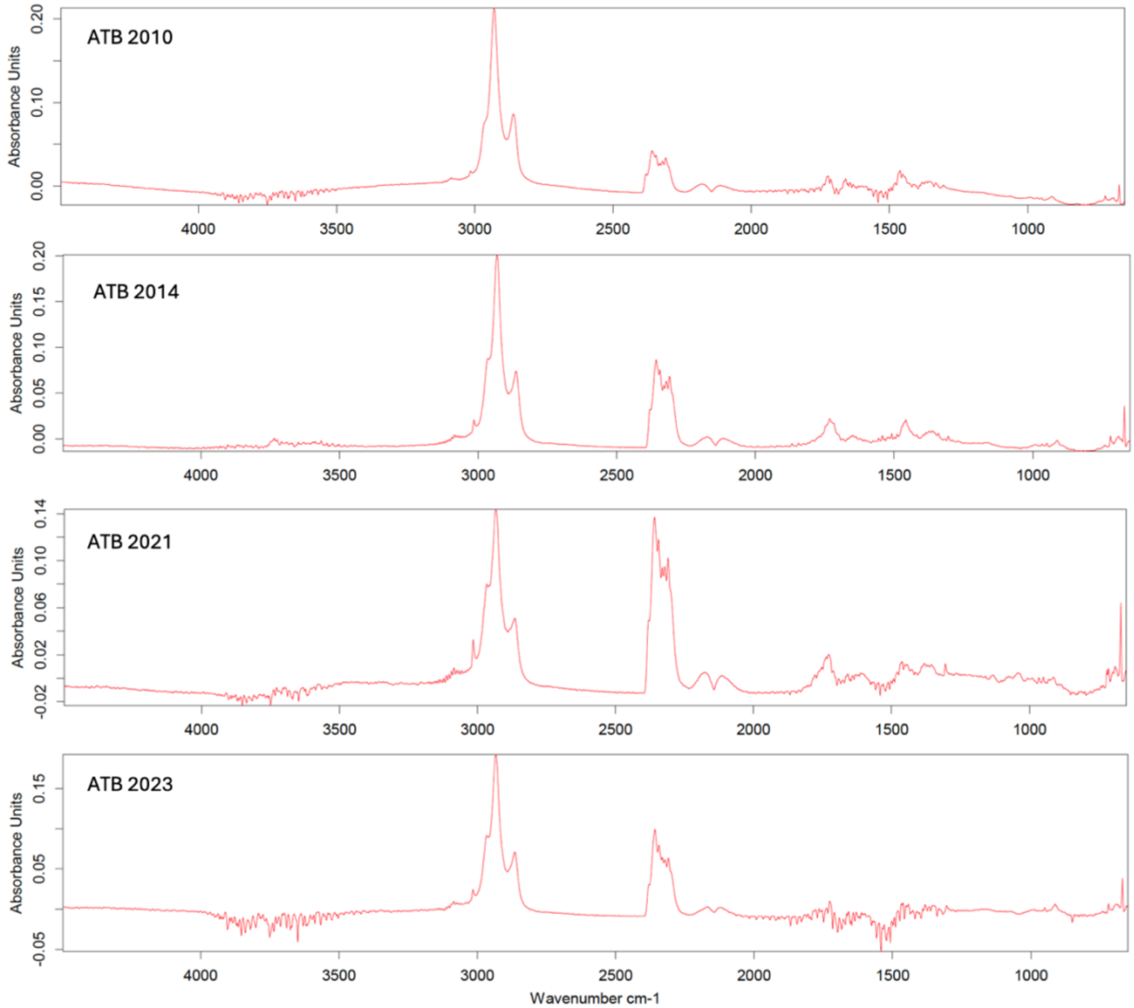

Figure C15. Spectra of ATB evolved gasses from 2010, 2014, 2021, and 2023, extracted from peak Gram-Schmidt temperatures.

Extracted Spectra of 42 tonne ha^{-1} ATB Annual treatment Rate Soil

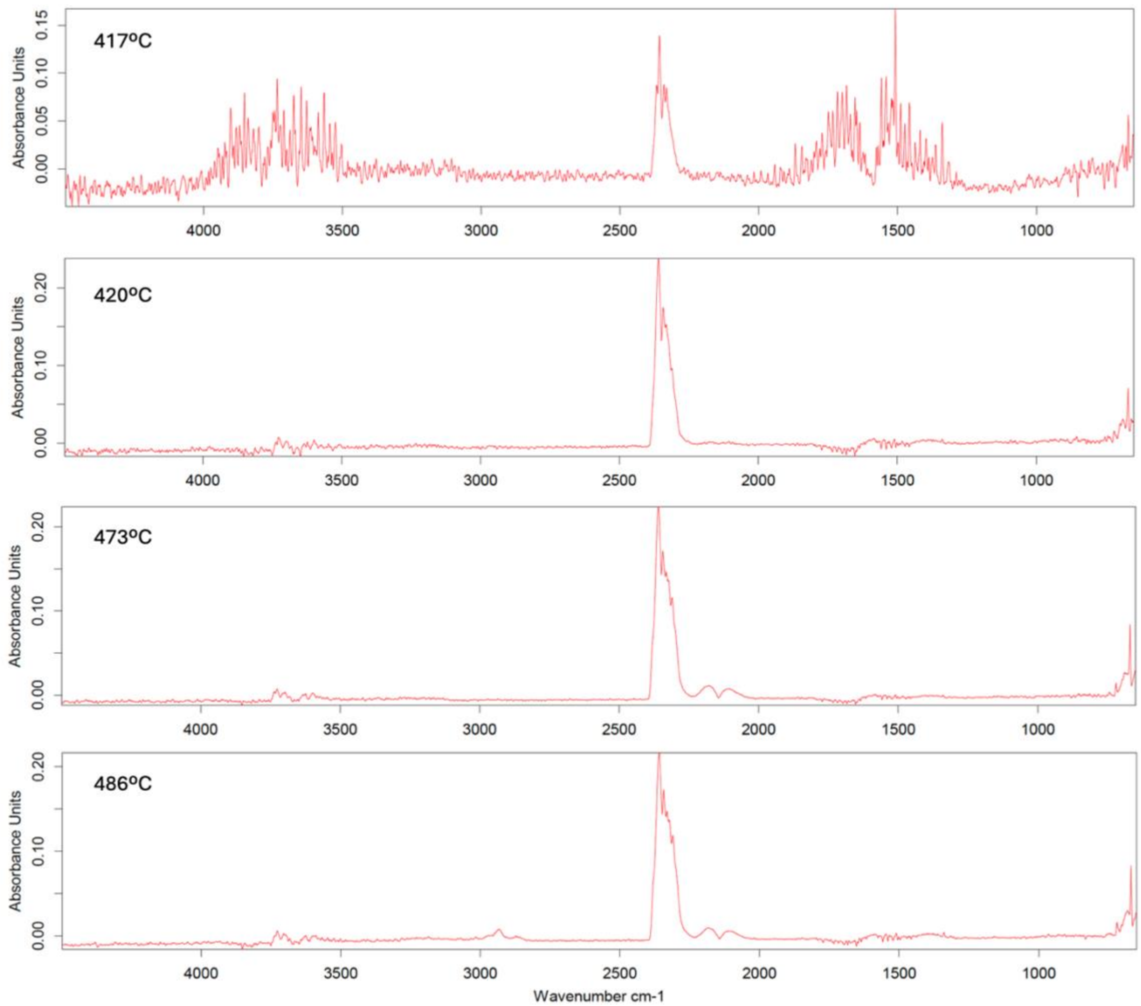

Figure C16. Spectra of the evolved gasses of soil that has received 42 tonnes ha^{-1} of ATBs annually and extracted from 417, 420, 473, and 486ºC.

Evolved Gas Spectral Matching

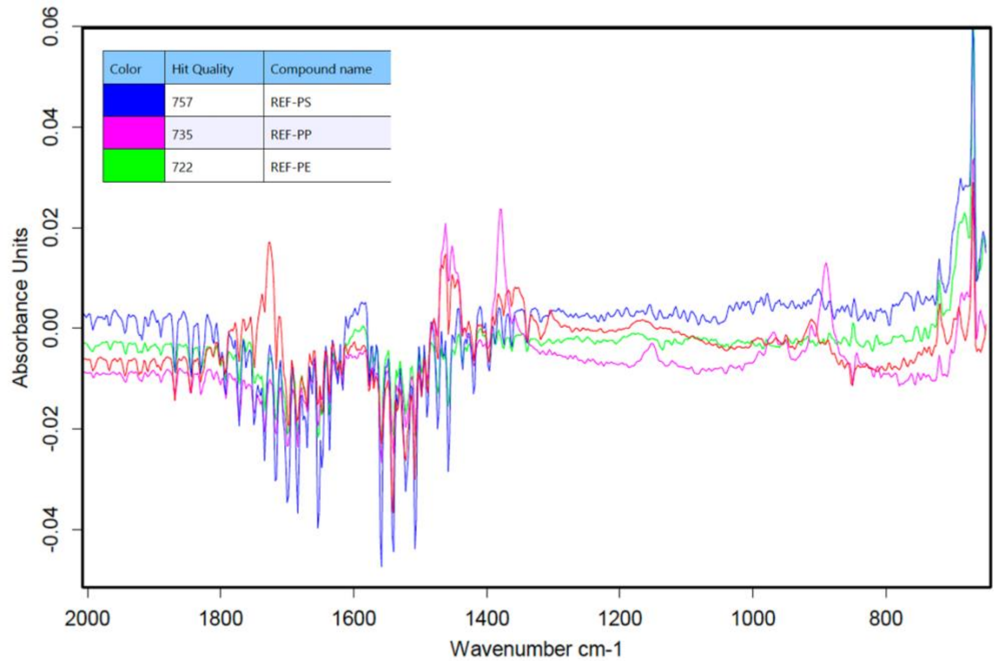

Figure C17. Automated evolved gas spectral matching of PS, PP, and PE from ATBs with reference polymer library.

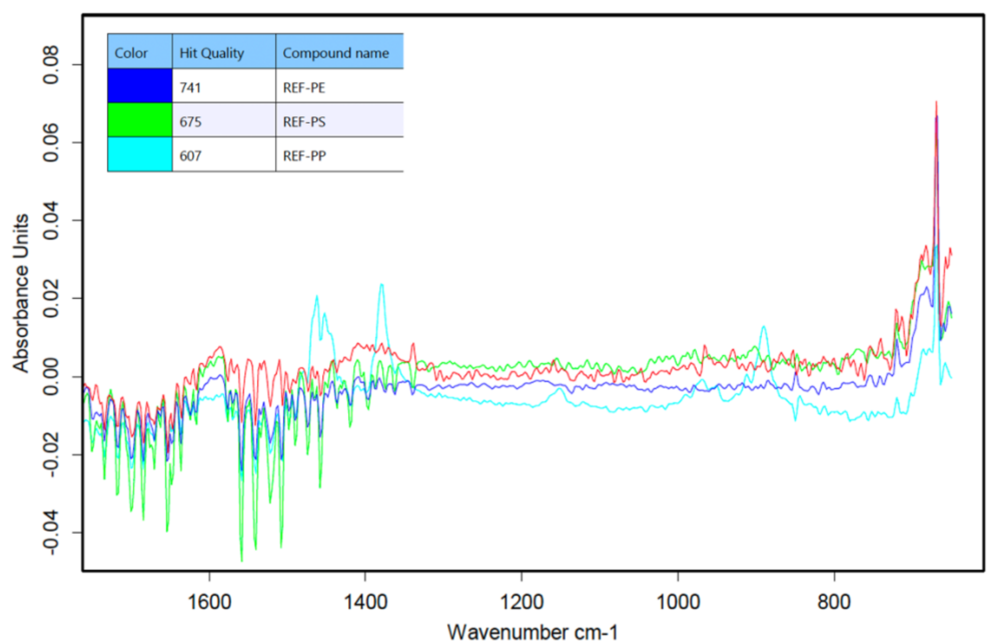

Figure C18. Automated evolved gas spectral matching of PE, PS, and PP from 42 tonne ha^{-1} ATB annually applied soils with reference polymer library.

APPENDIX D

OTHER SUPPORTING DOCUMENTS

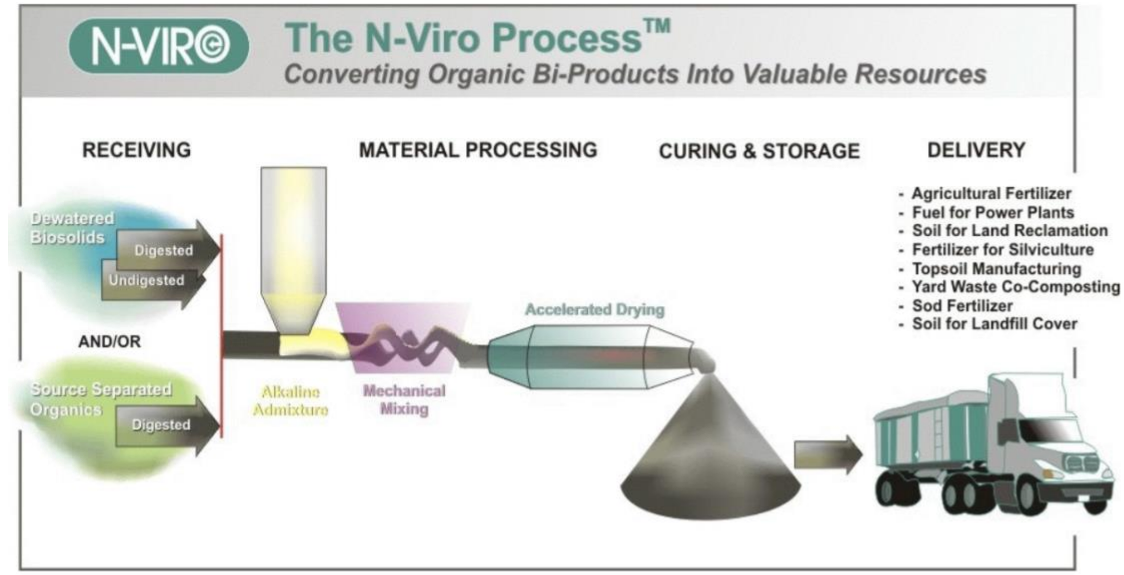

Figure 1C. A schematic of the patented N-Viro process of producing ATBs.

Figure 2C. Aerial view of field site in 2023.

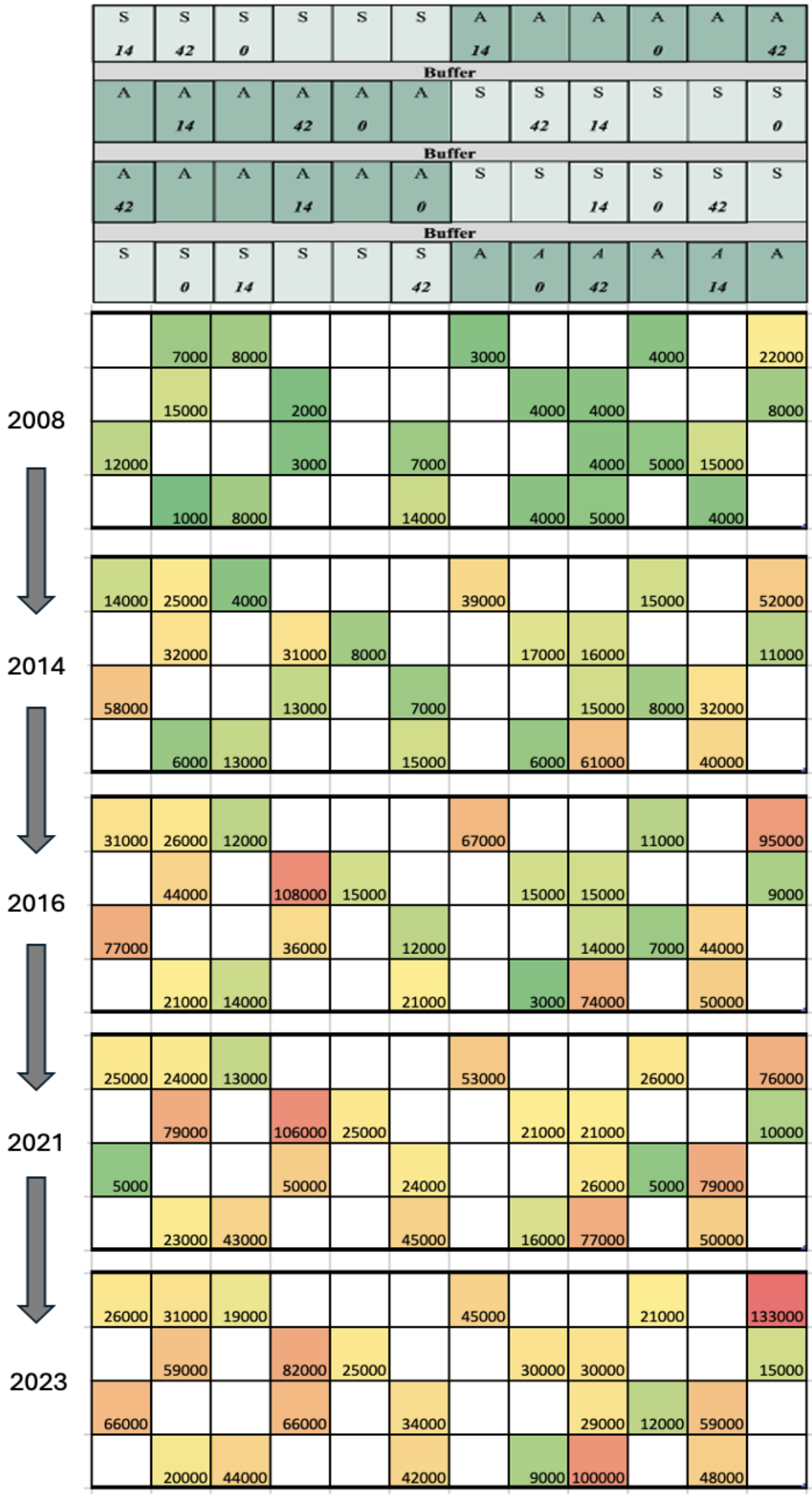

Figure 3C. Heat map of the field site over-time showing MP accumulation from 2008 to 2023.